

Patrícia Alexandra Soares Pinto

Synthesis of Bioactive Chalcones and Their Heterocyclic Derivatives as Potential Antitumor Agents

Dissertação para obtenção do Grau de Mestre em Química Farmacêutica Industrial,
sob orientação do Professor Doutor Jorge Salvador e da Professora Doutora Honorina Cidade,
apresentada à Faculdade de Farmácia da Universidade de Coimbra

Setembro 2016



Patrícia Alexandra Soares Pinto

Synthesis of Bioactive Chalcones and Their Heterocyclic Derivatives as Potential Antitumor Agents

Dissertation presented to the Faculdade de Farmácia da Universidade de Coimbra, to obtain the degree of Master in Industrial Pharmaceutical Chemistry

Work developed under the scientific supervision of Professor Jorge António Ribeiro Salvador and Professor Honorina Maria de Matos Cidade.



FFUC FACULDADE DE FARMÁCIA
UNIVERSIDADE DE COIMBRA



September 2016

IN ACCORDANCE WITH THE APPLICABLE LAW, IS NOT ALLOWED TO REPRODUCE ANY PART OF THIS DISSERTATION.

This work was developed in Laboratório de Química Orgânica e Farmacêutica, Departamento de Ciências Químicas, Faculdade de Farmácia da Universidade do Porto. This research was partially supported by the Structured Program of R&D&I INNOVMAR –Innovation and Sustainability in the Management and Exploitation of Marine Resources (reference NORTE-01-0145-FEDER-000035, Research Line NOVELMAR), funded by the Northern Regional Operational Programme (NORTE2020) through the European Regional Development Fund (ERDF) and by Foundation for Science and Technology (FCT) and COMPETE under the projects PTDC/MAR-BIO/4694/2014 (POCI-01-0145-FEDER-016790), PTDC/DTPFTO/1981/2014 (POCI-01-0145-FEDER-016581) and PTDC/AAGTEC/0739/2014 (POCI-01-0145-FEDER-016793).



Poster Communications – Original Research

Some results presented in this dissertation are part of the following abstracts and scientific poster communications:

P. Pinto*, P. M. A. Silva, S. Marques, J. Costa, J. Moreira, A. Palmeira, M. Pinto, J. Salvador, H. Bousbaa, H. Cidade, 2',4'-Dihydroxy-3,4,5-trimethoxychalcone Analogues: Synthesis, Biological Activity and Docking Studies. 11th YES Meeting (Young European Scientist) (Accepted in 11 July 2016).

P. Pinto*, P. Phianok, J. Costa, L. Moreira, J. Moreira, M. Pinto, J. Salvador, H. Cidade, Chalcones as Versatile Intermediates for the Synthesis of Potential Bioactive Agents. IJU16 - 9th Meeting of Young Researchers of U. Porto, Porto, Portugal, February 17-19, 2016.

P. Pinto*, P. Phianok, J. Costa, L. Moreira, J. Moreira, M. Pinto, J. Salvador, H. Cidade, Synthesis of Potential Bioactive Heterocyclic Chalcone Analogues. IJU16 - 9th Meeting of Young Researchers of U. Porto, Porto, Portugal, February 17-19, 2016.

P. Pinto*, P. Phianok, J. Costa, J. Moreira, M. Pinto, J. Salvador, H. Cidade, Synthesis of Potential Bioactive Chalcone Derivatives. 5th Portuguese Young Chemists Meeting and 1st European Young Chemists Meeting, Guimarães, Portugal, April 26-29, 2016.

***Presenting author**

Acknowledgements

Não existem palavras que façam justiça à gratidão pelas pessoas que contribuíram para a realização desta dissertação. Gostaria de agradecer a todos aqueles que de uma forma ou de outra colaboraram para o enriquecimento científico e, especialmente, pelo apoio emocional.

No entanto é com enorme prazer que gostaria de agradecer, particularmente ao Professor Doutor Jorge Salvador, meu orientador, pela disponibilidade sempre que possível ao longo da dissertação. À minha co-orientadora, Professora Doutora Honorina Cidade por todo o apoio laboratorial sempre que necessário, pela amizade demonstrada ao longo de todo o ano de trabalho. Gostaria de reconhecer toda a orientação e o seu pensamento crítico assim como os seus ensinamentos valiosos, foi incansável a sua ajuda.

Estimaria agradecer à Professora Doutora Madalena Pinto, pela oportunidade de realização da dissertação no Laboratório de Química Orgânica e Farmacêutica da Faculdade de Farmácia da Universidade do Porto, pela sua simpatia e pelo seu rigor científico.

À Dr.^a Sara Cravo que ao longo do ano esteve sempre disponível para me auxiliar em técnicas laboratoriais, em síntese, assim como em opiniões científicas. Obrigada pelo acompanhamento e pelo carinho demonstrado.

À Gisela Adriano pela prontidão em tudo que fosse necessário no laboratório.

Gostaria de agradecer também à Professora Doutora Andreia Palmeira, pela cooperação e ensinamentos no estudo de Docking, o seu contributo foi essencial para o enriquecimento deste trabalho. Ao Professor Doutor Hassan Bousbaa e às estudantes de mestrado Patrícia Silva e Sandra Marques o meu agradecimento pela realização de ensaios de atividade biológica realizada na CESPU.

Aos meus colegas e companheiros de Laboratório, pela cooperação e companheirismo, que tornaram o ambiente de trabalho mais agradável, em particular à Joana Moreira e ao João Costa pela boa disposição e disponibilidade em ajudar em tudo que fosse preciso.

Aos meus pais fantásticos e maravilhosos, a quem dedico com enorme emoção todo este trabalho, sem vocês isto não seria possível. Obrigada por todo o carinho, apoio e a nunca desistirem de mim. ADORO-VOS.

Ao meu Irmão, meu número 1, por toda compreensão e toda ajuda nos pequenos e grandes pormenores. Toda a passagem de aprendizagem fez de mim uma pessoa bem melhor. Obrigada pela presença em todos os momentos.

Aos meus avôs, meus ídolos de década, sempre preocupados em que tudo corresse 'às mil maravilhas', a confiança e apoio depositado em mim foi essencial.

À restante família, tios e primos, que de uma forma e de outra auxiliaram-me nos momentos bons e menos bons, com os melhores ensinamentos.

Aos meus amigos de coração, e a ti Miguel, a quem estou grata desde sempre e para sempre, a adolescência traz o que de melhor se pode ter. Obrigada pelas pequenas e grandes distrações e pela descontração nos momentos mais stressantes, pelo carinho e amor.

À minha amiga Mari e Raquel, amigas desde a licenciatura, que marcaram presença ao longo de todo o ano. As pequenas coisas demonstram o que de melhor tem a vida.

Tenho em mim todos os sonhos do mundo

Fernando Pessoa

Abstract

Chalcones have been intensively studied for their wide range of biological activities, namely antitumor, being this activity associated with, at least in part, to their ability to promote cell cycle arrest by interference with mitosis. Recently, as result of the search for new antitumor small molecules by LQOF-FFUP research group 2',4'-dihydroxy-3,4,5-trimethoxychalcone has been identified as an antimitotic agent. Inspired by the potential of this chalcone as antimitotic agent, six structure related chalcones (**P0**, **P4**, **P5**, **BT**, **BF**, **CI**) possessing a 3,4,5-trimethoxyphenyl ring, considered as crucial for the interaction with the colchicine binding site of α,β -tubulin, were synthesized by base catalysed Claisen Schmidt condensation via microwave assisted organic synthesis (MW).

As chalcones are interesting intermediates for the synthesis of bioactive heterocyclic compounds, chalcone derivatives such the pyrazole **P0-Pyr**, pyrazoline **CI-Pyr** and isoxazol **P0-iso** derivatives were also synthesized by molecular modification of chalcones enone moiety. Docking studies were carried out in order to predict the binding ability of synthesized chalcone derivatives, as well as structure related analogues with the colchicine binding site of α,β -tubulin. The antiproliferative activity of chalcones derivatives **P0**, **P4**, **P5**, **BT**, **BF** and **CI** on the growth of three human tumor cell lines (A375-C5, MCF-7 and NCI-H460) was assessed using SRB assay.

Keywords: Chalcones, Antitumor activity, Antimitotic activity

Resumo

As chalconas têm sido intensamente estudadas pela sua vasta gama de atividades biológicas, nomeadamente antitumoral, sendo esta associada, em parte à sua capacidade para promover a paragem do ciclo celular pela interferência da mitose.

Recentemente, como resultado da pesquisa de novos antitumorais pelo grupo de pesquisa do LQOF-FFUP, a 2',4'-di-hidroxi-3,4,5-trimetoxichalcona foi identificada como agente antimitótico. Inspirado pelo potencial desta chalcona como agente antimitótico, seis chalconas estruturalmente relacionadas (**P0**, **P4**, **P5**, **BT**, **BF**, **CI**) possuindo um anel 3,4,5-trimetoxifenilo, considerado como crucial para interação com o local de ligação da colchicina na α,β - tubulina, foram sintetizados por condensação de Claisen Schmidt por síntese orgânica assistida por microondas.

Considerando o potencial de chalconas como intermediários para a síntese de compostos heterocíclicos bioativos, foram sintetizados três derivados (o pirazol **P0-pyr**, a pirazolina **CI-pyr** e o isoxazol **P0-iso**) mediante a modificação molecular da porção enona do scaffold chalcona. Adicionalmente foram realizados estudos de docking dos compostos sintetizados, assim como de outros compostos estruturalmente relacionados, com o local de ligação da colchicina na α,β - tubulina a fim de prever a sua capacidade de ligação a este alvo. A atividade antiproliferativa das chalconas **P0**, **P4**, **P5**, **BT** e **BF** no crescimento de 3 linhas celulares tumorais humanas (A375-C5, MCF-7 e NCI-H460) foi avaliada usando ensaios de SRB.

Palavras-chave: Chalconas, Atividade Antitumor, Atividade Antimitótica

Table of Contents

Acknowledgements.....	vi
Abstract	viii
Resumo	ix
Table of Contents	x
List of Figures	xiii
List of Tables	xv
Abbreviations and Symbols	xvi
Outline of the Dissertation.....	xix
Chapter 1: Introduction	1
1.1. Cancer and Mitosis.....	2
1.1.1. Microtubule dynamics crucial to mitosis.....	4
1.1.2. Antimitotic agents (MTAs)	6
1.1.2.1. Microtubule stabilizing Natural Products	9
1.1.2.1.1. Microtubules stabilizers occupying Taxane binding domain	9
1.1.2.2. Microtubule destabilizing Natural Products	10
1.1.2.2.1. Microtubule inhibitors Natural Products.....	10
1.1.2.2.2. Microtubule inhibitors binding at colchicine binding domain	11
1.2. Flavonoids.....	19
1.2.1. Chalcones.....	22
1.2.1.1. Synthesis of chalcones	23
1.2.1.1.1. Aldol Condensation.....	23
1.2.1.1.2. Others Methods.....	27
1.2.1.2. Chalcones as intermediates for the synthesis of nitrogen heterocycles...30	
1.2.1.2.1. Pyrazole Derivatives.....	31
1.2.1.2.2. Isoxazole Derivatives	32
1.2.2. Biological activities.....	33
1.2.2.1. Chalcones as antimitotic agents	36
1.3. Aims and overview	54
Chapter 2: Results and Discussion	55
2.1. Chemistry.....	56

2.1.1. Synthesis	56
2.1.2. Molecular modification of chalcone derivatives.....	59
2.1.2.1. Synthesis of isoxazole derivatives	60
2.1.2.2. Synthesis of pyrazole derivatives.....	62
2.1.2.2.1. Synthesis of pyrazole derivatives by one-pot synthesis.....	62
2.1.2.2.1.Synthesis of pyrazole derivatives by two steps synthesis.....	63
2.2. Structure Elucidation	66
2.2.1. Chalcones.....	66
2.2.2. Isoxazole derivatives P0-iso	70
2.2.3. Pyrazoline derivative C I-pyrz.....	72
2.2.4. Epoxide derivatives P0-epo, P4-epo and BT-epo	74
2.2.5. Pyrazole derivative P0-pyrz.....	76
2.2.6. Chalcone bromine P0-br.....	78
2.3. Peak Purity	80
2.4. Docking Studies	81
2.5. Biological Activity	86
Chapter 3: Conclusions	87
Chapter 4: Experimental Procedures.....	89
3.1. Chemistry.....	90
3.1.1. Synthesis	90
3.1.1.1. General Methods	90
3.1.2. Synthesis of chalcone P5 by conventional heating.....	91
3.1.3. Synthesis of chalcones P0, P4, P5, B, BF and CI by MW irradiation.....	91
3.1.4. Synthesis of isoxazole derivative P0-iso	93
3.1.5. Synthesis of pyrazoline derivative C I-pyrz.....	94
3.1.6. Synthesis of epoxide derivatives P0-epo, P4-epo, P5-epo and BT-epo.....	94
3.1.7. Synthesis of pyrazole derivative P0-pyr	96
3.1.8. Synthesis of chalcone bromide P0-br.....	96
3.2. Peak Purity.....	98
3.3. Docking Studies.....	98
3.4. Biological Activity.....	99
3.4.1. Cell Culture	99

3.4.2. Growth inhibition assay Biological Activity	99
Chapter 5: References	100

List of Figures

Figure 1: Event of cell cycle.....	2
Figure 2: Representation of mitosis phases (adapted from (9)).....	3
Figure 3: Structures of tubulin dimer and microtubule	4
Figure 4: Microtubule polymerization and depolymerization dynamics.. ..	5
Figure 5: Different types of antimitotic agents.....	7
Figure 6: Illustration of tubulin binding sites.	7
Figure 7: Schematic diagram of putative events involved in MTAs-induced apoptosis (adapted from (21)).	8
Figure 8: Structure of (-)-combretastatin and combretastatins A, B, C and D.....	12
Figure 9: The structure of the flavonoids.....	19
Figure 10: Schematic representation of the major branch pathways of flavonoid biosynthesis.....	20
Figure 11: Chemical structure of quercetin (26), genistein (27) and flavopiridol (28).	21
Figure 12: General structure of chalcones.	22
Figure 13: Claisen-Schmidt condensation reaction.	23
Figure 14: Synthesis of chalcone derivatives using chlorotriptyl chloride as solid support by Neves et al. (49).	24
Figure 15: Synthesis of chalcone derivatives by SPOS using PEG as solid support by Peng et al. (50).	25
Figure 16: Synthesis of chalcones via Grinding technique by Zangade et al. (69).	26
Figure 17: Synthesis of chalcones by one-pot condensation reactions by Leanne et al. (70).....	26
Figure 18: Synthesis of chalcones by one-pot synthesis of chalcones by Xu et al. (71).	27
Figure 19: Synthesis of chalcones via palladium-catalyzed cross-coupling by Al-Masum et al. (72).	27
Figure 20: Synthesis of chalcone via Suzuki cross-coupling reaction by Selepe et al. (74).	28
Figure 21: Chalcone synthesis via Friedel-Crafts reaction.	29
Figure 22: Synthesis of chalcone via Julia-Kocienski olefination reaction by Kumar et al. (75).	29
Figure 23: Synthesis of chalcones via Heck coupling reaction by Bianco et al. (76).....	29
Figure 24: Some chalcone derivatives obtained by molecular modification of α,β -unsaturated ketone moiety of chalcone scaffold.	30
Figure 25: Synthesis of pyrazole derivatives through molecular modifications of chalcones.....	31
Figure 26: Synthesis of isoxazole derivatives through molecular modifications of chalcones.	33
Figure 27: Chalcones clinically tested for various health conditions.	34
Figure 28: Structure of some chalcones reported as chemopreventive agents.	34

Figure 29: Summarizes the molecular targets for the antitumor activity of chalcones.....	35
Figure 30: Building blocks used for the synthesis of chalcones.....	54
Figure 31: Reaction mechanism of Claisen-Schmidt condensation.....	56
Figure 32: Synthesis of chalcone derivatives by MAOS.....	57
Figure 33: Synthesis of isoxazoles and pyrazoles by molecular modification of chalcones.....	59
Figure 34: Synthesis of isoxazole derivatives.....	60
Figure 35: Synthesis of 1,3,5-trisubstituted pyrazole derivatives by Ponnala et al. (78).....	62
Figure 36: Structure of CI-pyrz	63
Figure 37: Synthesis of chalcone P0-br	64
Figure 38: Synthesis of chalcone epoxides.....	64
Figure 39: Synthesis of P0-pyr	66
Figure 40: Main correlations found in the HMBC spectra of chalcones.....	68
Figure 41: Main correlations found in the HMBC spectrum of P0-iso	71
Figure 42: Main correlations found in the HMBC spectrum of CI-pyrz	73
Figure 43: Main correlations observed in the HMBC spectra of chalcones P0-epo , P4-epo and BT-epo	75
Figure 44: Main correlations found in the HMBC spectrum of P0-pyrz	77
Figure 45: Main correlations observed in the HMBC spectrum of P0-br	79
Figure 46: The molecular docking model of tested and control models with tubulin.....	85

List of Tables

Table 1: Examples of MTAs.....	14
Table 2: Chalcones with antimetabolic activity.....	37
Table 3: Reaction Conditions used to synthesize chalcone P5.....	57
Table 4: Synthesized chalcones, with their respective yields and reaction time.....	58
Table 5: General experimental conditions for the synthesis of isoxazole derivatives (P0-iso, P4-iso and BT-iso).....	61
Table 6: Synthesis of chalcone epoxides.....	65
Table 7: IR data of chalcones P0, P4, P5, BT, BF and CI	66
Table 8: ¹ H NMR data of chalcones P0, P4, P5, BT, BF and CI	69
Table 9: ¹³ C RMN data of chalcones compounds P0, P4, P5, BT, BF and CI	69
Table 10: IR data of isoxazole derivative P0-iso	70
Table 11: ¹ H NMR ^a and ¹³ C NMR ^b data of isoxazole derivative P0-iso	71
Table 12: IR data of pyrazoline derivative CI-pyrz	72
Table 13: ¹ H NMR and ¹³ C NMR data of pyrazoline derivative CI-pyrz	73
Table 14: IR data of chalcones P0-epo, P4-epo and BT-epo	74
Table 15: ¹ H NMR data of epoxide derivatives P0-epo, P4-epo and BT-epo	75
Table 16: ¹³ C NMR data of epoxide derivatives P0-epo, P4-epo and BT-epo	76
Table 17: IR data of pyrazole derivative P0-pyrz	76
Table 18: ¹ H NMR and ¹³ C NMR data of pyrazole derivative P0-pyrz	77
Table 19: IR data of chalcone derivative P0-br	78
Table 20: ¹ H NMR and ¹³ C NMR data of chalcone derivative P0-br . ^a	79
Table 21: Purity values of chalcones P0, P4, P5, BT and BF	80
Table 22: Docking scores (Kcal.mol ⁻¹) for tubulin target for the compounds P0, P4, P5, BT, BF, P0-iso, P4-iso, P0-pyrz, P4-pyrz and BT-pyrz and controls (podophylotoxin, combretastatin-A4 and colchicine).....	83
Table 23: GI ₅₀ values obtained for chalcones P0, P4, P5, BT and BF on the growth of human tumor cell Lines ^a	86

Abbreviations and Symbols

^{13}C NMR	Carbon-13 Nuclear Magnetic Resonance
^1H NMR	Proton Nuclear Magnetic Resonance
AcOH	Acetic Acid
ANS	Anthocyanidin Synthase
$\text{BF}_3\cdot\text{OEt}_2$	Boron trifluoride diethyl etherate
Br_2	Bromine
Brd	Broad doublet
Bipy	2,2'-bipyridine
CC	Column Chromatography
CDCl_3	Deuterated Chloroform
CDKs	Cyclin-Dependent kinases
CHI	Chalcone isomerase
CHS	Chalcone Synthase
CIIMAR	Interdisciplinary Centre of marine and environmental research
CA4	Combretastatin A4
CA4P	Combretastatin A4 Phosphate
C4H	Cinnamic acid 4-hydroxylase
CrO_3	Chromium trioxide
DBU	1,8-Diazabicyclo [5.4.0]undec-7-ene
DED	Death Effector Domain
d	doublet
dd	double doublet
DD	Death Domain
DFR	Dihydroflanonol-4-Reductase
DISC	Death-Induced Signaling Complexes
DMSO	Dimethylformamide
DPPH	2,2-Diphenyl-1-Picrylhydrazyl
EtOAc	Ethyl Acetate
EtOH	Ethanol
FDA	Food and Drug Administration

FFUP	Faculdade de Farmácia da Universidade do Porto
FHT	Flavanone 3 β -Hydroxylase
FLS	Flavonol Synthase
FNS I	Flavone Synthase I
FTIR	Fourier Transform Infrared Spectroscopy
GI₅₀	Concentration of Compound that Inhibited 50% of the net cell growth
GDP	Guanosine Diphosphate
GTP	Guanosine Triphosphate
HMBC	Heteronuclear Multiple Bond Correlation
HPLC	High Performance Liquid Chromatography
HPLC-DAD	High Performance Liquid Chromatography with Diode Array Detector
HSQC	Heteronuclear Single Quantum Coherence
HTS	High-Throughput Screening
IC₅₀	Concentration of Compound that causes 50% growth inhibition
ILs	Ionic Liquids
IR	Infrared spectroscopy
KOH	Potassium Hydroxyde
LC	Liquid Chromatography
LQOF	Laboratório de Química Orgânica e Farmacêutica
m	multiplet
MAOS	Microwave-Assisted Organic Synthesis
Mp	Melting point
MW	Microwave
MRP	Multidrug Resistance Protein
MT	Microtubule
MTAs	Microtubule-Targeting Agents
NCI	National Cancer Institute
PAL	Phenylalanine Ammonia Lyase
PDB	Protein Databank
PEG	Polyethylene Glycol
Pgp	P-glycoprotein

PKs	Protein-Kinases
q	Quadruplet
Rt	Retention time
r.t	room temperature
RMSD	Root-Mean-Square Deviation
s	singlet
SAC	Spindle Assembly Checkpoint
SAR	Structure - Activity Relationship
STAT3	Signal Transducer and Activator of Transcription 3
SPOS	Solid Phase Organic Synthesis
t	triplet
THF	Tetrahydrofuran
TiO₂-SO₄²⁻	Sulfated titania
TLC	Thin Layer Chromatography
TNF	Tumor Necrosis Factor
TPCD	Tetrakis(pyridine)cobalt(I) Dichromate
WHO	World Health Organization
4CL	4-Coumarate: Coenzyme A Ligase
ΔΨ_m	Variation of the membrane potential
δ	Chemical shift
δ_c	Carbon chemical shift
δ_H	Proton chemical shift
ν	Wavenumber (cm ⁻¹)

Outline of the Dissertation

The present dissertation is structured in five chapters:

Chapter 1- INTRODUCTION

The first chapter is a focused review about cancer and mitosis, namely, antimetabolic agents. A brief review concerning chalcones, including synthesis as well as the biological activities described for this group of compounds, particularly their antitumor activity, is described in the second chapter. The aims of this dissertation are presented at the end of this subchapter.

Chapter 2- RESULTS AND DISCUSSION

The second chapter focus on the results and discussion of the developed research work, being sub-divided into five subchapters, which deal with the discussion of the results obtained concerning the synthesis, determination of the peak purity, biological activity and docking studies.

Chapter 3- CONCLUSION

The third chapter focus on the main conclusions and future work.

Chapter 4- EXPERIMENTAL SECTION

The fourth chapter refer the synthetic procedures adopted for the synthesis of chalcone derivatives. A reference to the procedure used for the evaluation of peak purity, biological activity and docking studies is also presented in this chapter.

Chapter 5- REFERENCES

Herein is presented a list of the references as well as the browsers used in this dissertation.

Chapter 1:

Introduction

1.1. Cancer and Mitosis

Cancer is the leading cause of mortality worldwide (1). According to the WHO report in 2012 approximately 3.7 million new cases of cancer were diagnosed being estimated that the number will increase 25% by 2030, to reach 4.6 million (2-3).

Cancer is a multifactorial heterogeneous disease that is associated with progressive and uncontrolled cell proliferation involving three distinct stages. Initiation, in which the mutation of a single cell occurs, promotion which is the proliferation of cell giving rise to a large number of daughter cells, containing the mutation created by the initiator, and progression in which the additional mutations result in malignancy (4).

Unrestricted growth is one of the hallmarks of tumor cells that distinguish them from normal cells, therefore tumor cells grow and divide themselves in order to increase malignant tissue, and eventually invade nearby parts of the body (5).

Mitosis represents a vulnerable phase of tumor existence and a main target for anticancer intervention. This is a complex and highly regulated event of the cell cycle (**Figure 1**) during which identical copies of the genome are moved to the two poles of a mitotic spindle giving rise to nuclei of the resulting daughter cells (6-8). Mitosis proceeds in five phases: prophase, prometaphase, metaphase, anaphase, and telophase (9) (**Figure 2**).

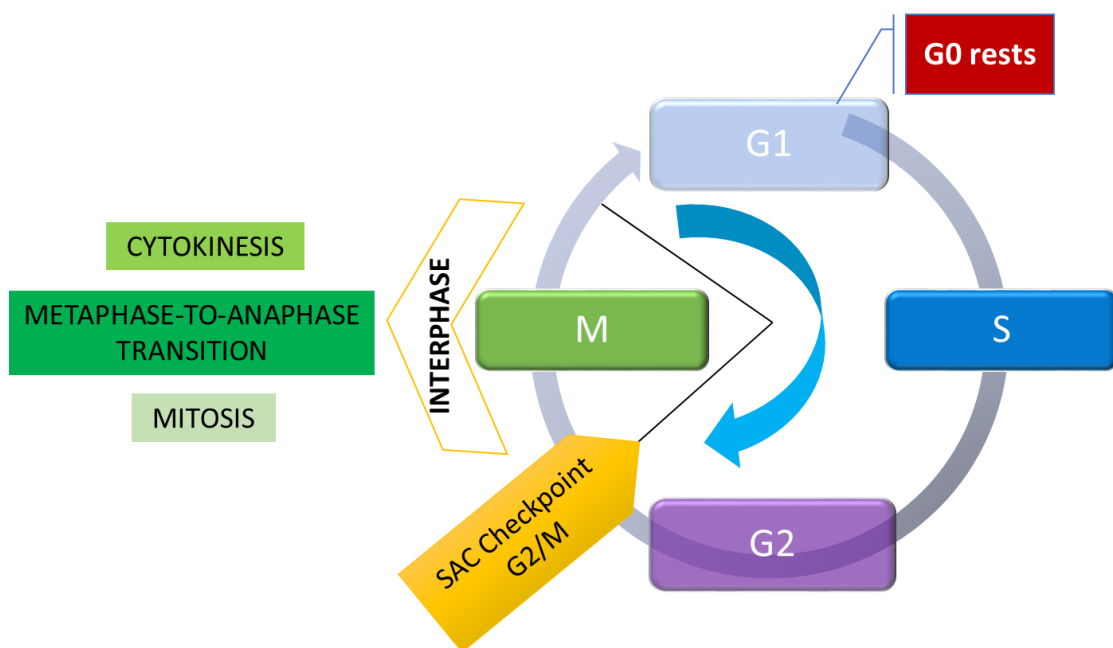


Figure 1: Event of cell cycle. Phases S (synthesis) and M (mitosis) are usually separated by two gap phases, G1 (gap 1) between M and S and G2 (gap 2) between S and M (gap 3). The three gaps provide time for the cell to monitor the internal and external environment to ensure that conditions are suitable and preparations are

complete before the cell entry to S phase and mitosis. The G₀ is a period in which cells exist in a quiescent state. G₀ phase is viewed as either an extended G₁ phase, where the cell is neither dividing nor preparing to divide, or a distinct quiescent stage that occurs outside of the cell cycle. Between G₂ and M phase there is a spindle assembly checkpoint (SAC), SAC check for chromosome attachment to spindle. Accordingly, the eucariotic cell cycle is divided into four sequential phases: G₁, S, G₂ and M (10).

In the prophase the chromatids condense and are released into the cytoplasm by nuclear envelope breakdown, which marks the transition into prometaphase and also represents the first irreversible transition into mitosis. During prometaphase, the initially unattached chromatids make connections to the microtubules (MTs) of the mitotic spindle and the mitotic checkpoint is active. At metaphase, every chromosome has made proper attachments to the mitotic spindle and has congressed to a central position. The next phase is anaphase, where chromatids are splitted and migrate to the spindle poles. Then in telophase, the now segregated chromosomes decondense and the nuclear envelope is formed. After telophase a septum between both daughter cells is formed (cytokinesis) (9, 11-14) (**Figure 2**).

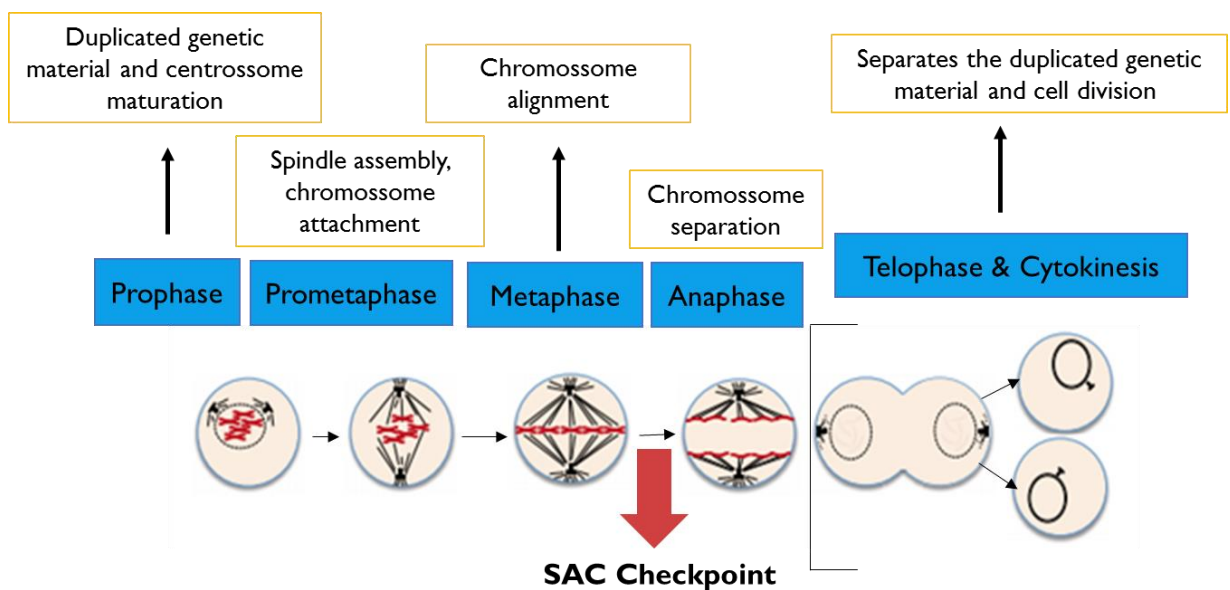


Figure 2: Representation of mitosis phases (adapted from (9)).

1.1.1 Microtubule dynamics crucial to mitosis

Microtubules are constituents of the intracellular cytoskeleton framework, being essential for many cellular functions in all eukaryotic cells, including tumor cells. They are important to cell division and mitosis, motility and cell-cell contacts, maintenance of cell shape, transport of vesicles, mitochondria and other components and cell signaling (12).

Microtubules are structures of about 25 nm diameter with the appearance of hollow tubes formed by 10–16 protofilaments (the most common being 13) (7). The basic polypeptidic component of microtubules is a heterodimer of α and β tubulin, which stands for a globular protein, that polymerizes to develop the protofilaments, which are in turn formed by longitudinal associates between α,β tubulin dimers (**Figure 3**) (7, 15). This tubulin heterodimers have two nucleotide binding sites, named N-site, for non-exchangeable, on the α subunit, always occupied by GTP, and E-site, for exchangeable, on the β subunit, which may have guanosine triphosphate (GTP) or guanosine diphosphate (GDP-P_i) linked when tubulin is in the heterodimeric form (**Figure 3**) (7, 15-16).

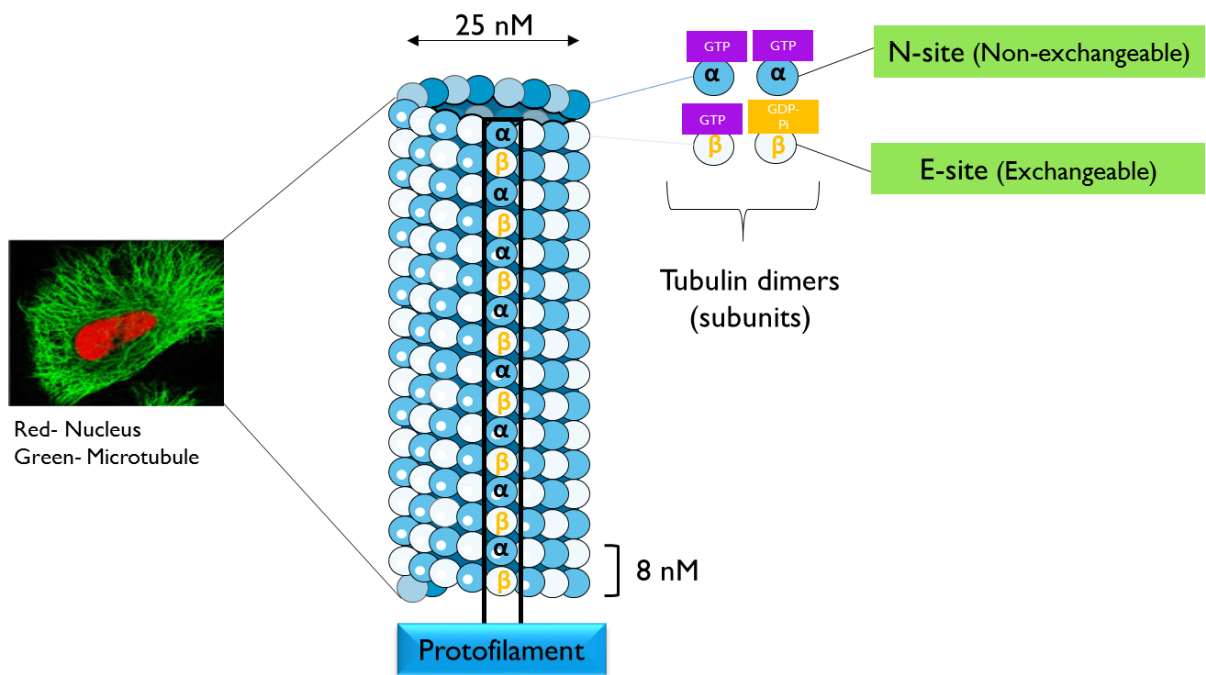


Figure 3: Structures of tubulin dimer and microtubule. Representation of nucleotide binding site on α and β tubulin with the presence of GDP and GTP, with corresponding sites N-site (non-exchangeable) and E-site (Exchangeable).

Microtubules can be considered as dynamic structures because they are in continuous assembly (microtubule stabilization) and disassembly (microtubule disruption), being microtubule dynamics fundamental for their physiological role.

The dynamic of polymerization of microtubules occurs by a nucleation-elongation mechanism by the reversible, non-covalent addition of α - and β -tubulin dimers at both ends of microtubules (**Figure 4**) (17-18). This polymerization of α,β -tubulin heterodimers results in an inherent heterogeneity between the two ends of the microtubule, designated as (-), minus or negative, with less dynamic and (+), positive or plus end, with more dynamic (**Figure 4**) The negative end with exposed α -tubulin are anchored at the organizing center while the positive end with exposed β -tubulin are disposed to the cell periphery (15, 17, 19).

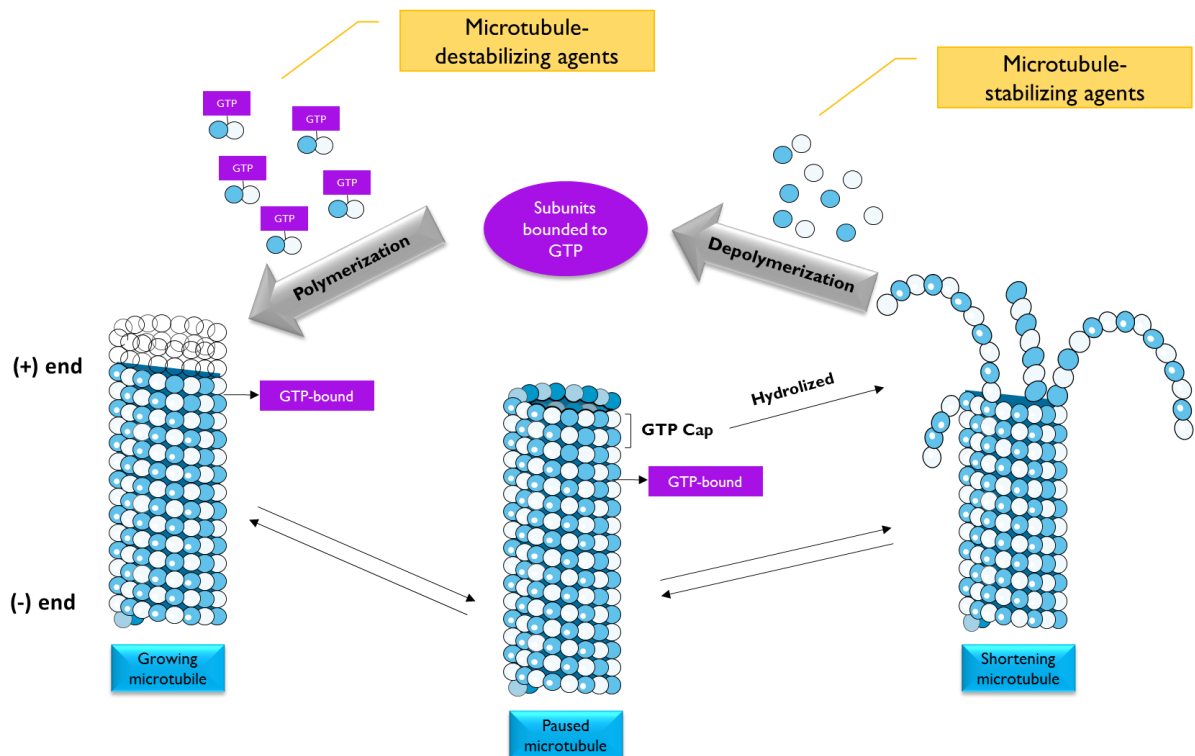


Figure 4: Microtubule polymerization and depolymerization dynamics. Heterodimers of α - and β -tubulin assemble to form a short microtubule nucleus. Nucleation is followed by elongation of the microtubule at both ends to form a cylinder that is composed of tubulin heterodimers arranged head-to-tail in 13 protofilaments. Each microtubule has a so-called plus (+) end, with β -tubulin facing the solvent, and a minus end (-), with α -tubulin facing the solvent.

Microtubules show complex polymerization dynamics that use energy provided by the hydrolysis of GTP at the time that tubulin with bound GTP is added to the microtubule ends. These dynamics are crucial to their cellular functions. During the association of α,β - tubulin heterodimer to the ends of microtubules, GTP in β -tubulin is hydrolyzed to GDP and resulting GDP in β -tubulin is unable to exchange. When the microtubule depolymerizes, the α,β -tubulin heterodimers are released and the GDP in β -tubulin is now able to exchange to GTP (**Figure 4**) (16, 19).

1.1.2 Antimitotic Agents (MTAs)

Among the current anticancer agents, chemotherapeutic approaches that make use of microtubule-targeting agents (MTAs), also known as antimitotic agents, have been used with a considerable scale of success in a wide range of tumor types (19). These MTAs affects the microtubule dynamics and thereby microtubule functions, leading to the disruption of the mitotic spindle function and blocking cell cycle progression at the transition from prometaphase/metaphase to anaphase. The activation of the SAC and microtubule dynamics induce prolonged mitotic arrest that eventually leads to cell death. This mitotic arrest is the major action of the distinct MTAs (9).

The majority of the antimitotic drugs are derived from naturally occurring compounds and according to their mechanism of action these drugs can be divided into distinct groups. MTAs either inhibit microtubule polymerization, destabilizing microtubules and decreasing microtubule polymer mass, or promote microtubule polymerization, stabilizing microtubules and increasing the polymer mass. The former group is commonly known as microtubule destabilizers or inhibitors and the last one is known as microtubule stabilizers. Nevertheless, at low but clinically relevant concentrations, both microtubule-stabilizing and -destabilizing drugs potently suppress microtubule dynamics without affecting microtubule polymer mass. Therefore, the primary action of both classes of drugs is the suppression of spindle-microtubule dynamics with no modifications to microtubule mass, being this latter effect greatly important for their therapeutic effect (20). In addition to the microtubule destabilizers and stabilizers, MTAs drugs with a mixed mechanism are also known (**Figure 5**) (15).

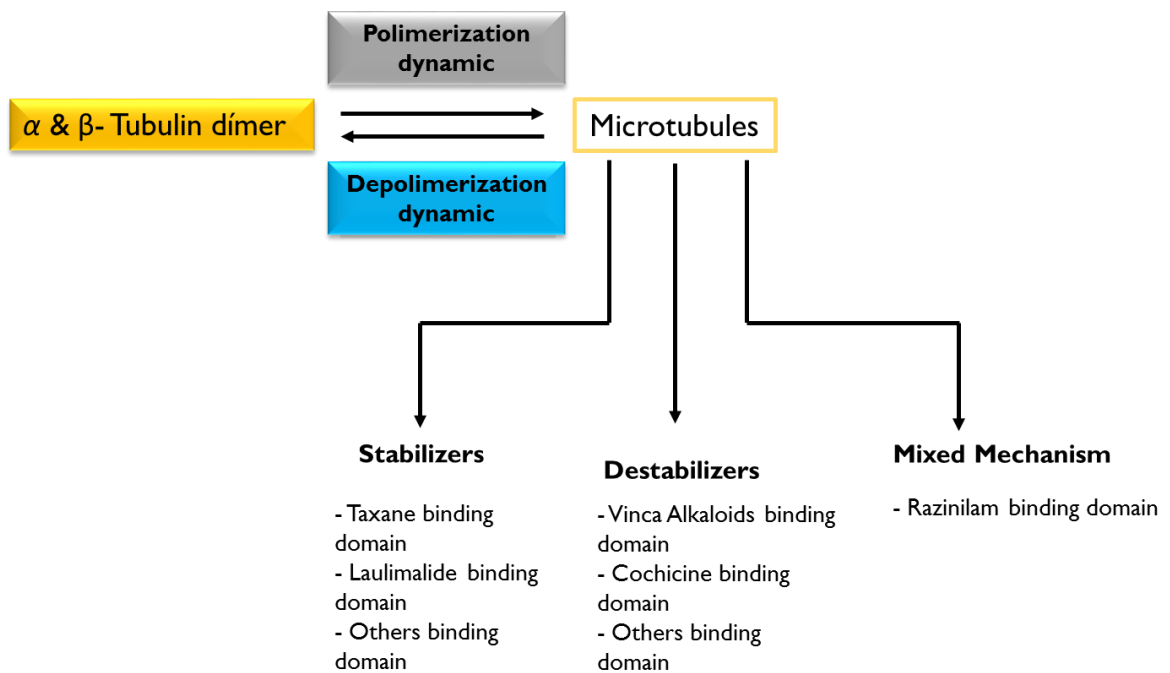


Figure 5: Different types of antimetabolic agents.

Most of the antimetabolic agents act by targeting three different sites on the tubulin heterodimer: the colchicine, the vinca alkaloid and the taxane binding sites. In addition to these three well characterized drug-binding sites, other binding sites are also known, namely the laulimalides binding site on β -tubulin (**Figure 6**) (19-20).

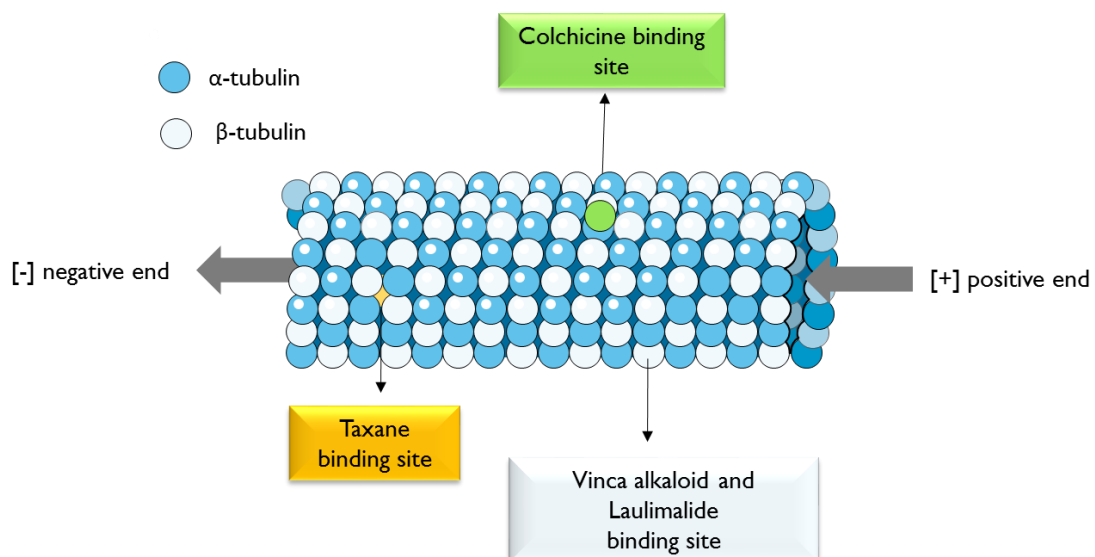


Figure 6: Illustration of tubulin binding sites.

The vinca binding domain is located at the plus end interface on the exchangeable GTP binding site in β -tubulin. The taxanes binding site is located within the lumen of the

microtubule, in a deep hydrophobic pocket at the lateral interface between adjacent protofilaments. However, the colchicine site is situated at the intra-dimer interface between β -tubulin and α -tubulin (21).

Most microtubule destabilizers bind to either the vinca domain or colchicine domain. On the opposite, agents that target the taxanes binding domain are known to act as microtubule stabilizers (6, 15). Lastly, antimetabolic agents with a mixed mechanism such as the alkaloid rhaznilam (20) target the rhaznilam domain, inhibiting the microtubule assembly. This MTA neither exactly behaves with tubulins as vinca alkaloids nor as taxanes

The interaction of chemotherapeutic agents that stabilize or destabilize microtubules results in suppression of microtubule dynamics that leads to damage of the mitotic spindle or to massive microtubule damage depending on drug concentration and time of exposure. These actions trigger apoptosis by inducing cell-cycle arrest at the G2–M phase or a general failure in microtubule-related functions depending on the level of microtubule damage. These effects, together with the abnormal exit of mitosis, lead to multinucleated cells and eventually to cell death, which are the major mechanisms involved in MTAs-induced apoptosis (Figure 7) (22).

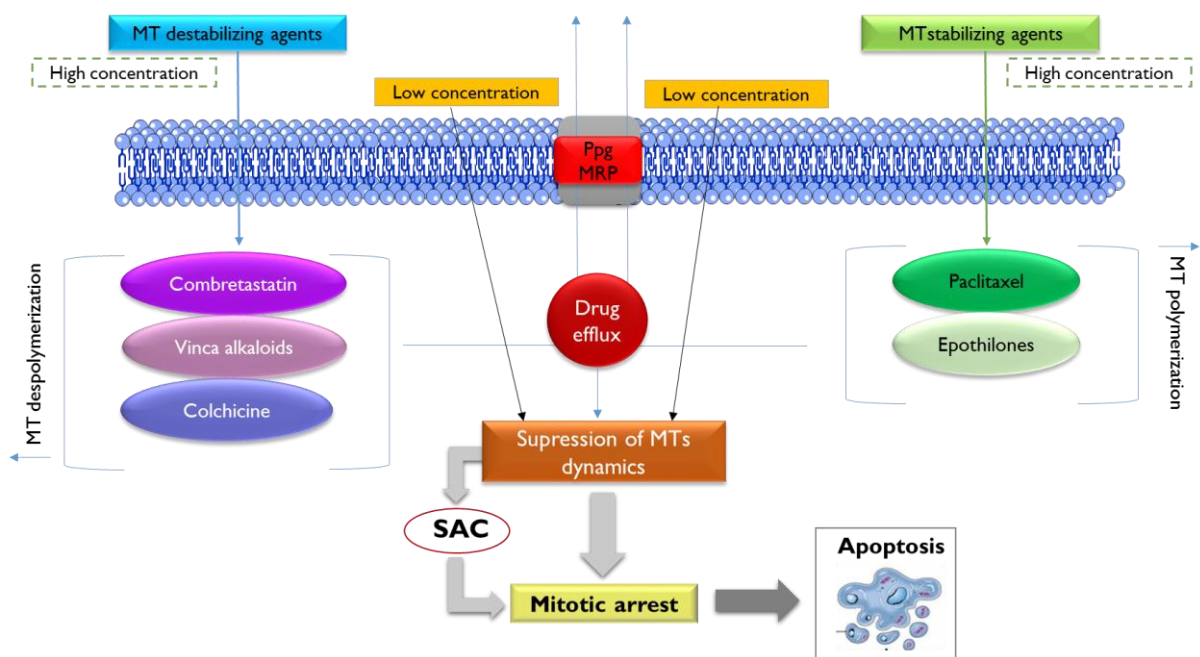


Figure 7: Schematic diagram of putative events involved in MTAs-induced apoptosis (adapted from (22)).

1.1.2.1 Microtubule Stabilizing Natural Products

1.1.2.1.1 Stabilizers binding Taxane binding domain

Paclitaxel (**1**, **Table 1**), a natural product isolated from the *Taxus brevifolia* (Pacific Yew) is one of the most promising compounds known to kill cancer cells by stabilizing the microtubule polymerization. It has been discovered as part of a broad screening program for natural products in the 1960s by the National Cancer Institute (NCI) in the USA. Paclitaxel (**1**, **Table 1**) has a complex structure consisting of a 14-membered taxane ring system connected to an oxetan ring and an amide side chain (12).

Unlike the antimitotic agents described up to that time, paclitaxel has shown to act by promoting the formation of unusually stable microtubules, instead of inhibiting the microtubules polymerization like vinca alkaloids (6, 11-12, 22).

The binding of microtubules with paclitaxel make them much more stabilized than without this taxane. Paclitaxel binds into a pocket in the second globular domain of β -tubulin facing the central role in a microtubule. These inhibits microtubule depolymerization by binding to β -tubulin, resulting in mitotic arrest and promotes microtubule stabilization by inducing conformational changes of β -tubulin that result in more stable lateral interactions between adjacent protofilaments.

Incubation of cells with high concentrations (≥ 200 nM) of paclitaxel stabilizes extensively microtubule polymerization. It was found that the binding of a very small number of paclitaxel molecules powerfully stabilizes the dynamics of the microtubules without increasing microtubule polymerization. Paclitaxel bind to GDP-bound β -tubulins and change their conformation to stabilize β -tubulins conformation to GTP-bound structures. (11, 15).

The high concentrations (≥ 200 nM) of paclitaxel leads to the formation of stable bundles of microtubules that disrupt the normal polymerization/depolymerization cycle of microtubules and thereby suppresses microtubule dynamics, resulting in the arrest of cells in mitosis. On the other hand, low concentrations of paclitaxel (≤ 20 nM) induce mitotic block without microtubule bundle formation. In both cases, the mitotic arrest in paclitaxel-treated cells leads to apoptosis (11).

Paclitaxel-induced apoptosis can occur either directly after a mitotic arrest or following an aberrant mitotic exit into a G1-like multinucleate state (11).

After the discovery of paclitaxel, other microtubule stabilizers that compete with paclitaxel for the same binding site were discovered, including the epothilones A (**2**) and B (**3**). Nevertheless, other microtubule stabilizers were also found targeting different microtubules

binding sites, such as laulimalide (4), peloruside (5) and discodermolide (6) (Table 1). (8, 11, 13, 15).

1.1.2.2. Microtubule Destabilizing Natural Products

1.1.2.2.1. Microtubule Inhibitors binding at Vinca binding domain

Vincristine and vinblastine (7, 8, Table 1) are alkaloids isolated from the extracts of the leaves of *Catharanthus roseus* in 1958 (12, 23). These natural products as well as their semisynthetic derivatives like vindesine (9), vinorelbine, and vinflunine are antimitotic drugs that have been successfully used in the treatment of cancer (15).

Despite substantial differences among the vinca alkaloids regarding their biological actions, the tubulin binding of these agents is similar. Compounds that bind to the vinca domain usually function as rapid, reversible and temperature independent inhibitors of tubulin assembly. Vinca alkaloids bind to β -tubulin close to the GTP - binding sites (the vinca domain) at the β - α -tubulin heterodimers interface. Binding at the vinca domain prevents curved tubulin from straightening and, in turn, interferes with growth and assembly of microtubules. As the microtubule is a dynamic protein, constantly polymerizing and depolymerizing, these structure poisoned dimers could easily be incorporated into the microtubule polymer, preventing further growth. The incorporation of the vinca alkaloids onto the heterodimer is rapidly reversible, and appears to occur at two sites per tubulin dimer (11-12).

Both high affinity and low-affinity binding sites have been identified. The binding of vinca alkaloids to the high-affinity sites located at the ends of microtubules results in the sub stoichiometric disruption of microtubules. Thus, low concentrations of vinca alkaloids modify the microtubule dynamics at the ends of microtubules, especially those involved in the mitotic spindle, which accelerates microtubule disassembly. This effect on mitotic spindle is usually not accompanied by gross microtubule disorganization. At higher concentrations, vinca alkaloids are able to bind in addition to low-affinity binding sites along the walls of microtubules leading to their disruption and disorganization (11).

According to Noble et al the mitotic-blocking action of low concentrations of vinca alkaloid agent in living cancer cells is due to the suppression of microtubule dynamics rather than microtubule depolymerization (23). Tubulin and microtubules are the main targets of the vinca alkaloids, which depolymerize microtubules and destroy mitotic spindles at the high concentrations, therefore leaving the dividing cancer cells blocked in mitosis with condensed chromosomes (20, 23).

In addition to vinca alkaloids, a large number of compounds bind to vinca binding domain, including the vinblastine (7), vincristine (8), vindesine (9), noscapine (10), cryptophycins (11), phomopsin A (12), and dolastatins 10 (13) and 15 (14) (Table 1) (8, 11-12).

1.1.2.2. Microtubule Inhibitors binding Colchicine binding

domain

Colchicine (15, Table 1), an alkaloid isolated from *Colchicum autumnale*, was the first drug known to bind to tubulin. The structure of this alkaloid comprises three hexameric rings, A-B-C (15, Table 1). In 2009, U.S.A. Food and Drug Administration (FDA) approved colchicine as a monotherapy drug to treat familial mediterranean fever and acute gout flares (24).

Despite lack of clinical success, colchicine has been extensively studied for its mode of action and can effectively inhibit mitosis (11). Tubulin-colchicine binding is slow, strongly temperature-dependent, and practically irreversible. The colchicine binding site is located at the interface of the α - β -tubulin heterodimer, adjacent to the GTP binding site of α -tubulin. Colchicine binds to soluble tubulin leading to the formation of α tubulin-colchicine complex. It is known to bind to the unpolymerized tubulin subunits in a two-step reaction process that begins with the formation of an initial pre-equilibrium complex, which is reversible and bound with low affinity. This is followed by slow conformational changes in tubulin resulting in the formation of a poorly reversible final-state tubulin-colchicine complex. This conformational change in tubulin heterodimers, followed by addition of the colchicine-tubulin complex and soluble tubulin molecules at the ends of microtubules, is responsible for the suppressed assembly dynamics of microtubule ends (18, 22).

The interaction of colchicine with tubulin is attributable to the simultaneous binding of its trimethoxyphenyl A and 2-methoxytropone C rings, whereas the middle connecting B ring is involved in the peculiar binding kinetics characteristic of the colchicine-tubulin interaction (11). It has been considered that the trimethoxyphenyl unit of ring A is essentially required to bind with tubulin, while the B ring of colchicine along with C7 side chain mainly controls kinetics of colchicine-tubulin binding (15).

As with vinca alkaloids, colchicine inhibits microtubule formation by binding to the α , β dimer at lower concentrations and also depolymerization microtubules at higher concentrations (8, 11, 18).

So, despite the differences between the effects at high concentrations of the vinca/colchicine-like drugs and the taxane-like drugs, almost all of the microtubule-targeted antimetabolic drugs stabilize microtubule dynamics at their lowest effective concentrations.

In addition to colchicine, several natural products that bind in the colchicine domain and disrupt microtubule assembly *in vitro* and *in vivo* are known, such as podophyllotoxin (**16**), 2-methoxyestradiol (**17**), combretastatin A4 (CA4) (**18**) and CA4P (**19**) (**Table 1**) (8, 12, 15) Among those, natural combretastatins have proved to be one of the most promising antimetabolic agents.

Combretastatins (**Figure 8**) are stilbenoid phenols structurally diverse isolated from *Combretum caffrum*. This group of natural products are currently divided into four major groups on the basis of their structural characteristics. These include the A-series (*cis*-stilbenes), B-series (diaryl-ethylenes), C-series (quinone), and D-series (macrocyclic lactones). Among combretastatins, the *cis*-stilbene CA4 is the most potent naturally occurring combretastatin, showing a remarkable antimetabolic activity (7, 25-26).

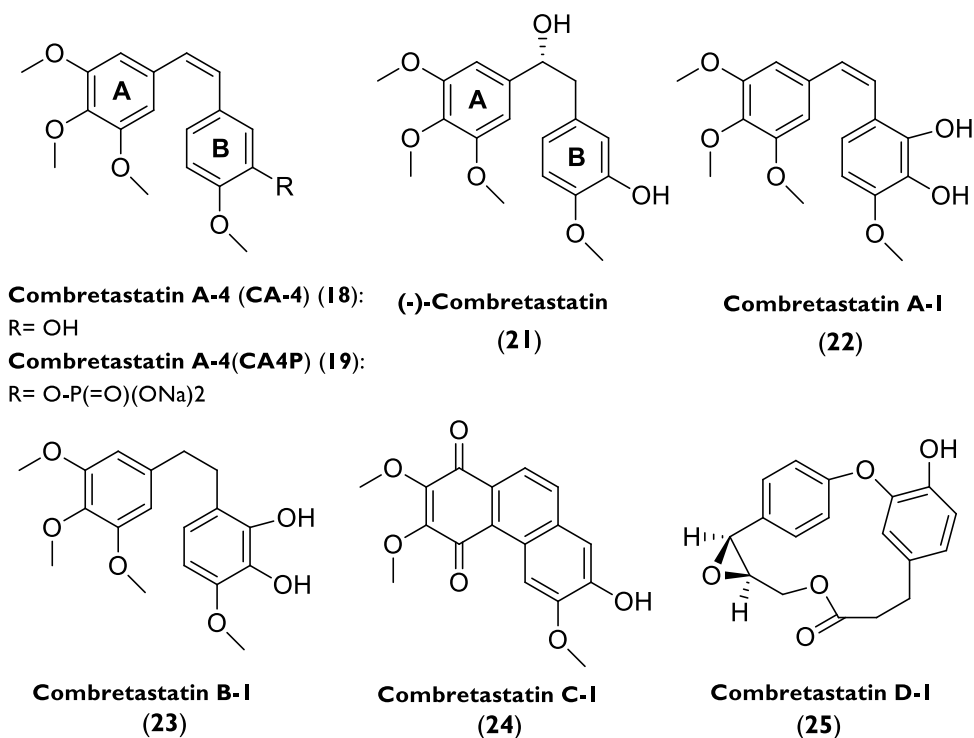


Figure 8: Structure of (-)-combretastatin and combretastatins A, B, C and D.

The antimetabolic effects of CA4 are due to inhibition of the function of microtubules, but this compound is not only considered an antimetabolic agent, but also exhibits antivasular and anti-angiogenic effects. In fact, the interference of CA4 in tubulin/microtubule polymerization dynamics has two main anticancer effects. It inhibits cancer cell proliferation through disturbance of mitotic spindle function, leading to cell apoptosis. In addition, it disrupts cell signaling pathways involved in regulating and maintaining the cytoskeleton of endothelial cells in tumor vasculature, leading to selective blockage of the blood flow through tumors. Whilst CA4 is a powerful antimetabolic compound, its dominant mode of action in tumor growth inhibition probably results from vasculature halt (27-28).

Nevertheless, due to poor solubility in aqueous media of CA4 the preparation of more soluble derivatives was required for intravenous administration, namely its disodium phosphate CA4P and the amino acid hydrochloride salt CA4P, a pro-drug which is soluble in saline solutions, but when cleaved by non-specific phosphatases yields CA4. This prodrug is currently being evaluated in phase II/III clinical trials as cytotoxic agent (15, 21, 24, 27).

In addition, the activity of CA4 is hampered by a short biological half-life and isomerization of the active *cis*-olefinic conformation into the corresponding inactive *trans* analogs under the influence of heat, light, and protic media. It could therefore be hypothesized that analogs that retain the potency and efficacy of CA4, but that have a different pharmacokinetic profile might be useful. To overcome these problems, new analogs of CA4 have been synthesized and developed in the recent years allowing the establishment of some structure activity relationships (SAR) considerations (24).

SAR studies on new analogs of CA4 have been directed at the effect of structural modifications on different parts of the molecule on the cytotoxicity, inhibition of microtubule polymerization and inhibition of the binding of colchicine to tubulin. The modifications described in the literature include: **i**) substituents on ring A; **ii**) substituents on ring B (hydroxy, alkoxy or other related substitutions). Among these modifications, the most important for mitotic activity is related to the substitution pattern of ring A (7).

It was considered that the presence of three methoxy groups at positions 3, 4 and 5 of A ring in all analogues was crucial to the interaction with tubulin. In fact, the replacement of these methoxy with ethoxy groups or the exchange of their position reduced the cytotoxicity of the CA4 analogues. Moreover, Luduena and Roach (29) explored several compounds possessing 3,4,5-trimethoxyphenyl moiety (3,4,5-trimethoxybenzaldehyde, 3,4,5-trimethoxybenzyl alcohol) for binding with tubulin. It was found that these compounds inhibit the binding of colchicine to tubulin and it was concluded that these units bind with tubulin at colchicine binding site, like CA4, colchicine and podophylotoxin (15, 29).

Table I: Examples of MTAs.

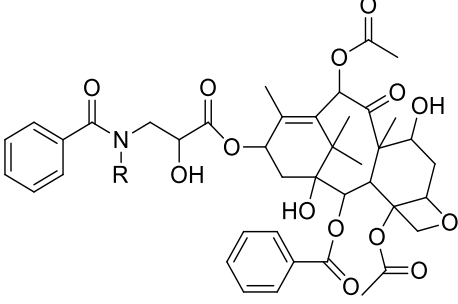
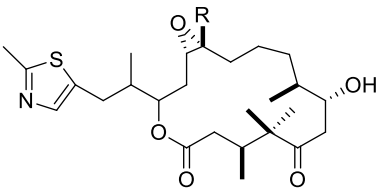
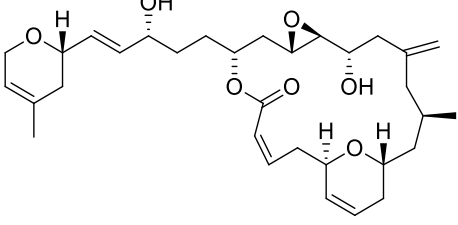
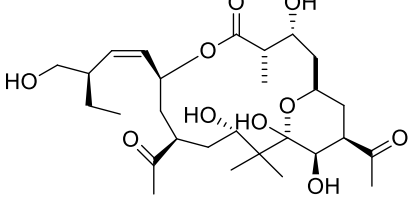
Compound	Microtubule binding site	Therapeutic application/ Clinical stage	Ref
Microtubule Stabilizers			
 <p>Paclitaxel (taxol®) (1)</p>	<p>Taxane binding domain</p>	<p>Ovarian, breast, lung bladder, prostate, melanoma, esophageal and other types of solid tumor cancers</p> <p>Clinical use</p>	<p>(11-12, 30)</p>
 <p>Epothilone A (2): R=H Epothilone B (3): R=OCH₃</p>	<p>Taxane binding domain</p>	<p>Breast, ovarian, prostate, lung, kidney, colorectal tumors.</p> <p>Refractory solid tumors</p> <p>Glioblastoma</p> <p>Epothilone analogue (Ixabepilone) in clinical use</p>	<p>(6, 18, 22, 30)</p>
 <p>Laulimalide (4)</p>	<p>Laulimalide binding domain</p>	<p>Lung and breast tumor</p> <p>Pre-clinical</p>	<p>(31-34)</p>
 <p>Peloruside (5)</p>	<p>Laulimalide binding domain</p>	<p>Lung and breast tumor</p>	<p>(20, 30)</p>

Table I: Examples of MTAs (*continued*).

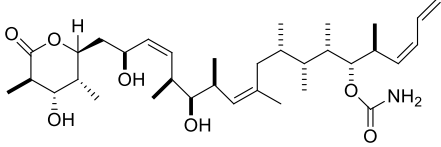
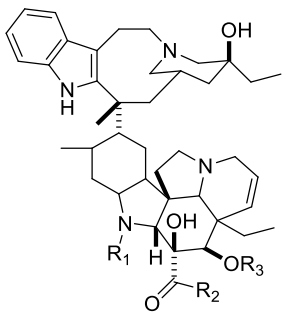
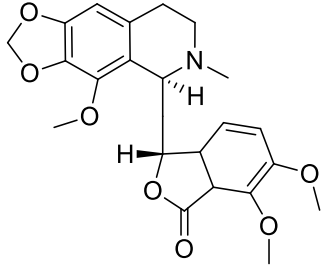
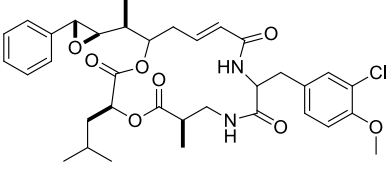
Compound	Microtubule binding site	Therapeutic application/ Clinical stage	Ref
Microtubule Stabilizers			
 <p style="text-align: center;">Discodermolide (6)</p>	Taxane binding domain	Breast tumor Phase I	(8, 35-36)
Microtubule Destabilizers			
 <p>Vinblastine (7): R₁=OCH₃; R₂=OCH₃; R₃= COOCH₃</p> <p>Vincristine (8): R₁=CHO; R₂=OCH₃; R₃=COOCH₃</p> <p>Vindesine (9): R₁=CH₃; R₂=NH₂; R₃=H</p>	Vinca binding domain	<p>Vinblastine- Hodgkin's lymphoma, testicular germ cell cancer.</p> <p>Vindesine - Leukemia and lung cancer.</p> <p>Vincristine- Non-Hodgkin's lymphoma, acute lymphoblastic leukemia, childhood leukemia.</p> <p style="text-align: center;">Clinical use</p>	(11-12, 17, 21)
 <p style="text-align: center;">Noscapine (10)</p>	Other binding domain	<p>-Treatment of multiple myeloma;</p> <p>- Non-Hodgkin's lymphoma (chronic lymphocytic leukemia)</p> <p style="text-align: center;">Phase I and II</p>	(12, 15, 18)
 <p style="text-align: center;">Cryptophycin I(11)</p>	Vinca binding domain	-Solid tumors Phase III	(11, 17-18)

Table I: Examples of MTAs (continued).

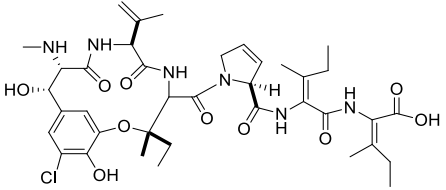
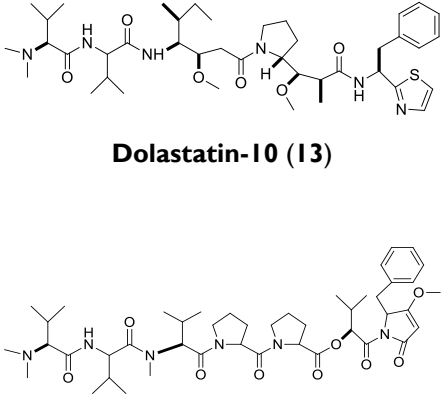
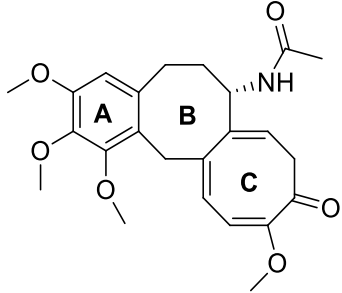
Compounds	Microtubule binding site	Therapeutic application/ Clinical stage	Ref
Microtubules Destabilizers			
 <p style="text-align: center;">Phomopsin A (12)</p>	Vinca binding domain	-Liver disease	(15)
 <p style="text-align: center;">Dolastatin-10 (13)</p> <p style="text-align: center;">Dolastatin-15 (14)</p>	Vinca binding domain	- Advanced colorectal cancer - Breast, kidney and prostate cancer Phase II	(6, 11, 15, 18, 21)
 <p style="text-align: center;">Colchicine (15)</p>	Colchicine binding domain	- Treatment for gout Clinical use	(11-12, 30)

Table I: Examples of MTAs (continued).

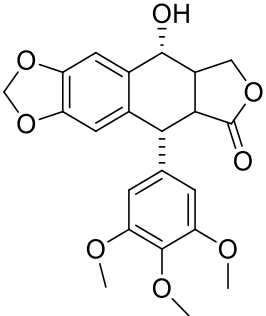
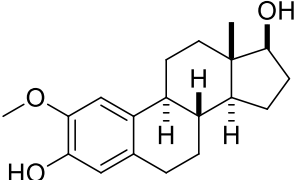
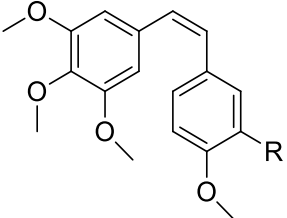
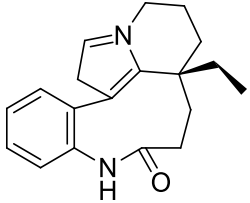
Compounds	Microtubule binding site	Therapeutic application/ Clinical stage	Ref
Microtubule Destabilizers			
 <p>Podophyllotoxin (16)</p>	Colchicine binding domain	<p>-Topical solution for the treatment of anogenital warts (external genital warts and perianal warts)</p> <p>In clinical use– topical application</p>	(6, 11, 15, 30)
 <p>2-Methoxyestradiol (17)</p>	Cochicine binding domain	<p>- Breast cancer</p> <p>Phase II completed (ovarian and prostate cancer)</p> <p>Phase I (Nanoparticles-prostate and solid malignancies)</p>	(13, 20)
 <p>Combretastatin A4 (CA4) (18): R= OH</p> <p>Combretastatin A4P (CA4P) (19): R=O-P(=O)(ONa)₂</p>	Colchicine binding site	<p>Combretastatin phosphate for the treatment of acute myelogenous leukemia.</p> <p>Thyroid, advanced solid tumors, non-small lung cancer</p> <p>Phase II/III</p>	(18)

Table 1: Examples of MTAs (*continued*).

Compounds	Microtubule binding site	Therapeutic application/ Clinical stage	Ref
Mixed Mechanism			
 <p data-bbox="375 898 571 931">Rhazinilam (20)</p>	Other binding domain	Treatment for breast carcinoma.	(8, 15, 32, 37)

1.1. Flavonoids

The flavonoids represent a large group of plant secondary metabolites possessing a variety of biological activities (1, 38).

Their structure comprises a fifteen-carbon atom phenylpropanoid core, along with two phenyl rings (A and B rings) joined by a three carbon atoms chain. Together they can be represented as C6–C3–C6. Flavonoids can be divided into numerous sub-classes according to the presence (or nonexistence) of a third ring (C ring), a double bond between carbon atoms 2 and 3, a carbonyl group on C-4, and hydroxyl group in the C ring (**Figure 9**) (38).

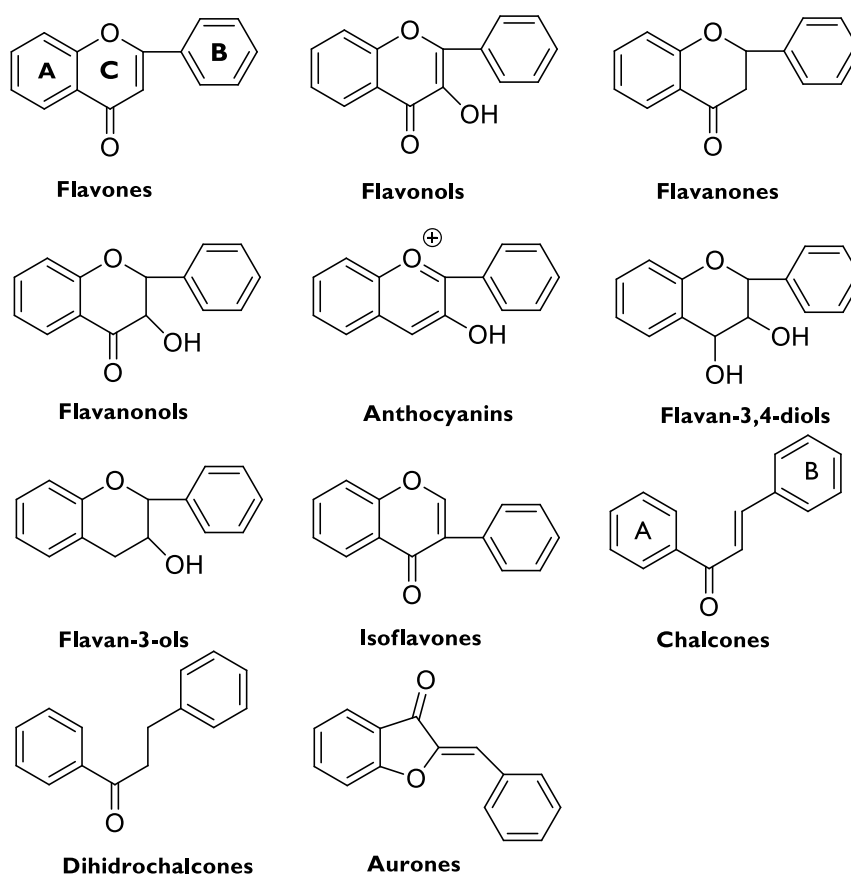


Figure 9: The structure of the flavonoids.

Flavonoids are phytochemicals that exist either as free glycones or conjugated glycosides. The core sequence can be extensively modified by rearrangement, alkylation, oxidation and glycosylation (38).

Flavonoids are biosynthesized through of the convergence of two pathways, the acetate-malonate and shikimate pathways, which give rise to the A and B rings, respectively being chalcones considered as the precursors of all flavonoids (**Figure 10**) (38-39).

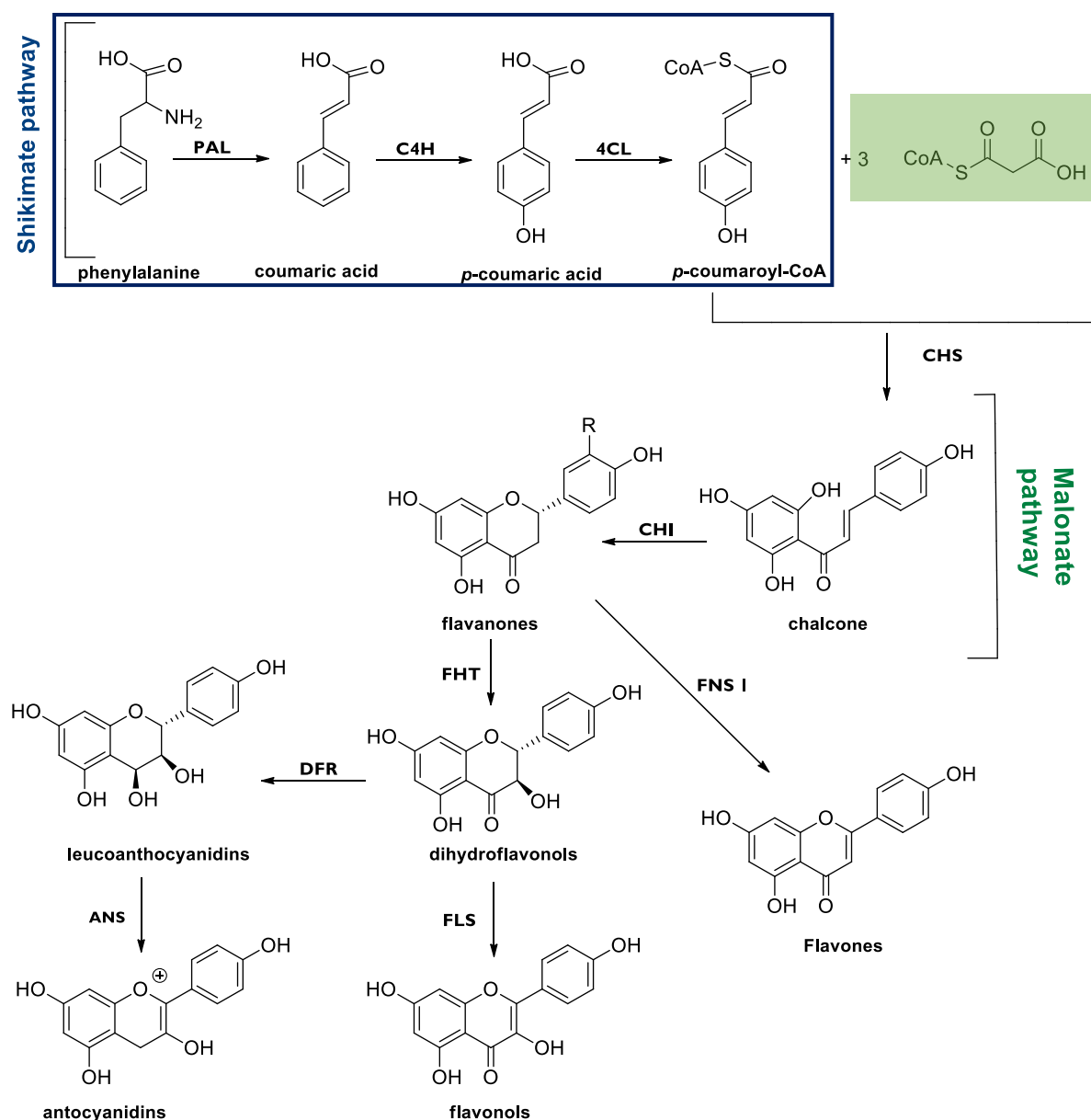


Figure 10: Schematic representation of the major branch pathways of flavonoid biosynthesis. Enzyme names are abbreviated as follows: Phenylalanine ammonia-lyase (PAL), cinnamate-4-hydroxylase (C4H), 4-coumaroyl: CoA-ligase (4CL), chalcone synthase (CHS), chalcone isomerase (CHI), Flavone synthase (FNSI), Flavanone 3 β -hydroxylase (FHT), Flavanone 3 β -hydroxylase (FLS), Dihydroflavonols reductase (DFR), Anthocyanidin synthase (ANS) (Adapted from (38-39)).

In addition to their important physiological function in plants, flavonoids have demonstrated to show significant pharmacological activities, including antioxidant, antitumor, anxiolytic, anti-inflammatory, antiviral, and antiprotozoal activities (1, 38).

The wide range of structural patterns has resulted in flavonoids being recognized as a rich source of compounds with potential anticancer properties. The capability of flavonoids to block the cell cycle, induce apoptosis, disrupt mitotic spindle formation or inhibit angiogenesis makes them into prominent agents in anticancer research (1). In addition, these compounds are reported to interfere with the activity of several molecular targets related to carcinogenesis, such as cyclin-dependent kinases, several protein-tyrosine kinases, aromatase, topoisomerase, or protein kinase C (40).

In recent years, flavonoids and their synthetic analogs have been extremely researched regarding the treatment of ovarian, breast, cervical, pancreatic, and prostate cancer, resulting in the entrance of some flavonoids in late phase of clinical trials for several oncological indications such as quercetin (26), genistein (27) or flavopiridol (28), a synthetic analog of the natural alkaloid rohitukin (Figure 11) (1).

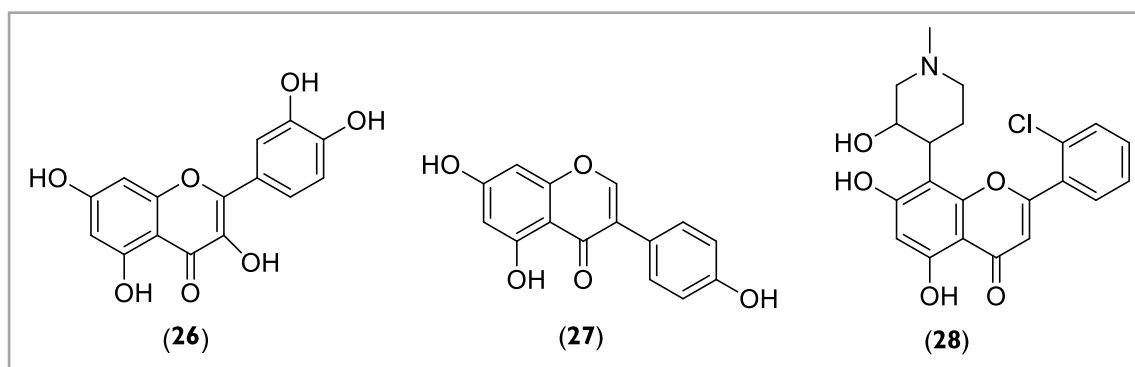


Figure 11: Chemical structure of quercetin (26), genistein (27) and flavopiridol (28).

It has been observed that even a high intake of plant-based dietary flavonoids is safe and not associated with any adverse health effect. In addition, the interaction of dietary flavonoids with the gut has numerous implications for human health and flavonoids in the diet may act as chemopreventive agents against the development of cancer. Apart from their cancer chemopreventive efficacy, such flavonoids could be developed as an alternative medicine to get the beneficial effects in combination treatment by reducing the dose and associated systemic toxicity of chemotherapeutic agents for similar efficacy (40).

1.2.1. Chalcones

Chalcones (1,3-diphenyl-2-propen-1-ones) are open-chain flavonoids in which the two aromatic rings are joined by a three-carbon α,β -unsaturated carbonyl system (41). The $C\alpha$ - $C\beta$ double bond can exist either in the (*E*) or (*Z*) - configuration, being the (*E*)-form the thermodynamically most stable and consequently, the majority of the chalcones are isolated as (*E*) isomers (**Figure 12**) (42).

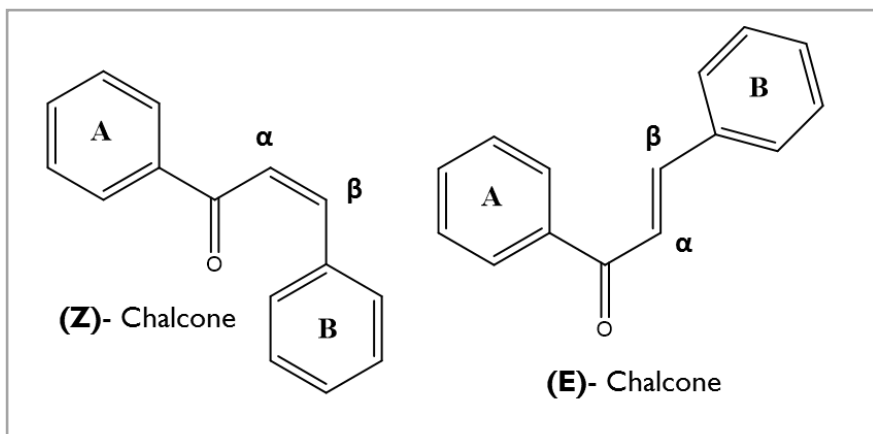


Figure 12: General structure of chalcones.

Chalcones are one of the major classes of natural compounds that are especially abundant in fruits (e.g., citrus, apples), vegetables (e.g., tomatoes, shallots, bean sprouts, potatoes) and various plants and spices (e.g., licorice), many of which have been used for centuries in traditional herbal medicine (41, 43).

The natural high abundance, easy synthesis and diversity of biological activities have attracted great research interest for these class of compounds.

A great number of natural chalcones are polyhydroxylated. Other common substituents include methoxy and prenyl groups. Apart from these features, the synthetically derived chalcones may also contain other substituents such as halogens, alkyl, amino, nitro, nitril, acetamido, and carboxylic groups, among others (41, 43-44).

1.2.1.1. Synthesis of Chalcones

Considering the promising biological activities described for natural chalcones several synthetic methods leading to natural mimic chalcones along with new molecules with different substitution patterns have been extensively reported in the past years. The main methodologies used are summarized in the next sub-sections.

1.2.1.1.1. Aldol Condensation

The Claisen-Schmidt condensation is the method usually used for synthesizing chalcones. In this method chalcones are prepared by condensation of acetophenone and benzaldehyde derivatives resulting in the formation of an α,β -unsaturated ketone moiety (**Figure 13**) (41-42).

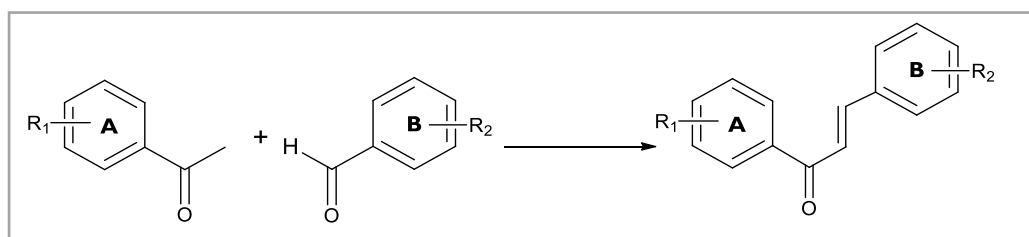


Figure 13: Claisen-Schmidt condensation reaction.

Traditionally these reactions are carried out in the presence of bases under homogeneous conditions, at room temperature or at reflux for several hours, and the benzaldehyde derivative is used in excess (45). The most used catalyst is aqueous methanolic or ethanolic NaOH or KOH, but other bases can be used namely ethanolic sodium ethoxide, and K_2CO_3 . These reactions can also be performed in acidic conditions using HCl, $BF_3 \cdot OEt_2$, B_2O_3 , and *p*-toluenesulfonic acid (42).

Traditional Claisen Schmidt reactions in homogeneous conditions present several hurdles, such as catalyst recovery and waste disposal problem (46-47). Therefore, a growing number of new techniques and procedures have been reported for the synthesis of these compounds namely using solid-phase synthesis (SPOS), heterogeneous catalysis, and acidic ionic liquids (42) (**Figure 14**).

The fundamentals of SPOS were introduced over forty years ago for peptide chemistry by R. Bruce Merrifield (48-49). Since then, many common reactions have been successfully

transferred from their solution-phase origins to a variety of solid supports, namely aldol condensation reactions. For instance the research group of LQOF-FFUP prepared a small library of chalcones *via* solid-phase synthesis by base-catalyzed aldol condensation of substituted 2'-hydroxyacetophenones and benzaldehydes, using the 2-chlorotrityl chloride as the solid support (**Figure 14**) (38, 50).

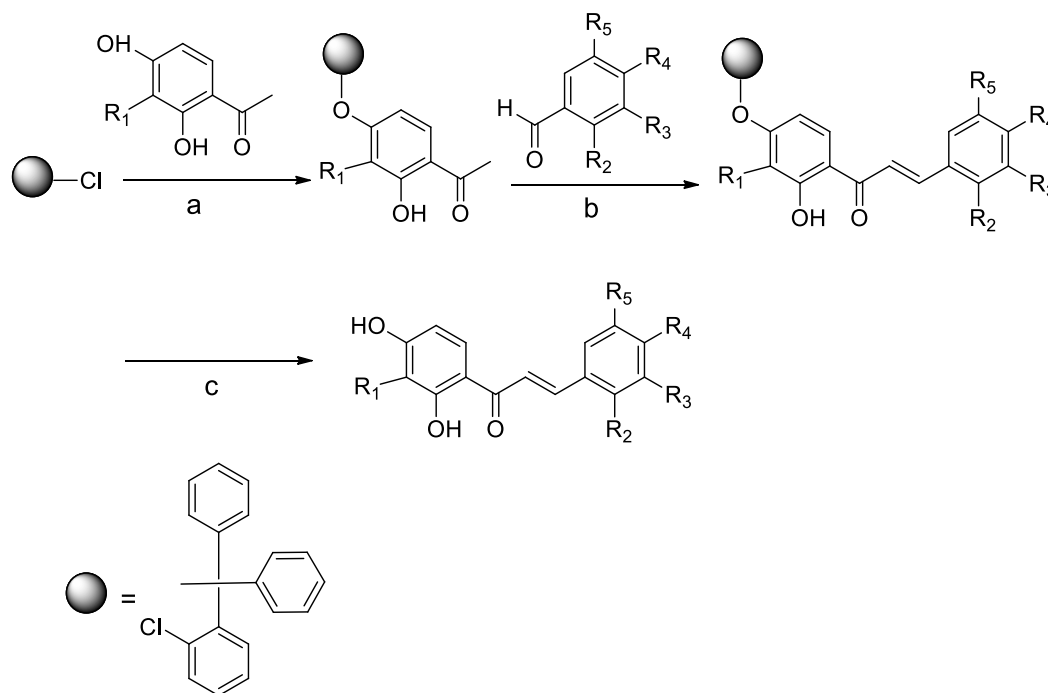


Figure 14: Synthesis of chalcone derivatives using chlorotrityl chloride as solid support by Neves *et al.* (50).

In this method 2-chlorotrityl chloride-supported acetophenones were treated with substituted benzaldehydes under basic conditions affording the solid-supported chalcones. Moreover, several patents focus on the use of combinatorial chemistry to carry out the condensation reaction using the Polyethylene Glycol (PEG) as solid support in order to prepare chalcones. PEG-supported 2-hydroxychalcones were obtained by the reaction of PEG-supported benzyloxy-2-hydroxy-acetophenones with appropriate substituted benzaldehydes in alkali medium (**Figure 15**) (46, 51).

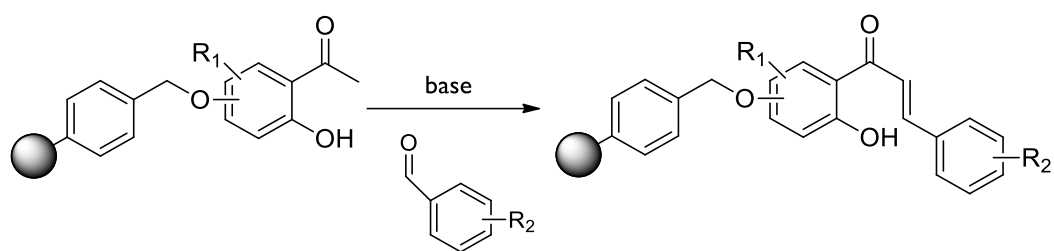


Figure 15: Synthesis of chalcone derivatives by SPOS using PEG as solid support by Peng et al. (51).

The use of heterogeneous catalysis has received much attention over the past few years, being described the use of several catalysts such as zeolites (52), alumina (53), barium hydroxides (54), MgO (55), and hydroxyapatite, among others (56). Nevertheless, some of these catalysts still require expensive toxic solvents to facilitate the heat and mass transfer of the liquid phase in reaction systems (57-59). Therefore, other alternatives have been developed namely the use of acidic ionic liquids.

Ionic Liquids (ILs) have attracted growing interest in the last decades for their variety of applications as solvents and catalysts in organic synthesis. They have received many attentions due to their peculiar chemical and physical properties, such as wide liquid range with melting point around room temperature, good stability in air and moisture, high solubility including inorganic, organic and even polymeric materials, and negligible vapor pressure (47, 60). In addition, the ILs, which are nonvolatile and nonflammable at ambient as well as higher temperatures, can also be potential green alternative solvents and catalysts for chemical synthesis. In recent years, some articles have reported the use of ionic liquids in the synthesis of chalcone derivatives (61-63).

Other more environment friendly methods applied for the synthesis of chalcones includes microwave assisted organic synthesis (MAOS) and solvent-free reactions. The use of the microwave irradiation in synthesis fastens the organic reactions, presenting several advantages over conventional heating, such as short reaction time, high selectivity, easy work up, high conversions and yields and cleaner products (64). In addition, solvent free reactions can be carried out by MW irradiation which holds a strategic position as the solvents are often very toxic, expensive, and problematic to use. Therefore, microwave irradiation has been used in the synthesis of chalcones through the condensation between acetophenone and benzaldehyde derivatives, in presence of several bases such as potassium carbonate in free-solvent conditions (65).

Beyond the anhydrous K_2CO_3 , other catalysts have been used, such as $TiO_2-SO_4^{2-}$ and re-usable hydroxyapatite. The $TiO_2-SO_4^{2-}$ is prepared by sol-gel method through H_2SO_4 , which

increase the acidity of TiO₂ due to the sulphate present (66). The hydroxyapatite is used as heterogeneous catalyst, having high reactivity because the water combined with hydroxyapatite operates as co-catalyst (56).

Grinding techniques has been also used for the synthesis of chalcones, in alternative to MW irradiation and conventional heating. In this technique reaction occurs through generation of local heat by grinding of crystals of substrate and reagent by mortar and pestle. Such reactions are simple to handle, have reduce pollution, are comparatively cheaper to operate and may be regarded as a more economical and ecologically favorable procedure in chemistry (45, 67-68). Using this technique Zangade *et al.* synthesized several chalcone derivatives by the reaction of substituted 2-acetyl-1-naphtol and diversely substituted benzaldehydes in the presence of solid KOH in a porcelain mortar under solvent-free conditions for 4-8 min (**Figure 16**) (67, 69).

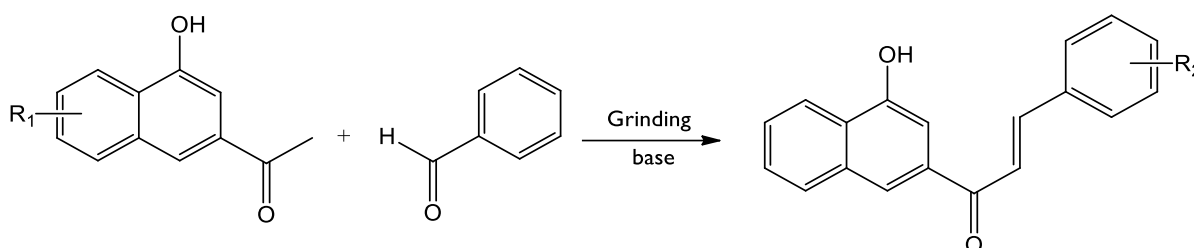


Figure 16: Synthesis of chalcones via Grinding technique by Zangade *et al.* (69).

One variation to the classic Claisen Schmidt reaction is the synthesis of chalcone through the aldol condensation of benzaldehydes previously produced *in situ* by the oxidation of primary alcohols and their subsequent reaction with ketones. This is an one-pot-condensation reaction, which as the advantage of avoiding the lengthy separation process and purification of the intermediate, saving time and resources and increasing chemical yield. Chen *et al.* and Xu *et al.* (70-71) patented new methods of synthesis of chalcones using one-pot condensations. In the procedure patented by Chen *et al.* CrO₃ is slowly added to a mixture of a primary alcohol and the corresponding ketone. This oxidizing agent generates *in situ* the aldehyde that after reacts with the ketone to give the final chalcone derivative (**Figure 17**). This methodology has been used for the synthesis of furochalcones in moderate to high yields (65- 98%).

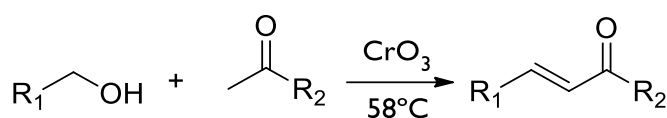


Figure 17: Synthesis of chalcones by one-pot condensation reactions by Chen *et al.* (70).

Xu et al. prepared some chalcone derivatives by a similar method using copper salt, 2,2'-bipyridine (Bipy), and TEMPO catalysts instead of CrO₃ (**Figure 18**).

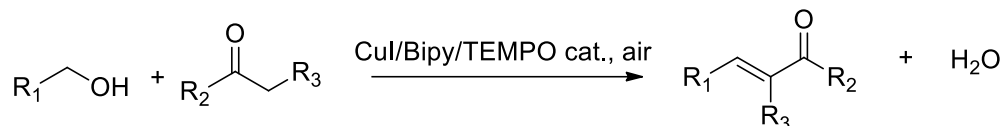


Figure 18: Synthesis of chalcones by one-pot synthesis of chalcones by Xu et al. (71).

1.2.1.1.2. Others Methods

There are some other well-known reactions that have been used for the synthesis of chalcones including direct cross-coupling, Suzuki, Friedel-Crafts, Julia-Kocienski olefination and Heck reactions (45-46).

Chalcones can be synthesized through one pot synthesis by palladium-catalyzed cross-coupling reactions of benzoyl chlorides and potassium styryltrifluoroborates under MW heating. This method has been used for the first time by Al-Masum et al in the synthesis of several chalcones using K₂CO₃ as base and 1,4-dioxane as solvent (**Figure 19**).

This process presents advantages, such as the fact that potassium styryltrifluoroborates is non-toxic, easily prepared and removable (72).

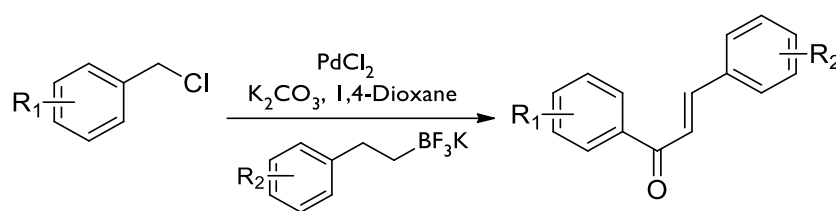


Figure 19: Synthesis of chalcones via palladium-catalyzed cross-coupling by Al-Masum et al. (72).

Other derivatives have been obtained by a Suzuki cross-coupling reaction between organoboron compounds and organic halides, catalyzed by palladium in the presence of base. The synthesis of chalcones by the Suzuki-Miyaura reaction was first proved by Eddarir and co-workers in 2006 (73). Two pathways were used, the first one involved coupling of arylboronic acids with cinnamoyl chloride, whereas the second pathway involved coupling of styrylboronic

acid with benzoyl chlorides (**Figure 20**). Moderate yields (41–51%) were obtained for pathway A, whereas good to excellent yields (68–93%) were obtained for pathway B (73-74).

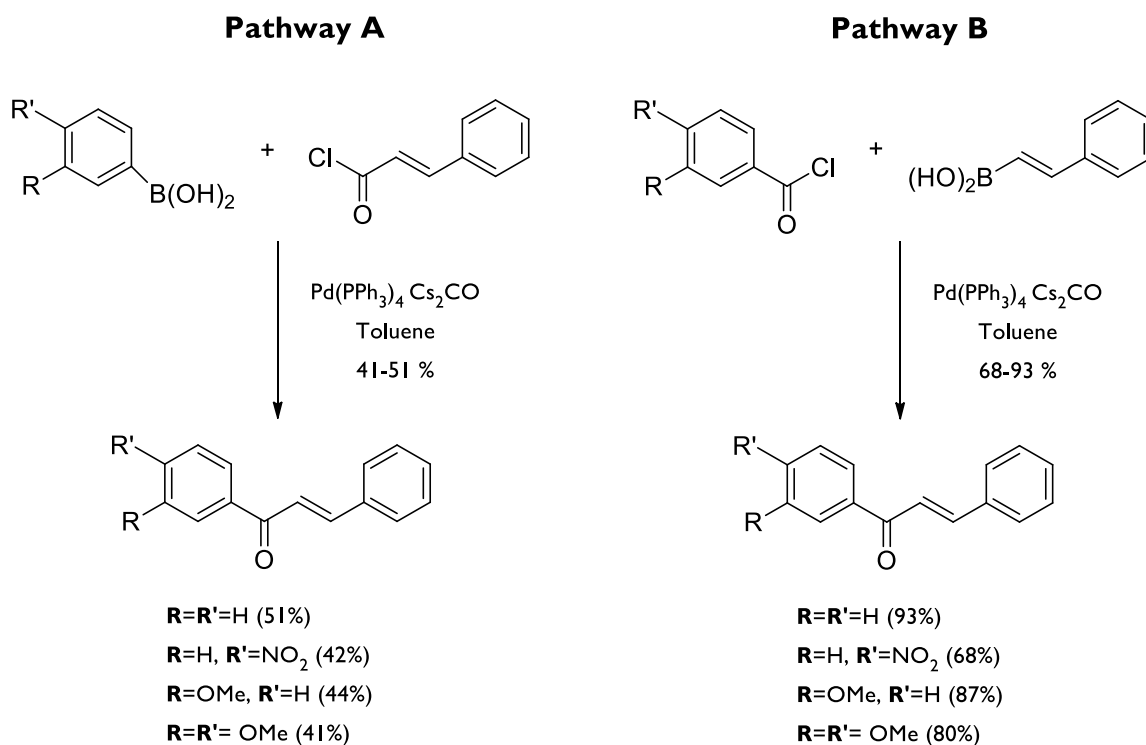


Figure 20: Synthesis of chalcone via Suzuki cross-coupling reaction by Selepe et al. (74).

Additional methods for the synthesis of chalcones include the Friedel-Crafts acylation of phenols. In this reaction the phenol originates the chalcone A-ring, while the acylating agent originates both the B-ring and the three carbon bridge to form C6-C3-C6 unit (**Figure 21**). Several catalysts have been used namely anhydrous aluminum chloride (45-46, 75).

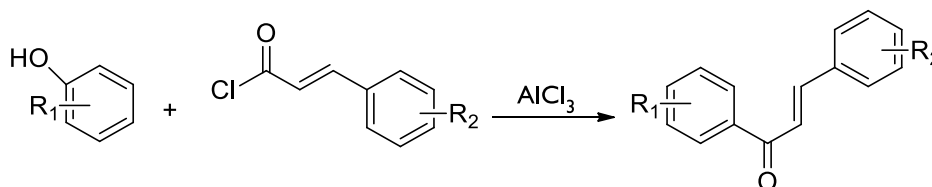


Figure 21: Chalcone synthesis via Friedel-Crafts reaction.

The Julia-Kocienski olefination reaction of benzaldehydes using heteroarylsulfonylarylethanones as coupling reagents in the presence of DBU in THF has also been used in the one-pot synthesis of several chalcone derivatives (**Figure 22**) (45, 76).

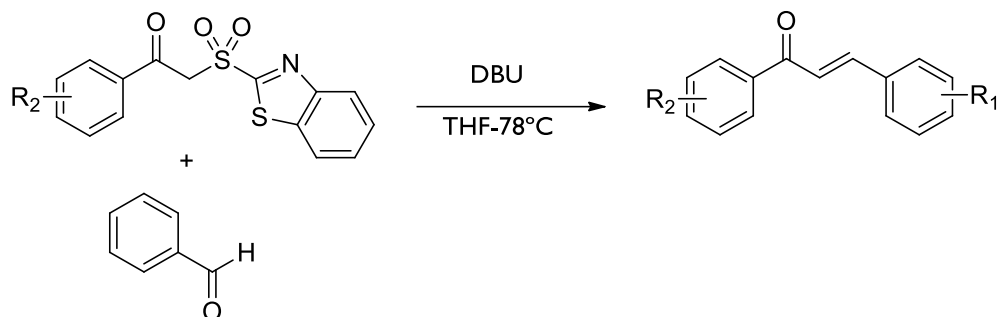
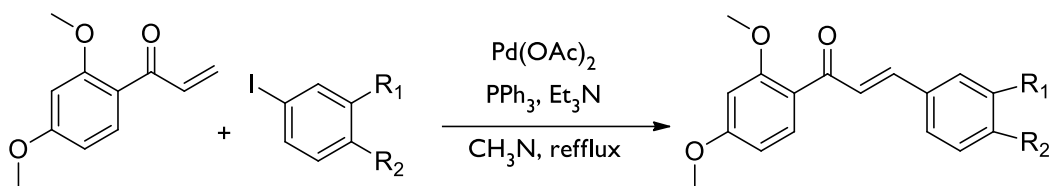


Figure 22: Synthesis of chalcone via Julia-Kocienski olefination reaction by Kumar et al. (76).

The Heck coupling reaction of aryl vinyl ketones with aryl iodides mediated by Palladium (II) acetate was also reported as a method for the synthesis of chalcones in good to excellent yields (**Figure 23**) (77).



e.g. R₁ = R₂ = H (96%)

R₁ = H, R₂ = OMe (95%)

Figure 23: Synthesis of chalcones via Heck coupling reaction by Bianco et al. (77).

1.2.1.2. Chalcones as intermediates for the synthesis of nitrogen

heterocycles

The chalcone framework could be easily incorporated into more complex structures in order to design new potentially bioactive compounds. In fact, several chalcone derivatives have been obtained by the molecular modification of the three-carbon α, β -unsaturated carbonyl system. Possessing two electrophilic reactive centers at α, β -unsaturated ketone group, due to delocalization of electron density in the $-C=C-C=O$ system, chalcone is ready to participate in addition reactions via attack to the carbonyl group (1,2-addition) or involving the β carbon (1,4-conjugate addition), leading to the synthesis of promising bioactive compounds with a more rigid structure, like isoxazole and pyrazole, among other derivatives (**Figure 24**) (42).

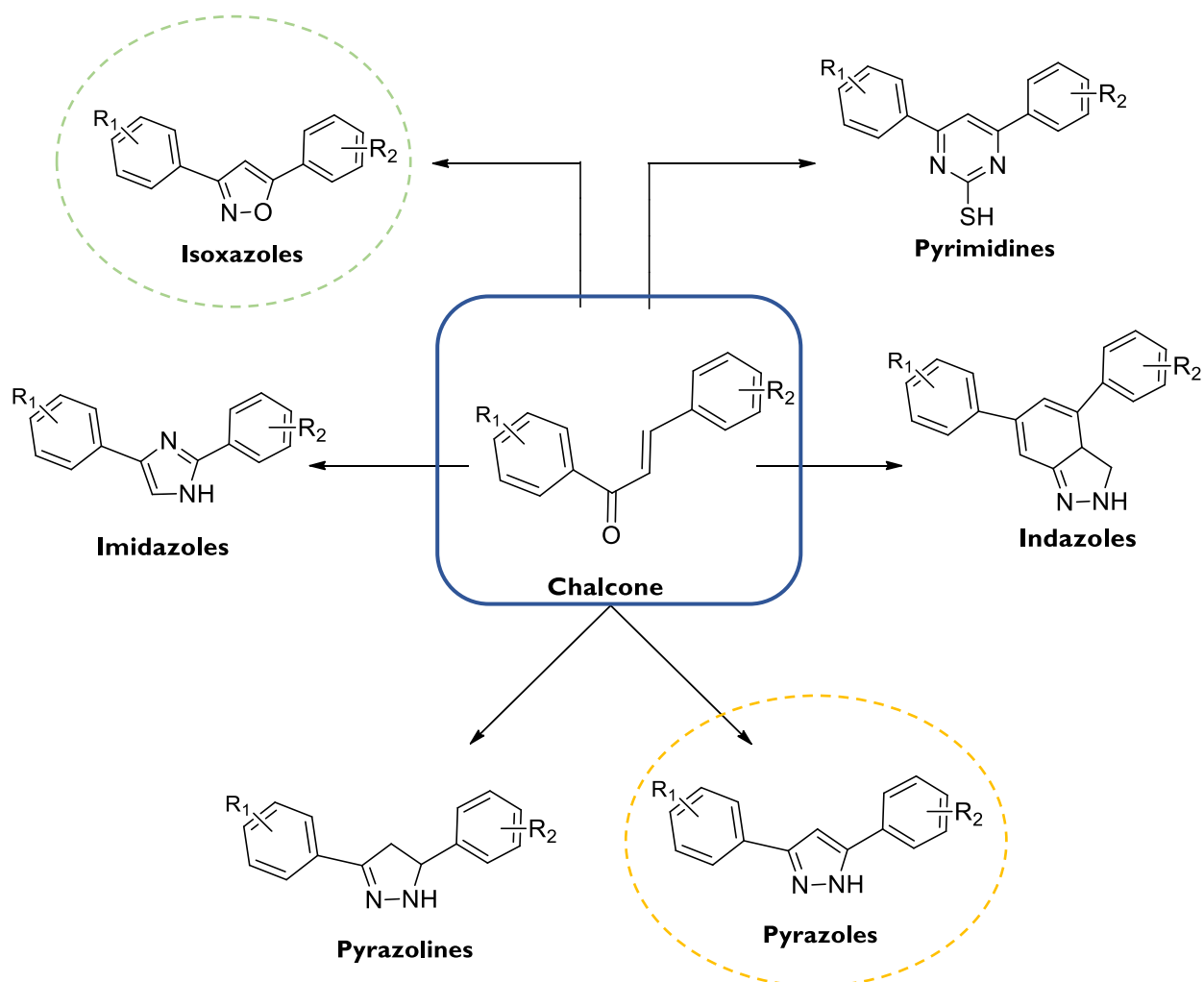


Figure 24: Some chalcone derivatives obtained by molecular modification of α, β -unsaturated ketone moiety of chalcone scaffold.

I.2.1.2.1. Pyrazole Derivatives

Pyrazoles are very important in Medicinal Chemistry as they constitute the basic framework of several drugs having a wide diversity of pharmacological and medicinal applications. Among the biological activities described for pyrazoles, the antitumor activity has been systematically reported, being considered that the introduction of this ring in the chalcone scaffold is associated with an improved antitumor activity (78).

One of the most important pathways to synthesize pyrazole derivatives are through the reaction of chalcones with dipolar molecules or 1,2-binucleophiles, such as hydrazine derivatives. These direct or two-steps transformation are usually carried under acidic conditions, being ethanol or acetic acid the most common solvents (**Figure 25**) (42).

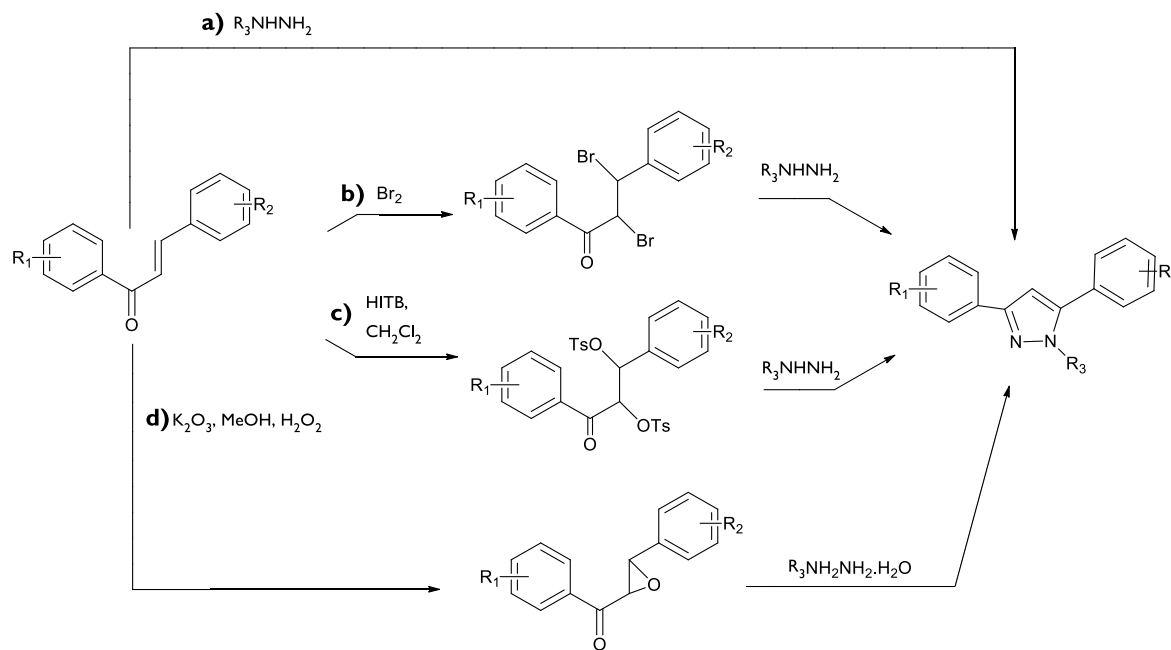


Figure 25: Synthesis of pyrazole derivatives through molecular modifications of chalcones.

Some pyrazole derivatives have been prepared through one-pot reactions of chalcones with several hydrazine derivatives, including phenylhydrazine and hydrazine hydrate in the presence of iodine (79-80), or tetrakis(pyridine)cobalt(I) dichromate (TPCD) (81), using ethanol or acetic acid as solvents (**Figure 25; a**). In addition to classic methods, ecofriendly

one-pot approaches have been used to synthesize pyrazole derivatives, including MAOS (82-85).

In some approaches of two steps synthesis of pyrazole derivatives, chalcones are firstly converted into chalcone dibromides by treatment with bromine, and afterward these derivatives afforded pyrazoles by the reaction with benzoylhydrazines (86), phenylhydrazines (79) or hydrazine hydrate (87-91) (**Figure 25; b**).

An alternative approach to chalcone bromides is the synthesis of chalcone α,β -ditosylates, which subsequently can be transformed into pyrazoles by the reaction of α,β -ditosylate chalcones with hydrazine derivatives (**Figure 25; c**) (92).

The two steps reactions involving the synthesis of chalcones epoxides through reaction of chalcone derivatives with potassium carbonate in methanol and H_2O_2 followed by the cycloaddition reaction of hydrazine hydrate with chalcone-epoxide have also been described as an effective procedure to obtain 3,5-diaryl-1*H*-pyrazoles (**Figure 25; d**) (93)

1.2.1.2.2. Isoxazole Derivatives

Isoxazoles are a class of heterocyclic compounds with a remarkable number of applications. They can be used as intermediates for the synthesis of several derivatives. In fact, the structural feature that distinguishes isoxazoles from other heterocycles is that they are aromatic but contain a weak nitrogen-oxygen bond which is a potential site of ring cleavage. Therefore, isoxazoles are very advantageous intermediates since the ring system stability allows the manipulation of substituents to give functionally complex derivatives (94). Moreover, isoxazoles show a wide spectrum of biological activities such as anti-inflammatory, anticonvulsant (95), insecticidal (96) and anticancer (97) activities.

3,5-Diarylisoxazoles can be prepared through the reaction of chalcones with hydroxylamines, using NaOH or KOH as base. NaOAc and glacial acetic acid in ethanol has also been used in the synthesis of 3,5-diarylisoxazoles (**Figure 26; a**) (90). These isoxazole derivatives can also be synthesized by a two-step approach. Firstly, chalcones are converted into the corresponding α,β -ditosylate derivatives, which then reacted with hydroxylamine giving the isoxazoles (**Figure 26; b**). A similar approach for the synthesis of 3,5-isoxazoles

has been achieved by the reaction of α,β -dibromochalcones with hydroxylamine hydrochloride, in the presence of KOH (**Figure 26; c**) (42).

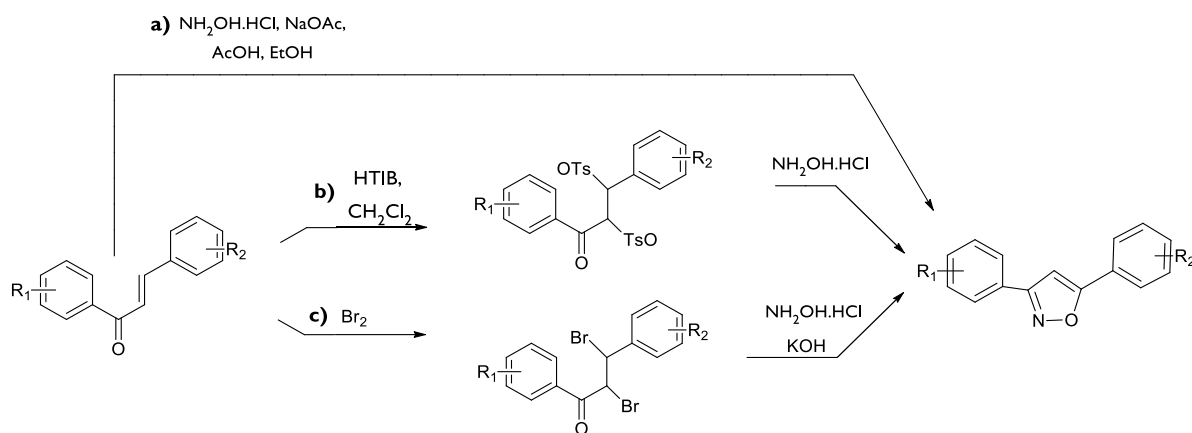


Figure 26: Synthesis of isoxazole derivatives through molecular modifications of chalcones.

1.2.1. Biological Activities

Chalcones display a broad range of biological activities including antioxidant (98), anti-inflammatory (99), antimicrobial (100-101), antimalarial (102), anti-leishmanial (102), antiprotozoal (103), antiulcer (104), antihistaminic (105), antifouling (106) and antitumor activities (107).

In addition, chalcones have also been described for their ability to modulate the activity of several molecular targets such as microtubules, kinases, tyrosine kinases, aurora kinases, oxidoreductases, tyrosinases, sex hormone converting enzymes (aromatase, 5α -reductase, 17β -hydroxysteroid dehydrogenase), aldolase reductase, thioredoxin reductase, monoamine oxidase (MAO), hydrolases, esterases, ABC transporters, topoisomerases, and cholesteryl ester transfer protein (19, 107).

The wide interest in these compounds is evidenced by the fact that several chalcone derivatives have been marketed or clinically tested for various health conditions (e.g., metochalcone - choleric/diuretic; sofalcone- anti-ulcer/mucoprotective; and hesperidin methylchalcone – vascular protective) (**Figure 27**) (19).

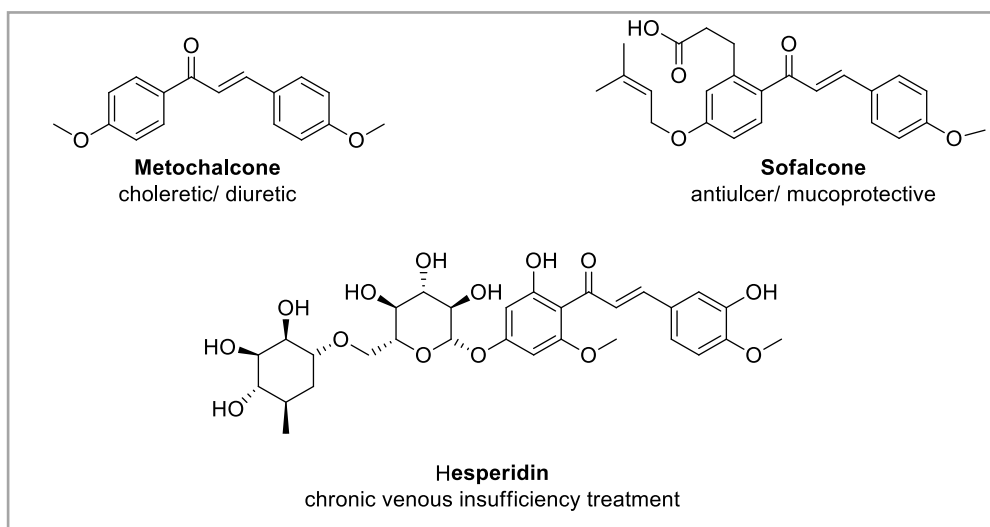


Figure 27: Chalcones clinically tested for various health conditions.

Among the activities reported for chalcones, the antitumor activity is one of the most exhaustively studied. Chalcones are reported as promising antitumor agents against most human tumor cell lines (44). They inhibit different steps of carcinogenesis from the very early stages, including tumor initiation, through promotion, progression, angiogenesis, and invasion, to the very late stages leading to metastasis (108). These compounds are also strongly implicated in the negative regulation of cell cycle progression and favor cell death mechanisms, predominantly apoptosis, in tumor cells. Additionally, they have the ability to uncouple mitochondrial respiration and thus collapse mitochondrial membrane potential (109). In addition, several chalcone derivatives such as xanthohumol (**29**) naringenin, (**30**) and isobavachalcone (**31**) have been reported as chemopreventive agents (**Figure 28**) (43-44).

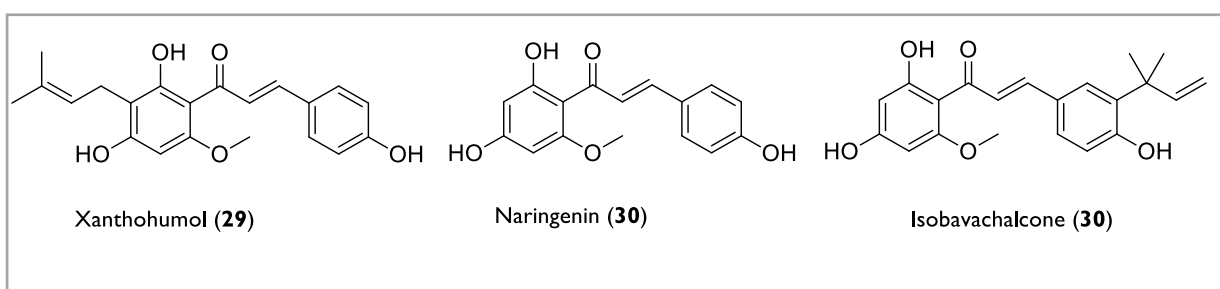


Figure 28: Structure of some chalcones reported as chemopreventive agents.

Given the importance of the antitumor activity of chalcones, several studies have been conducted in order to get some insights into the molecular mechanism of action of these compounds. In result of these studies it was demonstrated the interference of chalcones with several mechanisms and targets, namely, 5 α -reductase, aromatase, 17- β -hydroxysteroid dehydrogenase, ABCG2/Pgp/ BCRP HDAC/Sirtuin-1, P-glycoprotein, proteasome, VEGF, VEGFR-2 kinase, MMP-2/9, JAK/STAT signaling pathways, CDC25B, microtubule (tubulin), cathepsin-K, topoisomerase-II, P-53, Wnt, NF- κ B, B-Raf and mTOR (**Figure 29**) (19, 107).

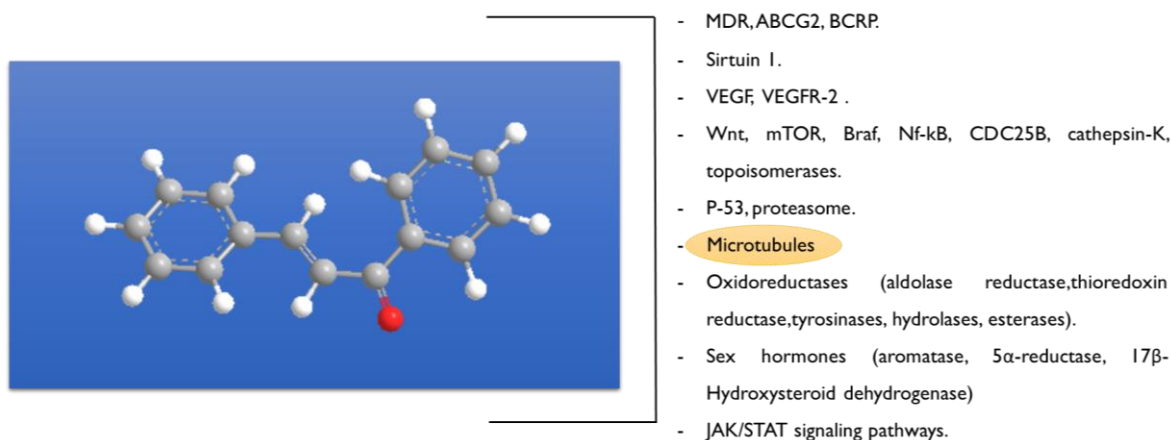


Figure 29: Summarizes the molecular targets for the antitumor activity of chalcones.

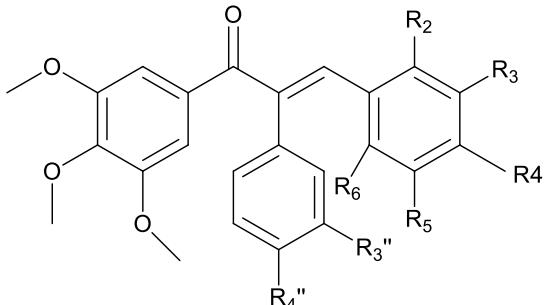
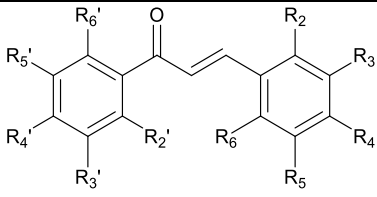
1.2.2.1. Chalcones as Antimitotic Agents

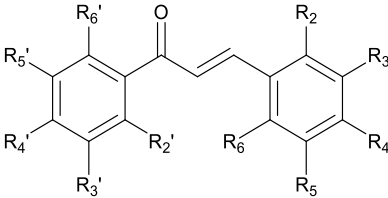
The effect of chalcones in mitosis by the interference with different targets has already been reported, making these compounds promising antimitotic agents (19, 107). (**Table 2** represents the chalcone derivatives with antimitotic activity in different human tumor cell lines.

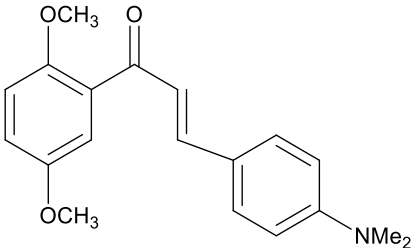
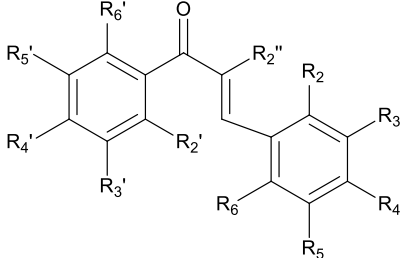
Among these antimitotic agents, polymethoxylated chalcones structurally similar to combretastatin A4 and colchicine have proved to bind to the tubulin effectively (110). Studies on these methoxylated chalcones suggested that the number and the position of methoxy substituents on the aromatic rings appeared to be critical for their cytotoxicity. The presence of a trimethoxylated phenyl A ring favors the binding to the colchicine binding site (15). In addition, the presence of this trimethoxylated phenyl moiety in B ring seems also to be important for antitumor activity. In fact, in the course of research work in LQOF-FFUP chalcone **CPX (60, Table 2)** was identified as a potent growth inhibitor of human tumor cell lines (50). Studies of the mechanism of action have demonstrated the ability of this compound to interfere with mitosis by affecting microtubules and causing mitotic catastrophe (5). Nevertheless, no studies have been undertaken to clarify the importance of this moiety in B ring of chalcones to the interaction with the colchicine binding site of tubulin.

Among the chalcones presented in **Table 2**, chalcones **42, 61, 62, 65, 111, 138-139, 143-144, 166** were found to be the most potent, displaying lower value to activity against several tumor cell lines.

Table 2: Chalcones with antimetabolic activity.

Chalcones	Cell line	Targets/ associated process/ IC _{50/75} ^a or tested concentration ^b	Ref
 <p> 31: R_{3''}=R₂=R₃=R₅=H; R₄= OCH₃; R_{4''}= OCH₃ 32: R_{3''}= F; R_{4''}= OCH₃; R₃= R₄= R₅= H; R₂= OH 33: R_{3''}= OH; R_{4''}= OCH₃; R₃= R₄= R₅= H; R₂= OH 34: R_{3''}= F; R₂= R₃= R₅= H; R₄=R_{4''}= OCH₃ 35: R_{3''}=R₃= R₄= R₅= H; R₂= OH 36: R_{3''}= OTBDMS; R_{4''}= OCH₃; R₃= R₄= R₅= H; R₂= OH 37: R_{4''}= OCH₃; R₂= R₃= R₅= R₆= H 38: R_{3''}= OH; R_{4''}= OCH₃; R₂= R₃= R₅= H; R₄=CH₃ 39: R_{3''}= F; R_{4''}= OCH₃; R₂= R₃= R₅= H; R₄= CH₃ 40: R_{3''}= F; R₄=R_{4''}= OCH₃; R₂= R₃= R₅= H; </p>	MCF-7	-Cell cycle arrest at G2/M phase -Inhibition of tubulin polymerization (IC ₅₀) 31: 2.5± 0.1 μM	31: (27)
	K562	-Cell cycle arrest at G2/M phase -Inhibition of tubulin polymerization (IC ₅₀) 32: 7.2 μM 33: 5.5 μM 34: 2.1 μM 35,36: >10 μM 37: 9.5 μM 38: 2.6 μM 39: 4.4 μM 40: 2.6 μM	32-40: (110-111)
 <p> 41: R₄= OCH₃; R₅= OH; R₂=R₄=R₆=OCH₃; R₂=R₃=R₆= R₃=R₅= H; 42: R₃=R₆=R₂=R₄=R₆=OCH₃; R₄=R₅=R₃=R₅= H 43: R₂=R₅=R₆=OH; R₃= R₂=R₄=R₆=OCH₃; R₄=R₃=R₅= H 44: R₃=R₄=R₅= R₄=OCH₃; R₂=R₆=R₂=R₅=R₆= H; R₃=OH Pedicin (45): R₃= R₆= OH; R₂=R₄=R₆=OCH₃; R₂=R₃=R₄= R₅=R₆= H Calytropsin (46): R₄= OCH₃; R₆= OH; R₃=R₄=OH; R₂=R₃=R₅=R₂=R₅=R₆=H 47: R₂=R₅=R₆=OH; R₃=R₄=R₃= R₅=H; R₂=R₄=R₆= OCH₃; 48: R₂=R₄=R₆= R₃= R₄= R₅=H; R₃=R₅= R₂=R₆= OCH₃ 49: R₃= R₅=H; R₃=R₅= R₂=R₄=R₆= OCH₃ 50: R₂=R₄=R₆= R₃= R₅=H; R₃=R₆= R₂=R₄=R₆=OCH₃ 51: R₂=R₄=R₂=R₄=R₆= OCH₃; R₃=R₅=R₆=R₃=R₅=H 52: R₄= NH₂; R₂=R₄=R₆=R₂= R₆= OCH₃; R₃=R₅=R₃= R₅=H; </p>	K562	Cell cycle arrest at G2/M phase 41: Tested concentration at: 1.5 μM	41: (112)
	K562	Inhibition of tubulin polymerization 42: Tested concentration at: 0.5 μM	42: (113-114)
	K562	Inhibition of tubulin polymerization 43: Tested concentration at: 10 μM	43: (113-114)

	A549	-Cell cycle arrest at G2/M phase -Inhibition of tubulin polymerization (IC ₅₀) 44: 3.7 ± 0.14 μM	44: (115)
	KB	-Inhibition of tubulin polymerization (IC ₅₀) 45: 300 μM	45: (116)
	OVCAR-3, A549	Inhibition of tubulin polymerization (IC ₅₀) 46: 0.66 μM	46: (117)
	K562	Inhibition of tubulin polymerization (Tested concentration) 47-52: 10 μM	47-52: (118-120)
	MCF-7	-Cell cycle arrest at G2/M phase -Inhibition of tubulin polymerization (IC ₅₀) 53: 31 ± 3.4 μM 54: 2.6 ± 0.2 μM 55: >40 μM 56: >40 μM	53-56: (32)
 <p>53: R₂=R₆'=R₂=R₃=R₄=R₆= H; R₃'=R₄'= R₅'= R₅'=OCH₃; R₄'=B(OH)₂ 54: R₂=R₆'=R₂=R₃=R₆=H; R₃'=R₄'= R₅'= R₅'=OCH₃; R₄'=OH 55: R₂=R₅'=R₆'=R₂=R₆=H; R₃'=R₃'=R₄'= R₅'= OCH₃; R₄'=B(OH)₂ 56: R₂'=R₅'=R₆'=R₂=R₆=H; R₄'= OH; R₃'=R₄'= R₅'= R₃'=OCH₃ 57: R₂'= R₃'=R₄'=R₅'=R₆'= R₂'= R₃'=R₄'= R₅'=R₆'= H 58: R₄'= OCH₃; R₆'= OH; R₂'= R₅'= OCH₃ Isoliquiritigenin (59): R₂'= R₄'=R₆'=R₂'= R₄'=R₅'=R₆'= H; R₃'=R₅'=R₃'= OH CPX (60): R₂'=R₄'=R₆'=R₂'=R₃'=H; R₃'= R₅'= OH; R₄'= R₅'= R₆'= OCH₃</p>	HeLa	-Cell cycle arrest at G2/M phase -Inhibition of tubulin polymerization (IC ₅₀) 57: >10 μM	57: (130)
	Jurkat, U937, PBMCs	-Inhibition of tubulin polymerization (IC ₅₀) 58: 3.2 (Jurkat), 16.0 (U937), 39.8 (PBMCs) μM	58: (120)
	A549, Hep G2	Inhibition of tubulin polymerization and	59: (121)

		<p>cell cycle arrest at G2/M phase</p> <p>59: Tested concentration at: 20 µg/mL</p>	
	MCF-17	<p>Inhibition of tubulin polymerization and cell cycle arrest at G2/M phase</p> <p>60: Tested concentration at: 16 µM</p>	60: (5)
 <p>MDL27048 (61)</p>	HeLa, SV40-3T3	<p>Inhibition of tubulin polymerization</p> <p>Tested concentration at: 0.2 µM</p>	(122, 123-124)
 <p>62: R₂=R₆'=R₂=R₅=R₆=H; R₃'=R₄'=R₅'=R₄'=OCH₃; R₃=NH₂ SD400 (63): R₂=R₆'=R₂=R₅=R₆=H; R₃'=R₄'=R₅'=R₄'=OCH₃; R₂'=CH₃; R₃=OH; 64: R₂=R₆'=R₂=R₅=R₆=H; R₃'=R₄'=R₅'=R₄'=OCH₃; R₂'=CH₃; R₃=F 65: R₂=R₆'=R₂=R₅=R₆=H; R₃'=R₄'=R₅'=R₄'=OCH₃; R₂'=CH₃; R₃=NH₂ 66: R₂=R₆'=R₂=R₅=R₆=H; R₃'=R₄'=R₅'=R₄'=OCH₃; R₂'=H; R₃=OH 67: R₂=R₆'=R₂=R₅=R₆=H; R₃'=R₄'=R₅'=R₄'=OCH₃; R₂'=F 68: R₂=R₆'=R₂=R₅=R₆=H; R₃'=R₄'=R₅'=R₄'=OCH₃; R₂'=F; R₃=OH 69: R₂=R₆'=R₂=R₅=R₆=H; R₃'=R₄'=R₅'=R₄'=OCH₃; R₂'=H; R₃=R₄=[OCH₂O]phenyl 70: R₂=R₆'=R₂=R₅=R₆=H; R₃'=R₄'=R₅'=OCH₃; R₂'=H; R₃=R₄=[OCH₂CH₂O]phenyl</p>	HDMEC	<p>Cell cycle arrest at G2/M phase</p> <p>62: Tested concentration at: 0.3 µM</p>	62: (113, 125)
	K562	<p>-Cell cycle arrest at G2/M phase</p> <p>-Inhibition of tubulin polymerization (IC₅₀)</p> <p>63: 2.4 µM</p> <p>64: 3.5 µM</p> <p>65: 0.3 µM</p> <p>66: 1.8 µM</p> <p>67: 4.6 µM</p> <p>68: 0.6 µM</p> <p>69-70: 12 µM</p>	<p>63-65: (126)</p> <p>66-68: (114)</p> <p>69-70: (127)</p>

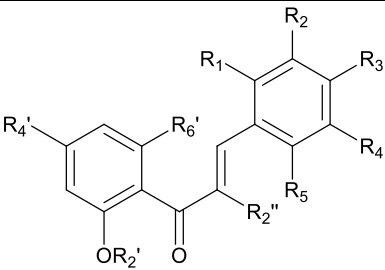
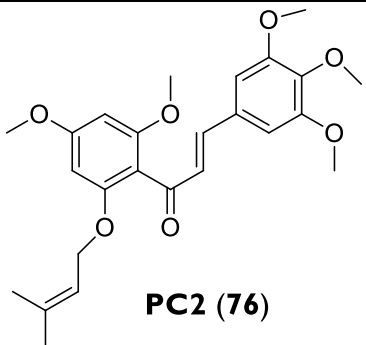
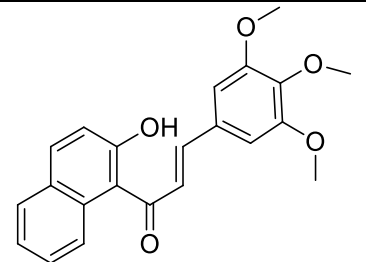
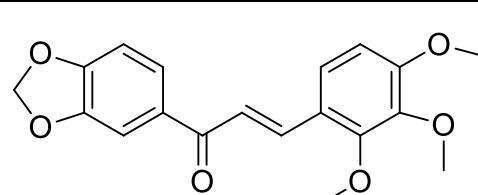
 <p>71: R₄'=H, OH, OMe, OEt, propoxy, isopropoxy, OBn, NH₂; R₂=R₆=R₂'=R₁=R₂=R₃=R₄=R₅=H</p> <p>72: R₆'= H, OH, OMe, OEt, Pr, iso-Pr, OBn; R₂'=R₄'=R₂'=R₁=R₂=R₃=R₄=R₅=H</p> <p>73: R₂'= H, Me, OEt, OBn; R₄'=R₆'=R₂'=R₁=R₂=R₃=R₄=R₅=H</p> <p>74: R₂'= H,OH, OMe, OEt, OBn; R₂'=R₄'=R₆'=R₁=R₂'=R₃=R₄=R₅=H</p> <p>75: R₁-R₅= H, halo, OH, OMe, NH₂, NHMe, NMe₂; R₂'=R₄'=R₆'=R₂'=H</p>	K562	<p>Cell cycle arrest at G2/M phase (Tested concentration)</p> <p>71-75: 10 μM</p>	71-75: (118)
 <p>PC2 (76)</p>	MCF-7, NCI-H460	<p>Mitotic spindle damage</p> <p>Tested concentration at: 12 μM</p>	(128)
 <p>HTN (77)</p>	HCT116	<p>Inhibition of tubulin polymerization and cell cycle arrest at G2/M phase</p> <p>Tested concentration at: 10 μM</p>	(129)
 <p>78</p>	HeLa	<p>-Inhibition of tubulin polymerization (IC₅₀)</p> <p>>10 μM</p>	(130)

Table 2: Chalcones with antimetabolic activity (continued).

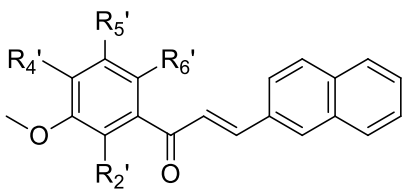
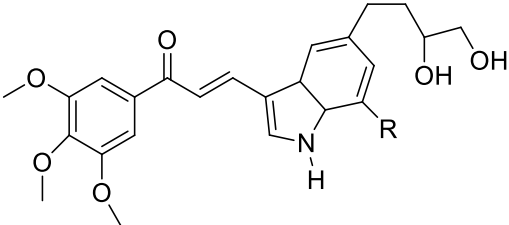
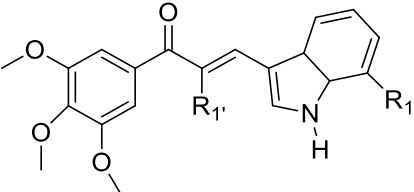
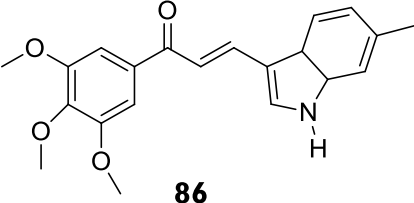
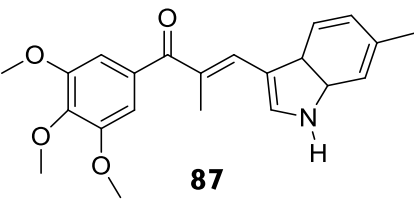
Chalcones	Cell lines	Targets/ associated process/ IC _{50/75} ^a or tested concentration ^b	Ref
 <p> 79: R₂'=R₅'=R₆'= H; R₄'=OH 80: R₂'=R₆'= H; R₄'=R₅'=OCH₃ 81: R₂'=OH; R₄'=OCH₃; R₅'=R₆'= H </p>	HeLa	-Inhibition of tubulin polymerization (IC₅₀) 79: 3.6 μM 80: 2.2 μM	79,80: (130)
	Capan-1 pancreatic	Inhibition of tubulin polymerization and cell cycle arrest at G2/M phase 81: Tested concentration at: 5.0 μM	81: (131)
 <p> AM-I32 (82): R=H AM-I38 (83): R= CH₃ </p>	LLC	Inhibition of tubulin polymerization and cell cycle arrest at G2/M phase (Tested concentration) 82: 1.12 μM 83: 1.19 μM	82,83: (132)
 <p> AM-97 (84): R₁'=R₁= CH₃ TK5048 (85): R₁'=R₁= H </p>	84: LLC 85: PC-14	Inhibition of tubulin polymerization and cell cycle arrest at G2/M phase (Tested concentration) 84: 1.43 μM 85: 10 μM	84,85: (132)

Table 2: Chalcones with antimittotic activity (*continued*).

Chalcones	Cell line	Targets/ associated process/ IC ₅₀ /75 ^a or tested concentration ^b	Ref
 86	HeLa S ₃	- Antiproliferative activity (IC ₅₀) 6.3 nM -Inhibition of tubulin polymerization	(113, 133)
 87	HeLa S ₃	- Antiproliferative activity (IC ₅₀) 0.7 nM -Inhibition of tubulin polymerization	(113, 133)

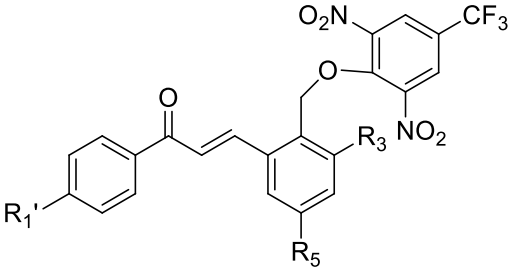
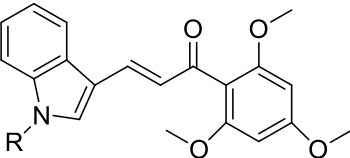
 <p> 88: R₁'= CH₃; R₃= Br; R₅=Br 89: R₁'= CH₃; R₃= Cl; R₅=Cl 90: R₁'= CH₃; R₃= H; R₅=Br 91: R₁'= CH₃; R₃= H; R₅=Cl 92: R₁'= OCH₃; R₃= Br; R₅=Br 93: R₁'= OCH₃; R₃= Cl; R₅=Cl 94: R₁'= OCH₃; R₃= H; R₅=Br 95: R₁'= OCH₃; R₃= H; R₅=Cl 96: R₁'= F; R₃= Br; R₅=Br 97: R₁'= F; R₃= Cl; R₅=Cl 98: R₁'= F; R₃= H; R₅=Br 99: R₁'= F; R₃= H; R₅=Cl 100: R₁'= Cl; R₃= Br; R₅=Br 101: R₁'= Cl; R₃= Cl; R₅=Cl 102: R₁'= Cl; R₃= H; R₅=Br 103: R₁'= Cl; R₃= H; R₅=Cl 104: R₁'= Br; R₃= Br; R₅=Br 105: R₁'= Br; R₃= Cl; R₅=Cl 106: R₁'= Br; R₃= H; R₅=Br 107: R₁'= Br; R₃= H; R₅=Cl </p>	<p>MCF-7 and A549</p>	<p>Inhibition of tubulin polymerization (IC₅₀)</p> <p> 88: 5.68±0.12 μM 89: 4.87±0.21 μM 90: 6.41±0.10 μM 91: 1.42±0.06 μM 92: 6.02±0.22 μM 93: 6.56±0.31 μM 94: 4.08±0.13 μM 95: 4.83±0.15 μM 96: 15.31±0.65 μM 97: 9.62±0.34 μM 98: 12.31±0.52 μM 99: 11.66±0.35 μM 100: 12.6±0.51 μM 101: 6.34±0.23 μM 102: 7.14±0.31 μM 103: 4.68±0.21 μM 104: 10.01±0.46 μM 105: 9.46±0.32 μM 106: 6.28±0.24 μM 107: 4.62±0.15 μM </p>	<p>88-107: (134)</p>
 <p>JAI-51 (108)</p>	<p>U118C, U118T, U138C, U138T, LN229C, LN229T, GL26C, and GL26T</p>	<p>-Cell cycle arrest at G2/M phase</p> <p>-Inhibition of tubulin polymerization (IC₅₀)</p> <p> 22±3 μM (U118C) 55±7 μM (U118T) 34±7 μM (U138T) 58±6 μM (U138C) 28±3 μM (LN229C) 68±6 μM (LN229T) 23±4 μM (GL26C) 60±8 μM (GL26T) </p>	<p>(135)</p>

Table 2: Chalcones with antimitotic activity (*continued*).

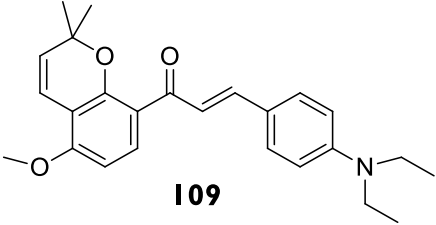
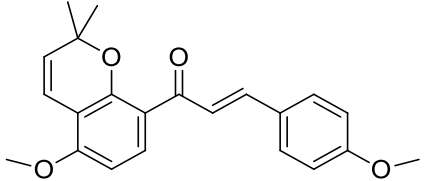
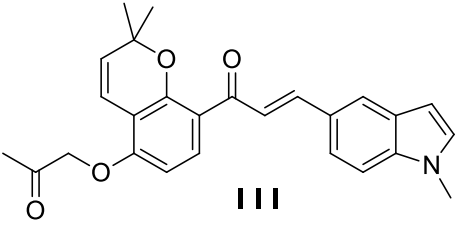
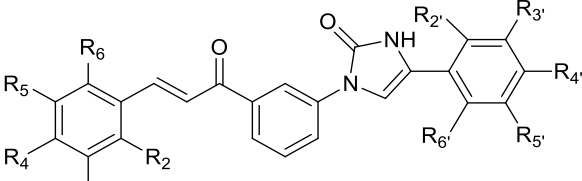
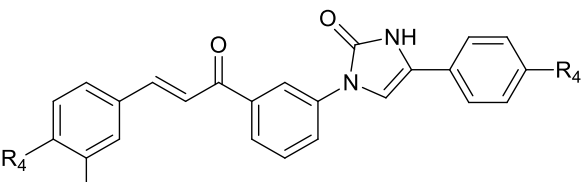
Chalcone	Cell line	Targets/ associated process/ IC _{50/75} ^a or tested concentration ^b	Ref
 <p>109</p>	HepG2	<p>Inhibition of tubulin polymerization and cell cycle arrest at G2/M phase</p> <p>Tested concentration at: 1.25 μM</p>	(136)
 <p>Millepachine (110)</p>	HepG2	<p>Inhibition of tubulin polymerization and cell cycle arrest at G2/M phase</p> <p>Tested concentration at: 1.25 μM</p>	(136)
 <p>111</p>	HepG2	<p>Inhibition of tubulin polymerization and cell cycle arrest at G2/M phase</p> <p>Tested concentration at: 0.50 μM</p>	(137)
 <p>112: R₄= OH; R₃=OCH₃; R₄'= H</p>	MCF-7	<p>Inhibition of tubulin polymerization and cell cycle arrest at G2/M phase</p> <p>Tested concentration at: 10 μM</p>	(138-139)
 <p>113: R₄= OH; R₃=OCH₃; R₄'= Cl</p>	MCF-7	<p>Inhibition of tubulin polymerization and cell cycle arrest at G2/M phase</p> <p>Tested concentration at: 10 Mm</p>	(138-139)

Table 2: Chalcones with antimitotic activity.

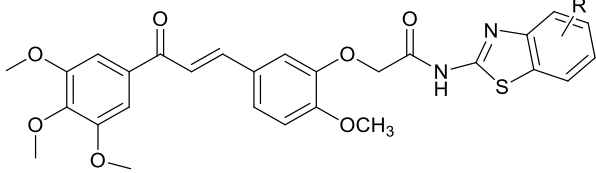
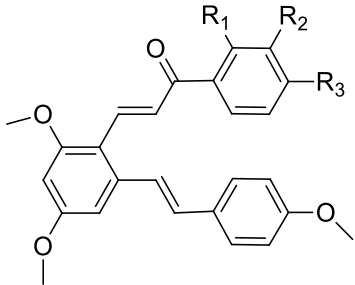
Chalcones	Cell line	Targets/ associated process/ IC _{50/75} ^a or tested concentration ^b	Ref
 <p>114: R= H 115: R= 6-trifluoromethoxy</p>	A549	<p>-Cell cycle arrest at G2/M phase</p> <p>-Inhibition of tubulin polymerization (IC₅₀)</p> <p>114: 3.5± 0.17 μM</p> <p>115: 5.2± 0.2 μM</p>	114,115: (115)
 <p>116: R₁= H; R₂= H; R₃=H 117: R₁= H; R₂= OCH₃; R₃=H 118: R₁= H; R₂=H; R₃= OCH₃ 119: R₁= H; R₂=H; R₃=OCH₂OCH₃ 120: R₁= H; R₂= H; R₃= O(OCH₂)₃CH₃ 121: R₁= H; R₂=H; R₃=OCH(CH₃)(CH₂)₂CH₃ 122: R₁= H; R₂= H; R₃=O(CH₂)₅CH₃ 123: R₁= H; R₂= H; R₃=O(CH₂)₁₁CH₃ 124: R₁= H; R₂= H; R₃=F 125: R₁= H; R₂= H; R₃=Cl 126: R₁= H; R₂= H; R₃=Br 127: R₁= H; R₂= Cl; R₃=H 128: R₁= H; R₂= Br; R₃=H 129: R₁= H; R₂= Cl; R₃=Cl 130: R₁= H; R₂= H; R₃=CF₃ 131: R₁= H; R₂= H; R₃=CH₃ 132: R₁= H; R₂= CH₃; R₃=CH₃ 133: R₁= CH₃; R₂= H; R₃=CH₃ 134: R₁= H; R₂= CH₃; R₃=CH₃ 135: R₁= H; R₂= H; R₃=NH₂ 136: R₁= H; R₂= H; R₃=N(CH₂CH₃)₂ 137: R₁= H; R₂= H; R₃=C₆H₄CH₃</p>	HepG2, B16-F10 and A549	<p>-Cell cycle arrest at G2/M phase</p> <p>-Inhibition of tubulin polymerization (IC₅₀)</p> <p>116: 34± 2μM</p> <p>117: 59± 10 μM</p> <p>118: 43± 10 μM</p> <p>119: 26± 5 μM</p> <p>120: 94± 9 μM</p> <p>121: 55± 4 μM</p> <p>122: 131± 16 μM</p> <p>123: 58± 6 μM</p> <p>124: 64± 3 μM</p> <p>125: 80± 13 μM</p> <p>126: 72± 8 μM</p> <p>127: 41± 2 μM</p> <p>128: 76± 4 μM</p> <p>129: 47± 1 μM</p> <p>130: 150± 15 μM</p> <p>131: 29± 2 μM</p> <p>132: 42± 6 μM</p> <p>133: 4.1± 0.4 μM</p> <p>134: 2.6± 0.6 μM</p> <p>135: 36± 9 μM</p> <p>136: 33± 4 μM</p> <p>137: 44± 5 μM</p>	116-137: (140)

Table 2: Chalcones with antimetabolic activity (*continued*).

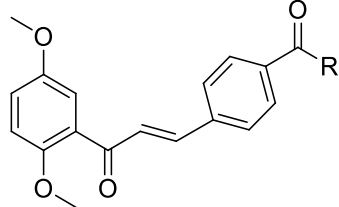
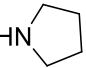
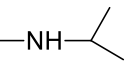
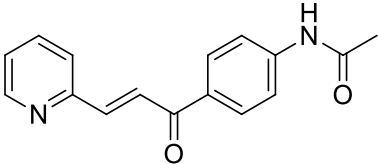
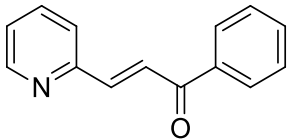
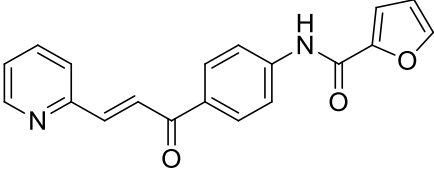
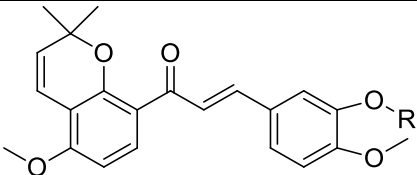
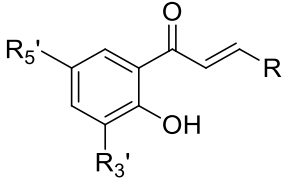
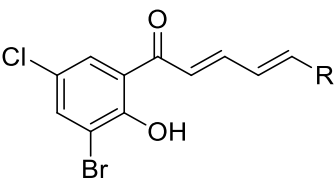
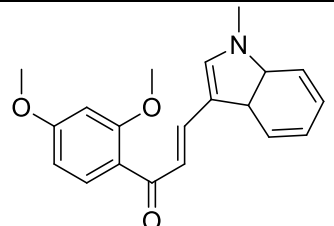
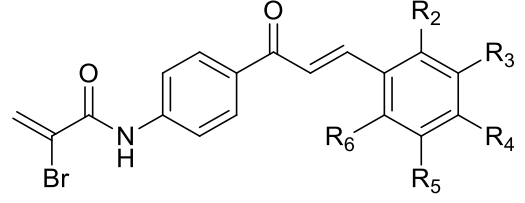
Chalcones	Cell line	Targets/ associated process/ IC _{50/75} ^a or tested concentration ^b	Ref
 <p>138: R= </p> <p>139: R= </p>	NTUB1	<p>-Cell cycle arrest at G2/M phase</p> <p>-Inhibition of tubulin polymerization (Tested concentration)</p> <p>138, 139: 0.3 μM</p>	138, 139: (141-142)
 <p>140</p>	SNU-398	<p>-Cell cycle arrest at G2/M phase</p> <p>-Inhibition of tubulin polymerization (IC₅₀)</p> <p>15.7 μM</p>	(143)
 <p>141</p>	SNU-398	<p>-Cell cycle arrest at G2/M phase</p> <p>-Inhibition of tubulin polymerization (IC₅₀)</p> <p>> 30 μM</p>	(143)
 <p>142</p>	SNU-398	<p>-Cell cycle arrest at G2/M phase</p> <p>-Inhibition of tubulin polymerization (IC₅₀)</p> <p>20 μM</p>	(119, 143)
 <p>143: R= butan-2-one</p> <p>144: R= pentan-2-one</p>	HepG2	<p>-Cell cycle arrest at G2/M phase</p> <p>-Inhibition of tubulin polymerization (Tested concentration)</p> <p>143, 144: 0.2 μM</p>	143,144: (144)

Table 2: Chalcones with antimitotic activity (continued).

Chalcones	Cell line	Targets/ associated process/ IC _{50/75} ^a or tested concentration ^b	Ref
 <p> I45: R_{3'}= Br; R_{5'}= Cl; R= 4-NEt₂-Ph I46: R_{3'}= Br; R_{5'}= Br; R= 4-NEt₂-Ph I47: R_{3'}= Br; R_{5'}= Cl; R= 4-CF₃-Ph I48: R_{3'}= Br; R_{5'}=Cl; R= 4-OCH₃-Ph I49: R_{3'}= Br R_{5'}= Cl R= phenyl I50: R_{3'}= Br; R_{5'}= Cl; R= 2-thienyl </p>	RPMI 8226, CCRF-CEM, U937-GTB, NCI-H69, 8226/Dox40 , 8226/LR5, CEM/VMI, U937/Vcr, H69AR, ACHN	<p>Inhibition tubulin polymerization (Tested concentration)</p> <p>I45-I50: 25 μM</p>	<p>I45-I50: (145)</p>
 <p> I51: R= phenyl I52: 1-benzyl-1H-indol-3-yl </p>	RPMI 8226, CCRF-CEM, U937-GTB, NCI-H69, 8226/Dox40 , 8226/LR5, CEM/VMI, U937/Vcr, H69AR, ACHN	<p>Inhibition tubulin polymerization(Tested concentration)</p> <p>I51,I52: 25 μM</p>	<p>I51,I52: (145)</p>
 <p>IPP51 (154)</p>	HeLa	<p>-Cell cycle arrest at G2/M phase</p> <p>-Inhibition tubulin polymerization</p> <p>I54: Tested concentration at: 5 μM</p>	<p>(146-147)</p>
 <p> I55: R₂=R₃=R₄=R₅=R₆=H I56: R₂=R₃=R₅=R₆=H; R₄=OCH₃ I57: R₂=OCH₃; R₃=R₄=R₅=R₆=H I58: R₂=R₃=OCH₃ ;R₄=R₅=R₆=H I59: R₂=R₃=R₄=OCH₃ ;R₅=R₆=H </p>	K562	<p>-Cell cycle arrest at G2/M phase</p> <p>-Inhibition tubulin polymerization (IC₇₅)</p> <p>I55: 2.77± 0.51 μM I56: 1.14± 0.21 μM I57: 2.94± 1.21 μM I58: 0.64± 0.15 μM</p>	<p>I55-I59: (148)</p>

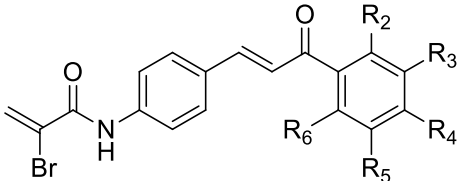
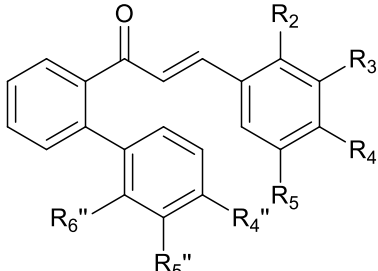
		159: $0.71 \pm 0.18 \mu\text{M}$	
 <p>160: $R_2=R_3=R_5=R_6=H$; $R_4=Br$ 161: $R_2=R_3=R_5=R_6=H$; $R_4=OEt$ 162: $R_2=Thienyl$; $R_3=R_4=R_5=R_6=H$</p>	K562	Inhibition tubulin polymerization (IC_{75}) 160: $0.84 \pm 0.18 \mu\text{M}$ 161: $0.85 \pm 0.21 \mu\text{M}$ 162: $0.82 \pm 0.13 \mu\text{M}$	160-162: (148)
 <p>163: $R_{5''}=R_2=R_5=H$; $R_3=OH$; $R_4=OCH_3$; $R_{4''}=F$; $R_{6''}=H$ 164: $R_{4''}=R_2=R_5=H$; $R_3=OH$; $R_4=OCH_3$; $R_{5''}=F$; $R_{6''}=H$ 165: $R_{4''}=R_2=R_5=H$; $R_{5''}=R_3=H$; $R_{6''}=OCH_3$; $R_4=B(OH)_2$ 166: $R_{4''}=R_2=R_5=H$; $R_{5''}=R_3=R_4=H$; $R_{6''}=N(CH_3)_2$</p>	A549	-Cell cycle arrest at G2/M phase -Inhibition tubulin polymerization (IC_{50}) 163: $1.3 \pm 0.0 \mu\text{M}$ 164: $3.4 \pm 0.2 \mu\text{M}$ 165: $3.6 \pm 0.0 \mu\text{M}$ 166: $0.49 \pm 0.27 \mu\text{M}$	163-166: (149)

Table 2: Chalcones with antimitotic activity (continued).

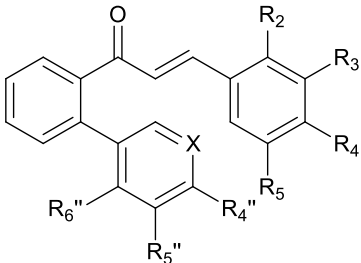
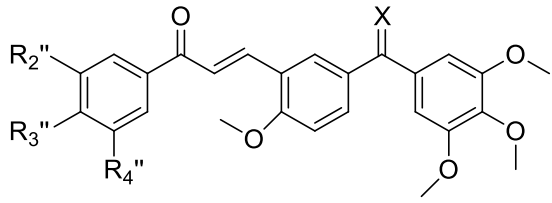
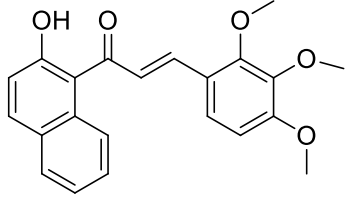
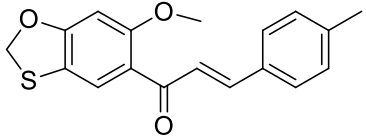
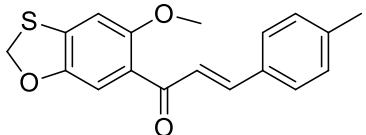
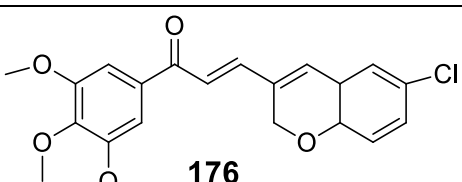
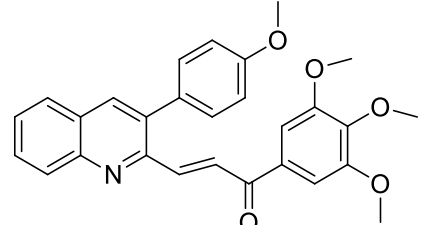
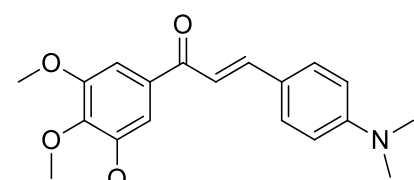
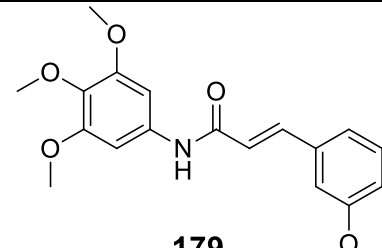
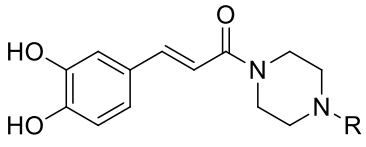
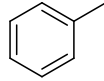
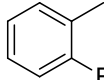
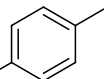
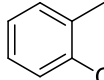
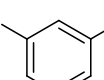
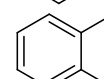
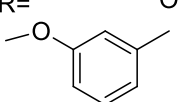
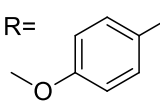
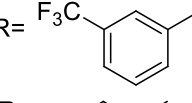
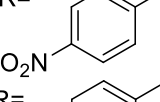
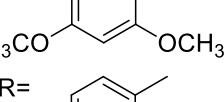
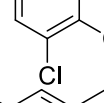
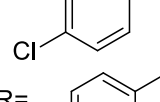
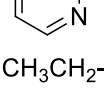
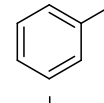
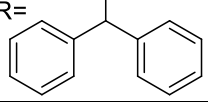
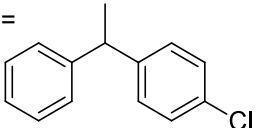
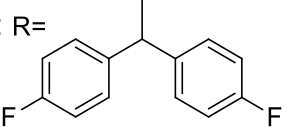
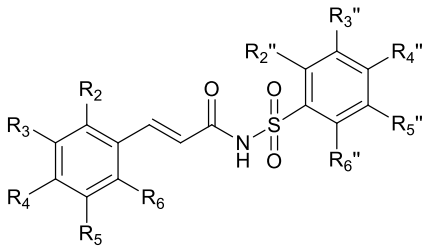
Chalcones	Cell line	Targets/ associated process/ IC _{50/75} ^a or tested concentration ^b	Ref
 <p>167: R_{4''}=R_{6''}=R₂=R₃=R₅=H; R_{5''}= F; X=CH; R₄=OCH₃ 168: R_{4''}=R_{6''}=R₂=R₃=R₅= H; R_{5''}= F; X=CH; R₄=OCH₃ 169: R_{4''}=R_{5''}= OCH₃; R_{6''}= R₂=R₅= H; R₃=OH; X=C(OCH₃); R₄=OCH₃</p>	A549	<p>-Cell cycle arrest at G2/M phase</p> <p>-Inhibition tubulin polymerization (IC₅₀)</p> <p>167: 1.8 ± 0.0 μM</p> <p>168: 4.0 ± 0.3 μM</p> <p>169: 2.8 ± 0.2 μM</p>	(149)
 <p>170: R_{2''}=H; R_{3''}=OCH₃; R_{4''}=NH₂; X=O 171: R_{2''}=H; R_{3''}=OCH₃; R_{4''}=OCH₃; X=O 172: R_{2''}=H; R_{3''}=OCH₂O; X=O</p>	MCF-7	<p>-Cell cycle arrest at G2/M phase</p> <p>-Inhibition tubulin polymerization (IC₅₀)</p> <p>170: 0.6 ± 0.03 μM</p> <p>171: 1.3 ± 0.10 μM</p> <p>172: 0.8 ± 0.02 μM</p>	(150)
 <p>HTN (173)</p>	HCT116	<p>Inhibition tubulin polymerization</p> <p>Cell cycle arrest at G2/M phase</p> <p>Tested concentration at: 10 μM</p>	(129)
 <p>AMG-175 (174)</p>	A549, HeLa, HHCT116	<p>Inhibition tubulin polymerization</p> <p>Cell cycle arrest at G2/M phase (IC₅₀)</p> <p>174: 5.80 μM</p>	(151)

Table 2: Chalcones with antimetabolic activity (*continued*).

Chalcones	Cell line	Targets/ associated process/ IC ₅₀ /75 ^a or tested concentration ^b	Ref
 AMG-190 (175)	A549, HeLa, HHCT116	Inhibition tubulin polymerization Cell cycle arrest at G2/M phase (IC₅₀) 175: 4.15 μM	(151-152)
 176	K562, SK-N-Mc	Inhibition tubulin polymerization (IC₅₀) 2.06 ± 0.22 μM	(153-154)
 177	MCF-7, MDA-MB-231, SKBR-3	-Cell cycle arrest at G2/M phase -Inhibition tubulin polymerization (IC₅₀) 14.4 ± 1.8 μM	(155)
 178	HeLa	- Cell cycle arrest at G2/M phase - Inhibition tubulin polymerization (IC₅₀) 2.8 μM	(130)
 179	HeLa	Cell cycle arrest at G2/M phase Tested concentration at: 25 μM	(156)

<p style="text-align: center;">  </p> <p>180: R= </p> <p>181: R= </p> <p>182: R= </p> <p>183: R= </p> <p>184: R= </p> <p>185: R= </p> <p>186: R= </p> <p>187: R= </p> <p>188: R= </p> <p>189: R= </p> <p>190: R= </p> <p>191: R= </p> <p>192: R= </p> <p>193: R= </p> <p>194: R= CH₃CH₂-</p> <p>195: R= </p> <p>196: R= </p>	HeLa	<p style="text-align: center;">-Cell cycle arrest at G2/M phase</p> <p style="text-align: center;">-Inhibition tubulin polymerization (IC₅₀)</p> <p>180: 3.14 ± 0.25 μM</p> <p>181: 7.78 ± 0.44 μM</p> <p>182: 7.39 ± 0.48 μM</p> <p>183: 5.46 ± 0.38 μM</p> <p>184: 5.28 ± 0.39 μM</p> <p>185: 1.72 ± 0.19 μM</p> <p>186: 3.08 ± 0.21 μM</p> <p>187: 1.86 ± 0.31 μM</p> <p>188: 5.89 ± 0.42 μM</p> <p>189: 4.86 ± 0.28 μM</p> <p>190: 2.98 ± 0.22 μM</p> <p>191: 4.42 ± 0.33 μM</p> <p>192: 4.93 ± 0.32 μM</p> <p>193: 11.61 ± 0.72 μM</p> <p>194: 12.78 ± 0.81 μM</p> <p>195: 9.28 ± 0.47 μM</p> <p>196: 0.92 ± 0.12 μM</p> <p>197: 1.56 ± 0.18 μM</p> <p>198: 1.44 ± 0.21 μM</p>	180-198: (157)
---	------	---	--------------------------

<p>197: R= </p> <p>198: R= </p>			
 <p>199: R₂'=R₃'=R₄'=R₅'=R₆'=R₂=R₃=R₄=R₅=R₆=H</p> <p>200: R₂'=R₃'=R₅'=R₆'=R₂=R₃=R₄=R₅=R₆=H; R₄'=CH₃</p> <p>201: R₂'=R₃'=R₅'=R₆'=R₂=R₃=R₄=R₅=R₆=H; R₄'=F</p> <p>202: R₂'=R₃'=R₅'=R₆'=R₂=R₃=R₄=R₅=R₆=H; R₄'=Cl</p> <p>203: R₂'=R₃'=R₅'=R₆'=R₂=R₃=R₄=R₅=R₆=H; R₄'=Br</p> <p>204: R₂'=R₃'=R₅'=R₆'=R₂=R₃=R₅=R₆=H; R₄'=F</p> <p>205: R₂'=R₃'=R₅'=R₆'=R₂=R₃=R₅=R₆=H; R₄'=F; R₄'=CH₃</p> <p>206: R₂'=R₃'=R₅'=R₆'=R₂=R₃=R₅=R₆=H; R₂'=H; R₄'=R₄'=F</p> <p>207: R₂'=R₃'=R₅'=R₆'=R₂=R₃=R₅=R₆=H; R₄'=F; R₄'=Cl</p> <p>208: R₂'=R₃'=R₅'=R₆'=R₂=R₃=R₅=R₆=H; R₄'=F; R₄'=Br</p> <p>209: R₂'=R₃'=R₅'=R₆'=R₂=R₃=R₄=R₅=R₆=H; R₄'=Cl</p> <p>210: R₂'=R₃'=R₅'=R₆'=R₂=R₃=R₅=R₆=H; R₄'=Cl; R₄'=CH₃</p> <p>211: R₂'=R₃'=R₅'=R₆'=R₂=R₃=R₅=R₆=H; R₄'=Cl; R₄'=F</p> <p>212: R₂'=R₃'=R₅'=R₆'=R₂=R₃=R₅=R₆=H; ; R₄'=R₄'=Cl</p> <p>213: R₂'=R₃'=R₅'=R₆'=R₂=R₃=R₅=R₆=H; R₄'=Cl; R₄'=Br</p> <p>214: R₂'=R₃'=R₄'=R₅'=R₆'=R₂=R₃=R₅=R₆=H; R₄'=Br</p> <p>215: R₂'=R₃'=R₅'=R₆'=R₂=R₃=R₅=R₆=H; R₄'=Br; R₄'=CH₃</p> <p>216: R₂'=R₃'=R₅'=R₆'=R₂=R₃=R₅=R₆=H; R₄'=Br; R₄'=F</p> <p>217: R₂'=R₃'=R₅'=R₆'=R₂=R₃=R₅=R₆=H; R₄'=Br; R₄'=Cl</p> <p>218: R₂'=R₃'=R₅'=R₆'=R₂=R₃=R₅=R₆=H; R₄'=R₄'=Br</p> <p>219: R₂'=R₃'=R₄'=R₅'=R₆'=R₂=R₃=R₅=R₆=H; R₄'=OCH₃</p> <p>220: R₂'=R₃'=R₅'=R₆'=R₂=R₃=R₅=R₆=H; R₄'=OCH₃; R₄'=CH₃</p> <p>221: R₂'=R₃'=R₅'=R₆'=R₂=R₃=R₅=R₆=H; R₄'=OCH₃; R₄'=F</p> <p>222: R₂'=R₃'=R₅'=R₆'=R₂=R₃=R₅=R₆=H; R₄'=OCH₃; R₄'=Cl</p> <p>223: R₂'=R₃'=R₅'=R₆'=R₂=R₃=R₅=R₆=H; R₄'=OCH₃; R₄'=Br</p> <p>224: R₂'=R₃'=R₅'=R₆'=R₂=R₃=R₄=R₅=R₆=H; R₄'=N(CH₃)₂</p> <p>225: R₂'=R₃'=R₅'=R₆'=R₂=R₃=R₅=R₆=H; R₄'=N(CH₃)₂; R₄'=CH₃</p> <p>226: R₂'=R₃'=R₅'=R₆'=R₂=R₃=R₅=R₆=H; R₄'=N(CH₃)₂; R₄'=F</p> <p>227: R₂'=R₃'=R₅'=R₆'=R₂=R₃=R₅=R₆=H; R₄'=N(CH₃)₂; R₄'=Cl</p> <p>228: R₂'=R₃'=R₅'=R₆'=R₂=R₃=R₅=R₆=H; R₄'=N(CH₃)₂; R₄'=Br</p> <p>229: R₂'=R₃'=R₄'=R₅'=R₆'=R₂=R₃=R₅=R₆=H; R₄'=NO₂</p> <p>230: R₂'=R₃'=R₅'=R₆'=R₂=R₃=R₅=R₆=H; R₄'=NO₂; R₄'=CH₃</p> <p>231: R₂'=R₃'=R₅'=R₆'=R₂=R₃=R₅=R₆=H; R₄'=NO₂; R₄'=F</p> <p>232: R₂'=R₃'=R₅'=R₆'=R₂=R₃=R₅=R₆=H; R₄'=NO₂; R₄'=Cl</p> <p>233: R₂'=R₃'=R₅'=R₆'=R₂=R₃=R₅=R₆=H; R₄'=NO₂; R₄'=Br</p> <p>234: R₂'=R₃'=R₄'=R₅'=R₆'=R₂=R₃=R₄=R₅=R₆=H; R₂'=NO₂</p> <p>235: R₂'=R₃'=R₅'=R₆'=R₂=R₃=R₄=R₅=R₆=H; R₂'=NO₂; R₄'=CH₃</p> <p>236: R₂'=R₃'=R₅'=R₆'=R₂=R₃=R₄=R₅=R₆=H; R₂'=NO₂; R₄'=F</p> <p>237: R₂'=R₃'=R₅'=R₆'=R₂=R₃=R₄=R₅=R₆=H; R₂'=NO₂; R₄'=Cl</p> <p>238: R₂'=R₃'=R₅'=R₆'=R₂=R₃=R₄=R₅=R₆=H; R₂'=NO₂; R₄'=Br</p>	<p>B16-F10</p>	<p>Cell cycle arrest at G2/M phase</p> <p>Inhibition tubulin polymerization (IC₅₀)</p> <p>199: 37 ± 5 μM</p> <p>200: 152 ± 3 μM</p> <p>201: 4.5 ± 0.4 μM</p> <p>202: 14.8 ± 0.3 μM</p> <p>203: 63 ± 1 μM</p> <p>204: 4.5 ± 0.5 μM</p> <p>205: 40 ± 8 μM</p> <p>206: 2.4 ± 0.4 μM</p> <p>207: 4.5 ± 0.2 μM</p> <p>208: 14.7 ± 0.7 μM</p> <p>209: 15.3 ± 0.7 μM</p> <p>210: 30 ± 1 μM</p> <p>211: 8.9 ± 0.2 μM</p> <p>212: 9.3 ± 0.5 μM</p> <p>213: 10.8 ± 0.6 μM</p> <p>214: 74 ± 8 μM</p> <p>215: 137 ± 14 μM</p> <p>216: 3.8 ± 0.2 μM</p> <p>217: 55 ± 1 μM</p> <p>218: 53 ± 6 μM</p> <p>219: 160 ± 9 μM</p> <p>220: 146 ± 5 μM</p> <p>221: 45 ± 7 μM</p> <p>222: 52 ± 3 μM</p> <p>223: 53 ± 8 μM</p> <p>224: 26 ± 2 μM</p>	<p>199-224: (158)</p>

		225: 37 ± 4 μM 226: 10 ± 5 μM 227: 14 ± 3 μM 228: 34 ± 5 μM 229: 50 ± 1 μM 230: 151 ± 12 μM 231: 6.3 ± 0.3 μM 232: 134 ± 14 μM 233: 163 ± 12 μM 234: 74 ± 9 μM 235: 102 ± 13 μM 236: 69 ± 5 μM 237: 78 ± 3 μM 238: 134 ± 10 μM	
--	--	---	--

^aIC₅₀: compound concentration required to inhibit tumor cell proliferation by 50%, IC₇₅: compound concentration required to inhibit tumor cell proliferation by 75%. ^b lower tested concentration

MCF-7: Breast adenocarcinoma; K562 :Human leukemic; BT20: Breast adenocarcinoma; KB: breast carcinoma ; OVCAR-3: Ovarian carcinoma; HeLa: Cervical adenocarcinoma; Jurkat: Human blood cancer; PBMCs: Peripheral blood mononuclear ; HepG2: Hepatocyte carcinoma; SV40T3: Simian virus ; HDMEC: Human endothelial cancer; NCI-H460: hypotriploid human cancer ; HCT116: Colon carcinoma ; Capan-1: Pancreatic adenocarcinoma; LLC: Lung carcinoma; PC-14: Lung carcinoma; HeLa S3: Cervix adenocarcinoma; GL26C, GL26T, U118C, U118T, U138C, U138T, LN229C, LN229T: Glioblastoma; B16-F10: Musculus skin melanoma ; NTUB1: Urothelial carcinoma; SNU-398: ; RPMI 8226: myeloma; CCRF-CEM: Leukemia ; NCI-H69: Small-cell lung cancer; 8226/DOX40: Doxorubicin resistant myeloma; 8226/LR5: Melphalan resistant myeloma; CEM/VMI: Teniposide resistant leukemia; H69AR: ; ACHN: Renal adenocarcinoma; U937-GTB: Lymphoma; HCT116: Colon colorectal carcinoma; SK-N-Mc: brain carcinoma; MDA-MB-231: Breast adenocarcinoma; SKBR-3: mammary gland/breast adenocarcinoma.

1.3. Aims and Overview

The main purpose of this dissertation was to obtain chalcone derivatives with antimitotic activity. Inspired by the potential of natural chalcones as antimitotic agents, namely chalcone **CPX (60, Table 2)**, already described by LQOF-FFUP research group as affecting microtubules (5), we aimed to synthesize structure related A ring analogues using the strategy of isosteric substitution as well as rigidification. In order to obtain isosters of **CPX (60)** six different acetophenones (**A0, A4, A5, ABF, ABT** and **ACI**) and 3,4,5-trimethoxybenzaldehyde were used as building blocks (**Figure 30**).

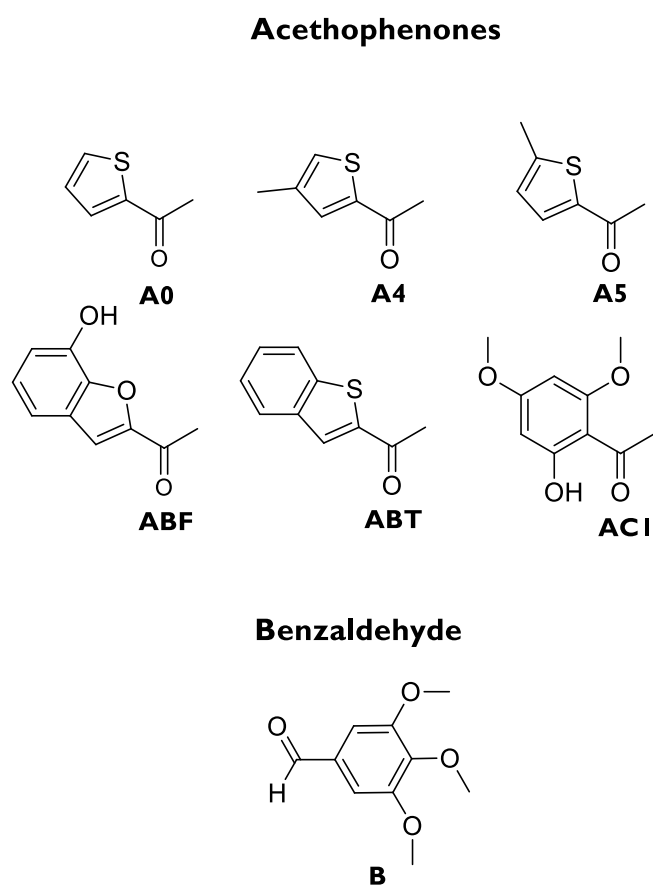


Figure 30: Building blocks used for the synthesis of chalcones.

Regarding the strategy of rigidification, as chalcones are interesting intermediates for the synthesis of bioactive heterocyclic compounds, chalcone derivatives such as pyrazole and isoxazole derivatives were also synthesized by molecular modification of chalcones enone moiety.

Chapter 2:

Results and Discussion

2.1. Chemistry

2.1.1. Synthesis

Chalcones were synthesized by base-catalyzed Claisen-Schmidt condensation of appropriately substituted acetophenones with the 3,4,5-trimethoxybenzaldehyde. The chalcones synthesized by this reaction include A-ring substituents supplied by the acetophenone and B-ring substituents given by the benzaldehyde (**Figure 31**).

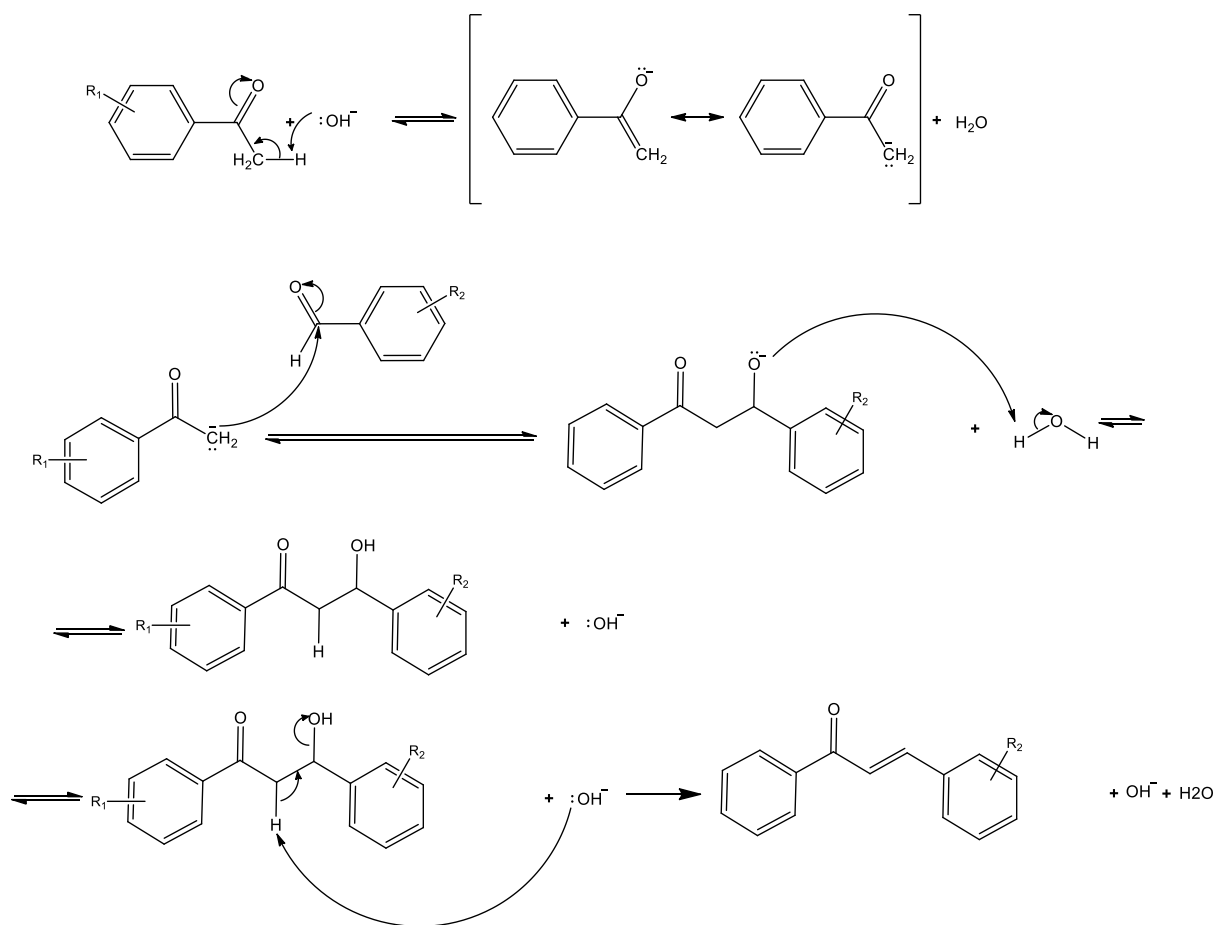


Figure 31: Reaction mechanism of Claisen-Schmidt condensation.

As described before, the synthesis of chalcones can be performed by Claisen-Schmidt condensation using conventional heating or MW irradiation. Therefore, these two methodologies were applied for the synthesis of chalcone **P5** in order to decide the best methodology to synthesize chalcone derivatives.

Chalcone **P5** was synthesized by the reaction of 2-acetyl-5-methylthiophene with 3,4,5-trimethoxybenzaldehyde in the presence of NaOH (**Table 3**).

Table 3: Reaction Conditions used to synthesize chalcone P5.

Reaction Conditions	Yield
65°C, 24h 30 min	13%
MW, 65 °C, 180W, 3h 30 min	16%

By conventional heating chalcone **P5** was obtained with only 13% yield with a very long reaction time (24 h 30 min). Several attempts to purify **P5** by flash column chromatography (CC) and crystallization were performed to fulfil purification, since it was clear the presence of impurities hard to separate from **P5**, namely 3,4,5-trimethoxybenzaldehyde, used as building block in excess. This was the main challenge and the reason for the low yield.

The synthesis by MW irradiation provided **P5** with almost the same yield (16%), once the purification process was also difficult, because of the similarity of retention factor of **P5** and 3,4,5-trimethoxybenzaldehyde, used as building block in excess. Nevertheless, the reaction time was reduced from 24 h 30 min in the conventional heating to only 3 h 30 min in MAOS. Consequently, the other chalcones (**P4**, **BT**, **BF**, and **CI**) were synthesized by MAOS (**Figure 32**).

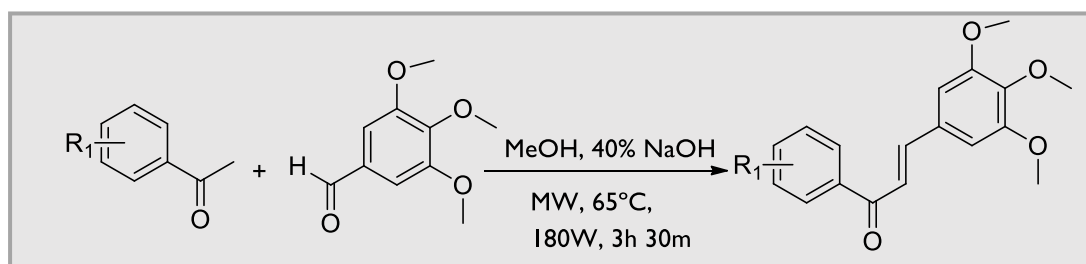
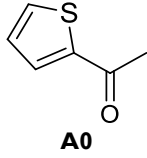
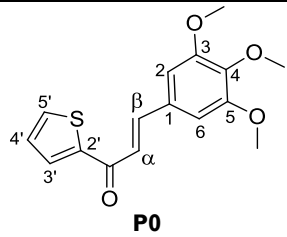
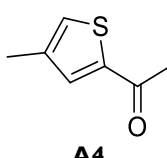
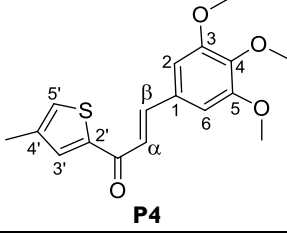
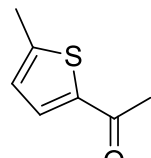
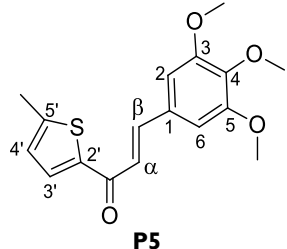
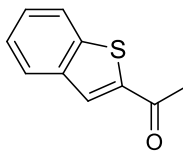
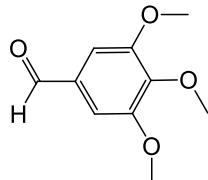
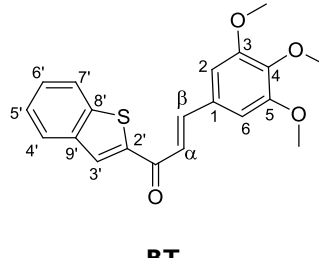
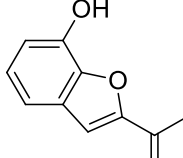
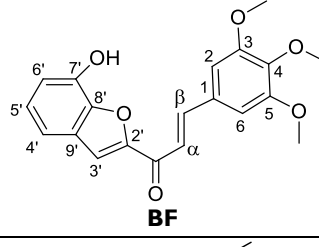
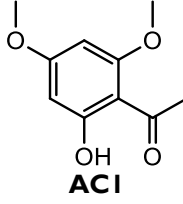
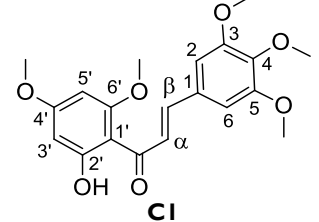


Figure 32: Synthesis of chalcone derivatives by MAOS.

Table 4 summarizes the reaction conditions, obtained products and the corresponding yield for the synthesis of chalcones **P0**, **P4**, **P5**, **BT** and **BF**.

Table 4: Synthesized chalcones, with their respective yields and reaction time.

Ketone	Benzaldehyde	Product	Time (min)	Yield (%)
 A0		 P0	3-4h	61
 A4		 P4		55
 A5		 P5		16
 ABT	 B	 BT		38
 ABF		 BF		12
 ACI		 CI		14

Chalcones **P0** and **P4** were obtained in good yields (61% and 55%, respectively). For all other reactions the obtained yields were low (12-38%), being this associated with the time consuming work-up procedures for purification, which involved a sequence of two CC procedures followed by crystallization.

2.1.2. Molecular modification of chalcone derivatives

Chalcones are interesting intermediates for the synthesis of heterocyclic compounds by molecular modification of the three-carbon α,β -unsaturated carbonyl system. In fact, possessing two electrophilic reactive centers at α,β -unsaturated ketone group, chalcones can participate in addition reactions via attack to the carbonyl group (1,2-addition) or involving the β carbon (1,4-conjugate addition), leading to the synthesis of promising bioactive compounds with a more rigid structure (42). Therefore, isoxazole and pyrazole derivatives have been synthesized by molecular modification of chalcones (**Figure 33**).

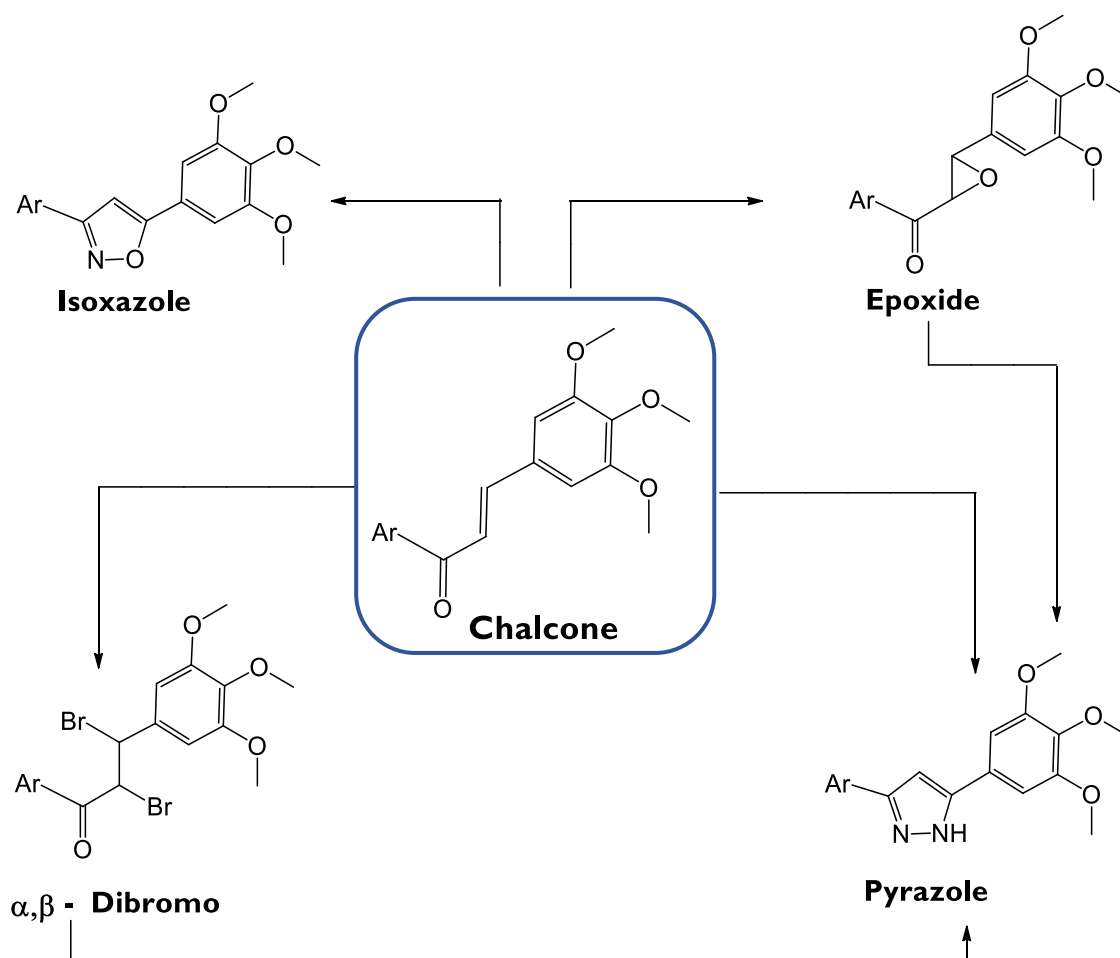


Figure 33: Synthesis of isoxazoles and pyrazoles by molecular modification of chalcones.

2.1.2.1. Synthesis of isoxazole derivatives

3,5-Diarylisoaxazoles can be prepared through the reaction of chalcones with hydroxylamines in the presence of NaOAc and glacial acetic acid (AcOH) (90, 96).

Alternatively, several authors used the same reaction in the presence of NaOH (159) or KOH (160-162) as base and ethanol as solvent.

The **P0**, **P4** and **BT** were used as building blocks for the synthesis of the isoxazole derivatives by the reaction with hydroxylamine hydrochloride in the presence of anhydrous NaOAc and glacial acetic acid in ethanol by MW irradiation (**Figure 34**) (89).

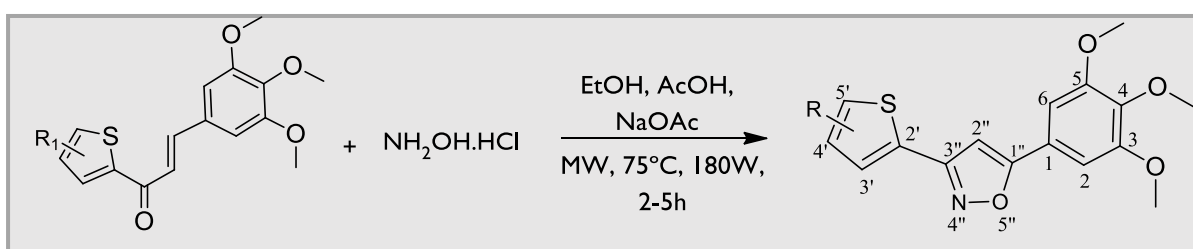
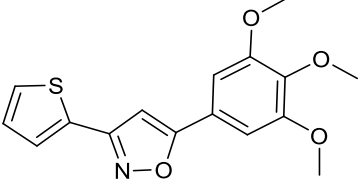
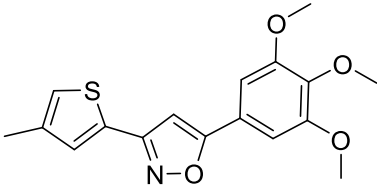
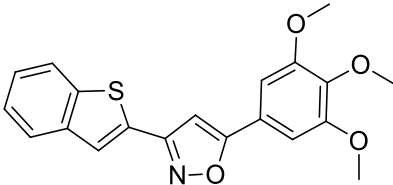


Figure 34: Synthesis of isoxazole derivatives.

Table 5 summarizes the reaction conditions and the results obtained for the synthesis of isoxazole derivatives.

Table 5: General experimental conditions for the synthesis of isoxazole derivatives (**P0-iso**, **P4-iso** and **BT-iso**).

Building block	Reaction conditions	Expected Products	Yield (%)
P0	NH ₂ OH.HCl, EtOH, AcOH, NaOAc, MW, 75°C, 180W, 3h	 <p>P0-iso</p>	22
P4		 <p>P4-iso</p>	N.O.
BT	NH ₂ OH.HCl, EtOH, AcOH, NaOAc, MW, 75°C 180W, 3h 30 min	 <p>BT-iso</p>	N.O.
	NH ₂ OH.HCl, EtOH, 40% NaOH, MW, 75- 100°C, 180-250W, 5 h		

N.O.: No product was obtained.

Derivative of chalcone **P0 (P0-iso)** was obtained in low yield (22%) as several products were detected in the reaction mixture, being needed a time consuming purification procedure which involved flash CC followed by preparative thin layer chromatography (TLC).

For the synthesis of derivatives **P4-iso** and **BT-iso** a complex mixture was obtained in the crude product being not possible to isolated the derivative even after flash CC and TLC purification procedures. Consequently, for the synthesis of **BT-iso** other reaction conditions were tried. Instead of the using NaOAc and glacial acid acetic in ethanol, the reaction with hydroxylamine hydrochloride was carried out in the presence of 40% sodium hydroxide in ethanol as described by *Patil et al.*, (91). Once again no product was detected in the reaction mixture after 5h.

2.1.2.2 Synthesis of pyrazole derivatives

Different methodologies for the generation of pyrazole derivatives are described in literature, namely one pot synthesis in which pyrazoles are synthesized by direct molecular modification of chalcones, and two steps reactions involving the conversion of chalcones to intermediates, such as chalcone epoxides and chalcones dibromides, which afterward are converted to pyrazoles. In this research work both one pot and two step approaches were used aiming to synthesize pyrazole derivatives, as described in the next sections.

2.1.2.2.1 Synthesis of pyrazole derivatives by one-pot synthesis

The first synthetic approach used for the synthesis of pyrazole derivatives was according to the one-pot method reported by *Ponnala et al.* for the synthesis of 1,3,5-trisubstituted pyrazoles, which was based on the cyclization of chalcones with a hydrazine derivative (phenylhydrazine) in the presence of iodine and anhydrous AcOH (**Figure 35**). (79-80).

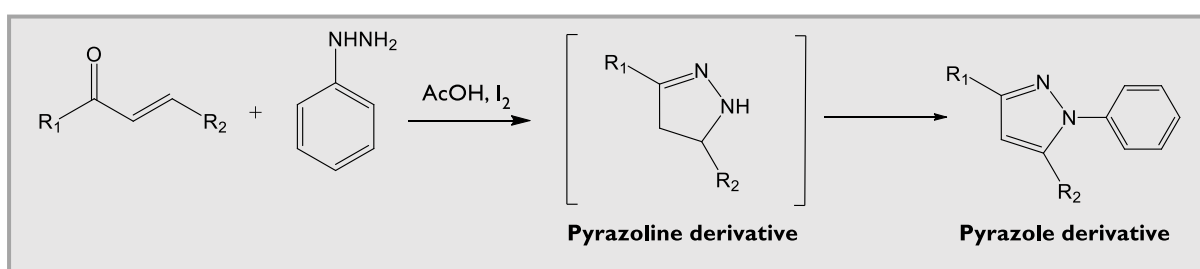


Figure 35: Synthesis of 1,3,5-trisubstituted pyrazole derivatives by *Ponnala et al.* (79).

In this research work hydrazine hydrate was used instead of phenylhydrazine, in order to synthesize the 3,5-disubstituted pyrazole derivative of chalcone **CI**, instead of the correspondent 1,3,5-trisubstituted pyrazole derivative. After purification by flash CC and TLC, the intermediate pyrazoline derivative **CI-pyrz (Figure 36)** was obtained, with 48% yield, instead of the pyrazole derivative.

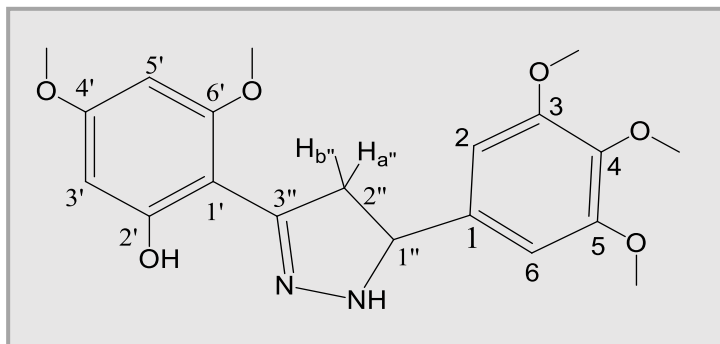


Figure 36: Structure of **CI-pyrz**.

As the one-pot synthesis approach failed to give the desired pyrazole derivative other approaches were carried out in order to synthesize the other pyrazole derivatives. Therefore, pyrazole derivatives were obtained by a two steps reaction involving firstly the synthesis of chalcone dibromides or chalcone epoxides and after the reaction of these intermediates with hydrazine hydrate to synthesize the correspondent pyrazoles, as described in the next sections.

2.1.2.2.2. Synthesis of pyrazole derivatives by two steps

synthesis

Taking into account the low chemical stability of oxirane rings the first strategy to synthesize pyrazole derivatives was through a two steps reaction involving the synthesis of α,β -dibromo chalcones as intermediates. Chalcone bromide **P0-br** was obtained by bromination of chalcone **P0** in carbon tetrachloride with bromine (**Figure 37**) (88).

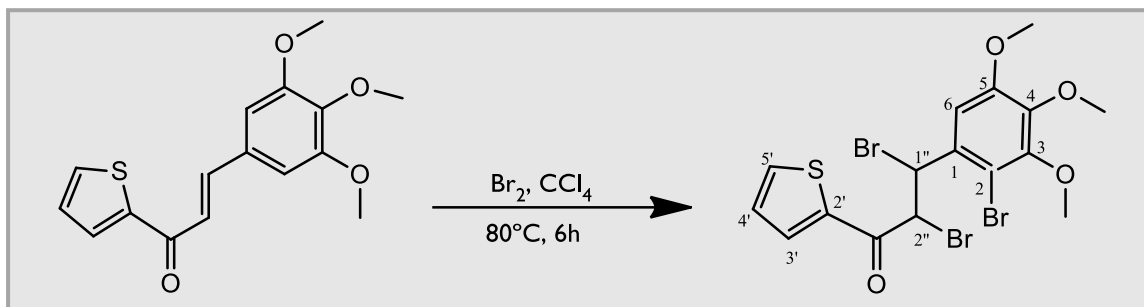


Figure 37: Synthesis of chalcone **P0-br**.

Instead of the expected α,β -dibromo chalcone, a tribromide derivative was obtained containing an additional bromine atom at C-2, with 78% yield. The formation of this product can be explained by the presence of three electron donating groups on B ring of chalcone **P0** that activates C-2 and C-6.

Consequently, pyrazole derivatives were synthesized by a two steps reaction involving the synthesis of chalcone epoxides as intermediates. Taking into account green chemistry principles, aqueous hydrogen peroxide is one of the oxidants of choice to prepare epoxides because of its ease of handling, high active oxygen content and the formation of water as the only by-product. Therefore, chalcone epoxides **P0-epo**, **P4-epo** and **BT-epo** were obtained by oxidation of chalcones with hydrogen peroxide in basic medium (**Figure 38**), according to the method reported by *LeBlac et al.* (93).

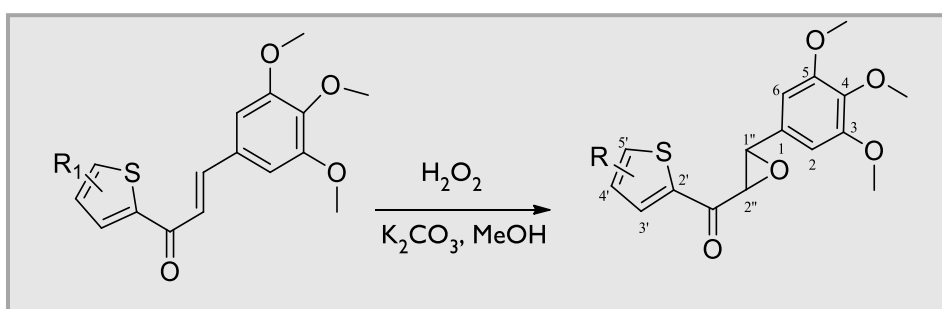
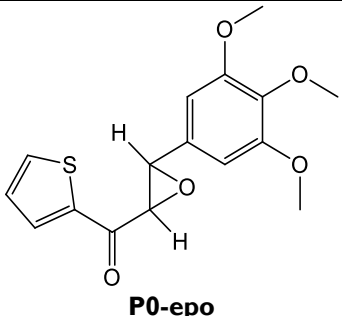
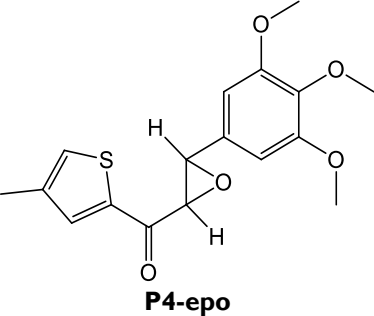
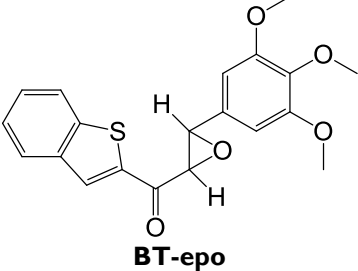


Figure 38: Synthesis of chalcone epoxides.

Table 6 summarizes the reaction conditions and the results obtained in the synthesis of epoxide derivatives.

Table 6: Synthesis of chalcone epoxides.

Building block	Reaction conditions	Product	Yield (%)
P0	K ₂ CO ₃ , MeOH, H ₂ O ₂ , r.t., 3-8h	 <p>P0-epo</p>	46
P4		 <p>P4-epo</p>	41
BT		 <p>BT-epo</p>	23

The epoxides **P0-epo**, **P4-epo** and **BT-epo** were obtained in 46%, 41% and 23% yield, respectively. The purification by crystallization of these compounds was not easy and contributed to the low yield obtained.

After the epoxidation step, pyrazole derivative **P0-epo** was synthesized by the reaction with hydrazine hydrate in the presence of *p*-toluenesulfonic acid in xylenes and dichloromethane (**Figure 39**) (93).

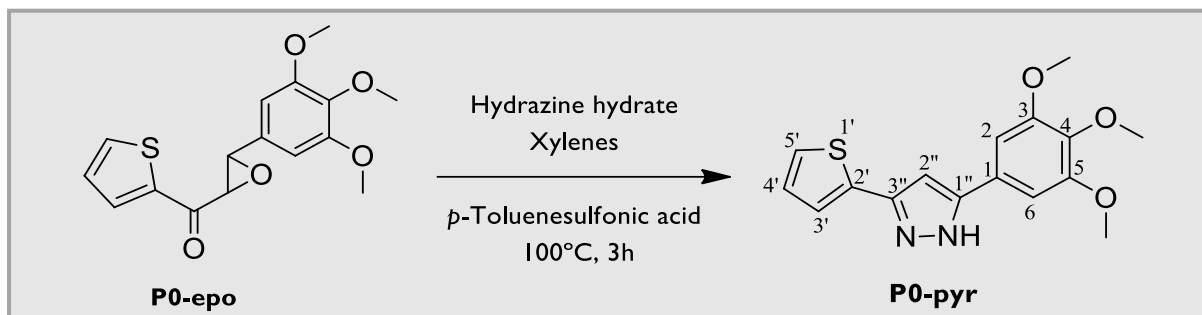


Figure 39: Synthesis of **P0-pyr**.

P0-pyr was obtained with a 4% yield. The low yield can be explained by the fact that this reaction was incomplete. Moreover, as more than one product was formed, a time consuming purification by flash CC and TLC was necessary to purify this product.

2.2. Structure Elucidation

2.2.1. Chalcones

The IR data of all chalcones were in accordance with the performed molecular modification (**Table 7**). Accordingly, this spectra revealed the presence of a large band of stretching vibration between 1627-1648 cm^{-1} , suggesting the formation of a α,β -unsaturated ketone moiety. In addition, the observation of bands at 2997-2823 cm^{-1} (aliphatic C-H), 1583-1403 cm^{-1} (C=C) and 1287-1248 cm^{-1} (C-O) were observed for all synthesized compounds.

Table 7: IR data of chalcones **P0**, **P4**, **P5**, **BT**, **BF** and **CI**.

Groups	ν (cm^{-1})					
	P0	P4	P5	BT	BF	CI
OH	-	-	-	-	3447	3469 3401
Aliphatic C-H	2971 2919 2832	2963 2917 2823	2997 2920 2849	2961 2918 2849	2918 2849	2966 2917 2831
C=O	1645	1648	1647	1641	1648	1627
C=C	1577 1467 1434 1415	1578 1504 1453 1416	1578 1560 1434 1420	1583 1503 1462 1422	1597 1578 1484	1572 1494 1436 1403
C-O	1287	1248	1283	1250	1287	1268

The ^1H and ^{13}C NMR data of chalcones **P0**, **P4**, **P5**, **BT**, **BF** and **CI** are reported in **Table 8** and **Table 9** respectively. The ^1H and ^{13}C NMR data of all synthesized chalcones have in common the signals of α,β -unsaturated ketone system (H_α : δ 7.70-7.26 d, C_α : δ 126.9-120.1, H_β : δ 7.89-7.74 d, C_β : δ 145.3-142.4, $\text{C}=\text{O}$: δ 192.3-179.5). The coupling constants of the vinylic system ($J_{\text{H}_\alpha\text{-H}_\beta} = 15.6\text{-}15.4$) confirm their (*E*) configuration. Additionally, the presence of two singlets of 6 protons at δ_{H} 3.96-3.92 s and one singlet of 3 protons at δ_{H} 3.92-3.90 s correlated with the signals at δ_{C} 56.6-56.2, and δ_{C} 61.1-61.0 in the 2D heteronuclear single quantum correlation (HSQC) spectra revealed the presence of three methoxy groups on B-ring linked to C-3, -5 and C-4, respectively. Also the signals of two equivalent aromatic protons in the positions -2 and -6 of the same ring were observed in ^1H NMR spectra (δ_{H} 6.91- 6.84 s) and ^{13}C NMR spectra (δ_{C} 106.1-105.6), confirming the presence of a 3,4,5-trimethoxyphenyl B ring for all synthesized chalcones.

As the precursor, for chalcone **P0** the characteristic signals of a thiophene A ring were observed in the ^1H and ^{13}C NMR data (H-5': δ_{H} 7.89 dd, H-3': δ_{H} 7.69 dd, H-4': δ_{H} 7.20 dd, C-5': δ_{C} 131.8, C-3': δ_{C} 133.9 and C-4': δ_{C} 128.2).

Alternatively for chalcones **P4** and **P5**, the NMR spectra revealed the presence of a 4-methyl or 5-methylthiophene A ring, respectively. In fact, instead of three double doublets between δ_{H} 7.89-7.20 observed for the signals of A ring of chalcone **P0**, only two signals of aromatic protons were observed in the ^1H NMR spectra of **P4** and **P5** and a signal of a methyl group (δ_{H} 2.34 and 2.57 s for **P4** and **P5**, respectively).

Instead of these signals for chalcone **BT** ^1H and ^{13}C NMR spectra display characteristic signals of a benzothiophene A ring, namely a singlet at δ_{H} 8.13 (H-3') correlated by HSQC to the signal at δ_{C} 128.8, and two multiplets for 2 aromatic protons at δ_{H} 7.95-7.90 (H-4' and H-7') and δ_{H} 7.52-7.41 (H-5' and H-6') correlated by HSQC to the carbon atoms signals at δ_{C} 125.9 and 125.1 (C-4' and C-7') and δ_{C} 127.5 and 127.4 (C-5' and C-6').

For chalcone **BF** ^1H and ^{13}C NMR spectra put in evidence the presence of a 2-hydroxybenzofuran A ring. Accordingly, one singlet at δ 7.68 correlated by HSQC with the signal at δ_{C} 114.2, two coupled double doublets at δ_{H} 7.29 dd and δ_{H} 7.06 dd, correlated by HSQC with the signals at δ_{C} 115.0 and δ_{C} 114.2, and a triplet at δ_{H} 7.21, correlated by HSQC with the signal δ_{C} 125.1, are observed in the ^1H NMR spectrum.

^{13}C NMR assignments were confirmed by HSQC and heteronuclear multiple bond correlation (HMBC) experiments.

Figure 40 represents the main correlations observed in the HMBC spectra of chalcones **P0**, **P4**, **P5**, **BT**, **BF** and **CI**.

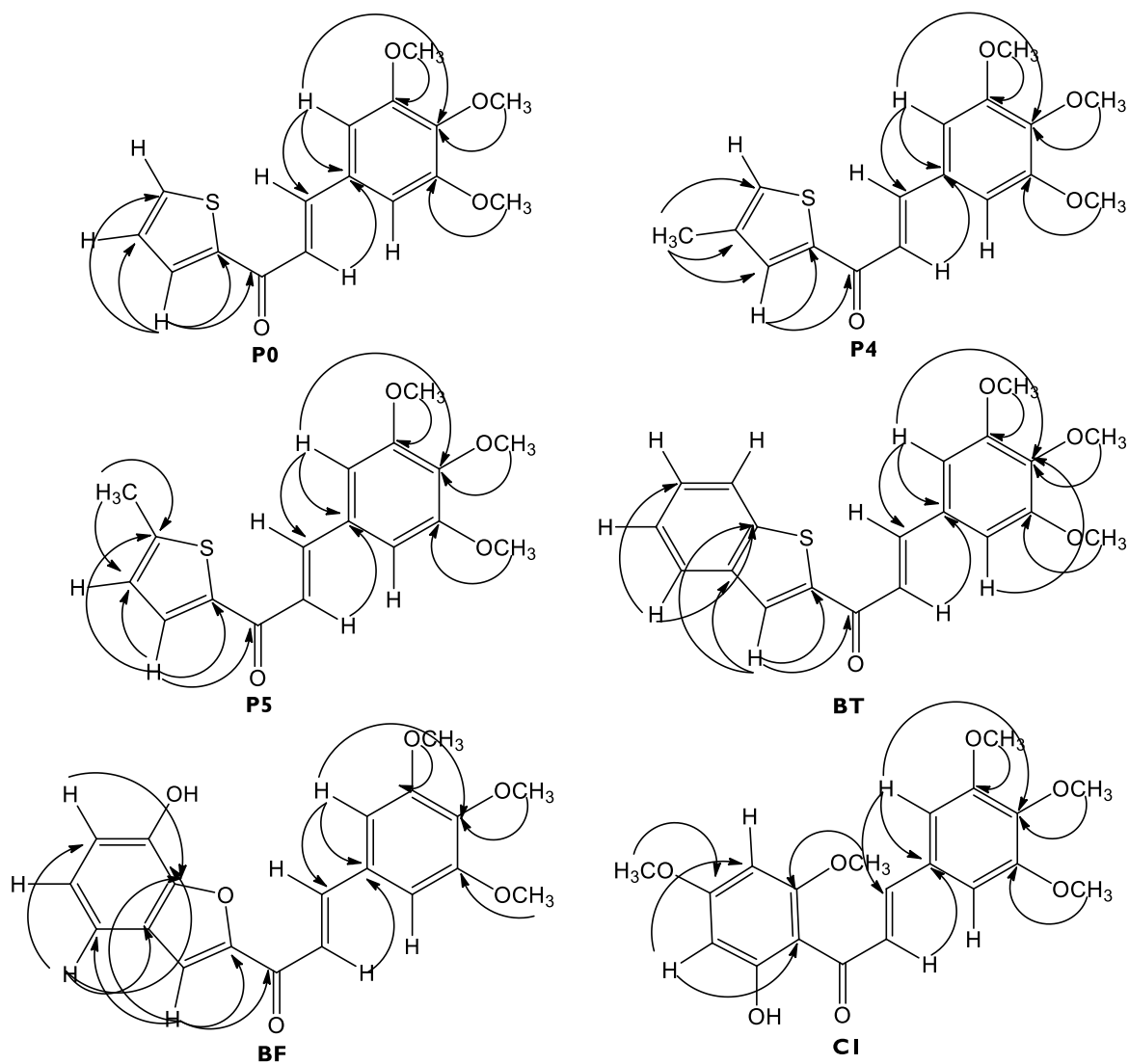


Figure 40: Main correlations found in the HMBC spectra of chalcones.

For chalcones **P0** and **CI** the ^1H and ^{13}C NMR data obtained are in accordance to the published data (163-166).

Table 8: ^1H NMR data of chalcones **P0**, **P4**, **P5**, **BT**, **BF** and **CI**.

	P0	P4	P5	BT	BF	CI
H-2, -6	6.87 (s)	6.86 (s)	6.85 (s)	6.91(s)	6.91(s)	6.84 (s)
3,5 - OCH ₃	3.93 (s)	3.93 (s)	3.93 (s)	3.96(s)	3.94 (s)	3.92 (s)
4 - OCH ₃	3.90 (s)	3.90 (s)	3.90 (s)	3.92(s)	3.92 (s)	3.90 (s)
H- α	7.31 (d, J=15.6)	7.27 (d, J=15.5)	7.26 (d, J=15.5)	7.58 (d, J=15.5)	7.43(d, J=15.6)	7.70 (d, J=15.6)
H- β	7.78 (d, J=15.5)	7.76 (d, J=15.5)	7.74 (d, J=15.4)	7.83 (d, J=15.5)	7.89 (d, J=15.6)	7.80 (d, J=15.6)
2'-OH	-	-	-	-	-	14.32 (s)
H-3'	7.69 (dd, J=5.0, 1.1)	7.69 (brd, J=1.2)	7.70 (d, J= 3.5)	8.13 (s)	7.68 (s)	5.96 (d, J=2.4)
H-4'	7.20 (dd, J=5.0, 3.8)	-	6.87 (d, J= 3.5)	7.95-7.90 (m)	7.29 (dd, J=7.8, 1.1)	-
4'-OCH ₃	-	-	-	-	-	3.91 (s)
4'-CH ₃	-	2.34 (s, -CH ₃)	-	-	-	-
H-5'	7.89 (dd, J=3.8, 1.1)	7.23 (dd, J=1.3, 1.1)	-	7.52-7.41 (m)	7.21 (t, J= 7.8)	6.11 (d, J=2.4)
5'-CH ₃	-	-	2.57 (s, -CH ₃)	-	-	-
H-6'	-	-	-	7.52-7.41 (m)	7.06 (dd, J=7.7, 1.1)	-
6'-OCH ₃	-	-	-	-	-	3.84 (s)
H-7'	-	-	-	7.95-7.90 (m)	-	-
7'-OH	-	-	-	-	n.o.	-
n.o. not observed; Values in parts per million (δ_{H}). Measured in CDCl ₃ at 300.13 MHz. J values (Hz) are presented in parentheses.						

Table 9: ^{13}C RMN data of chalcones compounds **P0**, **P4**, **P5**, **BT**, **BF** and **CI**.

	P0	P4	P5	BT	BF	CI
C-1	130.2	130.7	130.4	130.1	130.0	131.1
C-2,-6	105.7	105.7	105.6	105.8	106.1	105.6
C-3,-5	153.5	153.5	153.5	153.5	153.5	153.4
3,5-OCH ₃	56.3	56.3	56.2	56.3	56.3	56.6
C-4	140.5	140.4	140.3	140.7	140.9	140.1
4-OCH ₃	61.0	61.0	61.0	61.1	61.1	61.0
C- α	120.9	120.9	120.8	120.4	120.1	126.9
C- β	144.3	144.0	143.4	144.6	145.3	142.4
CO	182.0	181.9	181.5	183.3	179.5	192.3
C-1'	-	-	-	-	-	106.3
C-2'	145.5	145.0	143.6	143.0	153.6	162.4
C-3'	133.9	133.7	132.4	128.8	114.2	93.8
C-4'	128.2	139.0	126.9	125.9	115.0	168.4
4'-CH ₃	-	15.5	-	-	-	-

Table 9: ^{13}C RMN data of chalcones compounds (**P0**, **P4**, **P5**, **BT**, **BF** and **CI**) (continued).

	P0	P4	P5	BT	BF	CI
4'-OCH ₃	-	-	-	-	-	55.8
C-5'	131.8	129.8	150.1	127.5	114.2	91.3
5'-CH ₃	-	-	16.2	-	-	-
C-6'	-	-	-	125.1	125.9	166.2
6'-OCH ₃	-	-	-	-	-	52.8
C-7'	-	-	-	123.1	141.8	-
C-8'	-	-	-	145.2	144.6	-
C-9'	-	-	-	139.3	128.8	-
Values in parts per million (δ_c). Measured in CDCl ₃ at 75.47 MHz.						

2.2.2. Isoxazole derivatives **P0-iso**

In the IR spectrum of chalcone derivative **P0-iso** (**Table 10**) no band of stretching vibration characteristic of an α,β -unsaturated carbonyl system is observed, indicating the molecular modification of this moiety. Moreover, this spectrum revealed the presence of a large band of stretching vibration at 1387cm^{-1} (C-N) and 3444cm^{-1} (N-H) suggesting the formation of an isoxazole ring. In addition, the observation of bands between $2963\text{-}2850\text{cm}^{-1}$ (aliphatic C-H), $1540\text{-}1426\text{cm}^{-1}$ (C=C) and 1261cm^{-1} (C-O) were observed.

Table 10: IR data of isoxazole derivative **P0-iso**.

	ν (cm^{-1})
Groups	P0-iso
Aliphatic C-H	2963
	2918
	2850
Aromatic C=C	1540
	1470
	1426
C-O	1261
C-N	1387
N-H	3444

The ^1H and ^{13}C NMR data of chalcone derivative **P0-iso** are reported in **Table 11**. These spectra revealed the signals of A and B rings observed in the ^1H and ^{13}C NMR of its precursor (**P0**) (**Table 8** and **Table 9**). Nevertheless, instead of the signals of an α,β -unsaturated carbonyl system observed for **P0**, characteristic signals of an isoxazole ring are observed in the ^1H and ^{13}C NMR spectra, namely the signal of a proton at $\delta_{\text{H}} 6.60\text{ s}$ (H-2'') linked to a carbon at $\delta_{\text{C}} 97.3$ (C-2'') and signal of carbons at $\delta_{\text{C}} 165.5$ (C-3'') and $\delta_{\text{C}} 162.8$ (C-1'').

^{13}C NMR assignments were confirmed by HSQC and HMBC experiments. The main correlations observed in the HMBC spectrum are represented in **Figure 4I**.

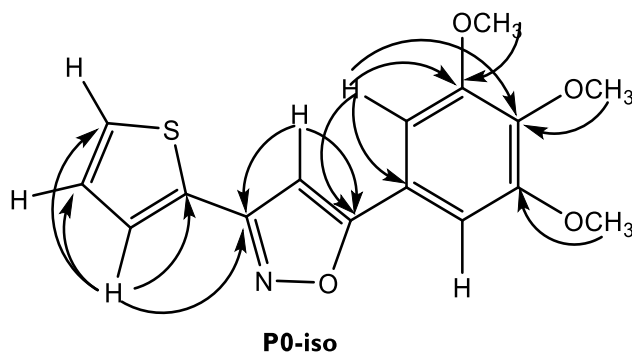


Figure 4I: Main correlations found in the HMBC spectrum of **P0-iso**.

Table II: ^1H NMR^a and ^{13}C NMR^b data of isoxazole derivative **P0-iso**.

	δ_{H}		δ_{C}
H-2,-6	7.07 (s)	C-1	124.3
H-3'	7.48 (dd, $J=5.1, 1.1$)	C-2,-6	104.1
H-4'	7.15 (dd, $J=5.5, 3.8$)	C-3,-5	153.6
H-5'	7.57 (dd, $J=3.8, 1.1$)	C-4	140.0
3,5 - OCH ₃	3.95 (s)	3,5-OCH ₃	56.3
4 - OCH ₃	3.91 (s)	4-OCH ₃	61.0
H-2''	6.66 (s)	C-2'	129.2
	-	C-3'	128.2
	-	C-4'	127.1
	-	C-5'	128.1
	-	C-1''	162.8
	-	C-2''	97.3
	-	C-3''	165.5

^aValues in parts per million (δ_{H}). Measured in CDCl₃ at 300.13 MHz. J values (Hz) are presented in parentheses.
^bValues in parts per million (δ_{C}). Measured in CDCl₃ at 75.47 MHz.

2.2.3. Pyrazoline derivative **CI-pyrz**

Instead of the band characteristic of an α,β -unsaturated carbonyl system observed in the IR spectrum of chalcone derivative **CI**, the spectrum of derivative **CI-pyrz** (**Table 12**) revealed the presence of large bands of stretching vibration at 1619 cm^{-1} (C-N) and 3431 cm^{-1} (N-H), suggesting the formation of a pyrazoline ring by molecular modification the enone moiety. In addition, the observation of bands at $2919\text{-}2850\text{ cm}^{-1}$ (aliphatic C-H), $1593\text{-}1459\text{ cm}^{-1}$ (C=C) and 1266 cm^{-1} (C-O) were observed.

Table 12: IR data of pyrazoline derivative **CI-pyrz**.

Groups	$\nu\text{ (cm}^{-1}\text{)}$ CI-pyrz
Aliphatic C-H	2919
	2850
Aromatic C=C	1593
	1508
	1459
C-O	1266
C-N	1619
N-H	3431

The ^1H and ^{13}C NMR data of chalcone derivative **CI-pyrz** are reported in **Table 13**. This derivative revealed the signals of A and B rings observed in the ^1H NMR and ^{13}C NMR of its precursor (**CI**) (**Table 8** and **Table 9**). In addition, the signals of two coupled protons at δ_{H} 3.03 dd and δ_{H} 2.79 dd linked to a carbon atom at δ_{C} 45.8 (C-2'') and one proton at δ_{H} 5.34 dd linked to a carbon atom at δ_{C} 79.5 (C-1'') revealed the presence of pyrazoline ring instead of the α,β -unsaturated carbonyl system.

This hypothesis was confirmed by the correlations found in the HMBC spectrum of **CI-pyrz** (**Figure 42**).

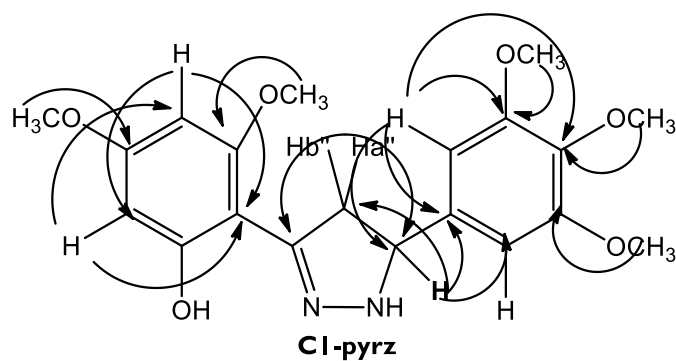


Figure 42: Main correlations found in the HMBC spectrum of **CI-pyraz**.

Table 13: ^1H NMR and ^{13}C NMR data of pyrazoline derivative **CI-pyraz**.

	δ_{H}		δ_{C}
H-2, -6	6.68 (s)	C-1	134.3
4 - OCH ₃	3.91 (s)	C-2,-6	103.2
3,5 - OCH ₃	3.89 (s)	C-3,-5	153.5
2'- OH	n.o	C-4	138.2
H-3'	6.18 (d, J=2.3)	3,5-OCH ₃	56.2
4'-OCH ₃	3.90 (s)	4-OCH ₃	60.9
H-5'	6.11 (d, J=2.3)	C-1'	105.9
6'-OCH ₃	3.83 (s)	C-2'	164.9
H-1''	5.34 (dd, J= 13.2, 2.9)	C-3'	93.6
H-2'' ^a ,b	3.03 (dd, J=16.5, 13.3) 2.79 (dd, J= 16.5, 2.9)	C-4'	166.0
5''- NH	n.o	4'-OCH ₃	55.7
	-	C-5'	93.3
	-	C-6'	162.3
	-	6'-OCH ₃	56.2
	-	C-1''	79.5
	-	C-2''	45.8
	-	C-3''	164.8

^an.o. not observed; Values in parts per million (δ_{H} and δ_{C}). Measured in CDCl₃ at 300.13 MHz. and at 75.45 MHz. J values (Hz) are presented in parentheses.

2.2.4. Epoxide derivatives P0-epo, P4-epo and BT-epo

In the IR spectra of chalcone epoxides **P0-epo**, **P4-epo** and **BT-epo** (Table 14) the band of carbonyl group appears at 1679-1654 cm^{-1} instead of 1648-1641 cm^{-1} observed for the building blocks, indicating that a molecular modification occurred at the α,β -unsaturated ketone system.

Table 14: IR data of chalcones **P0-epo**, **P4-epo** and **BT-epo**.

Groups	ν (cm^{-1})		
	P0-epo	P4-epo	BT-epo
Aliphatic C-H	2920	2996	2961
	2848	2960	2918
		2939	2850
C=O	1659	1654	1679
C=C	1590	1594	1593
	1467	1509	1510
	1432	1464	1465
	1417	1424	1429
C-O	1239	1245	1246

The ^1H NMR and ^{13}C NMR data of **P0-epo**, **P4-epo** and **BT-epo** (Table 15 and Table 16) reveal the signals of A and B rings observed in the ^1H NMR and ^{13}C NMR of their precursors (Table 8 and Table 9). Nevertheless, in ^1H NMR spectra of **P0-epo**, **P4-epo** and **BT-epo**, instead of the signals of vinylic protons, two doublets at δ_{H} 4.19-4.12 (H1'') and δ_{H} 4.15-4.00 (H2'') with $J = 1.8$ -1.7 Hz characteristic of epoxide protons are observed. Moreover, the ^{13}C NMR spectra show two signals at 59.7-59.0 and 62.0-60.9 corresponding to oxymethynic carbons of epoxide ring, confirming the formation of an epoxide by oxidation of the ethylene group.

As for other chalcones, ^{13}C NMR assignments were confirmed by HSQC and HMBC experiments. Figure 43 represents the main correlations observed in the HMBC spectra of chalcone epoxides.

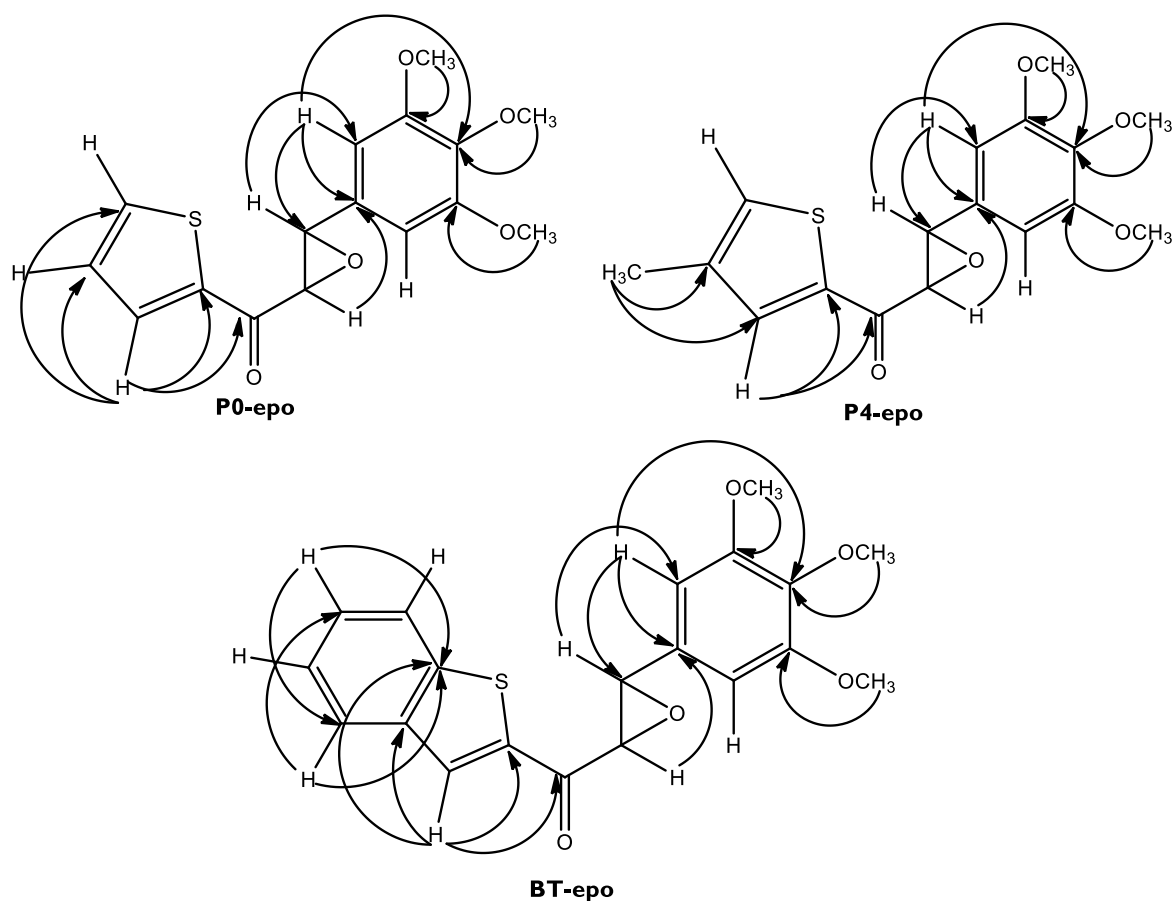


Figure 43: Main correlations observed in the HMBC spectra of chalcones **P0-epo**, **P4-epo** and **BT-epo**.

Table 15: ^1H NMR data of epoxide derivatives **P0-epo**, **P4-epo** and **BT-epo**.

	P0-epo	P4-epo	BT-epo
H-2,-6	6.57 (s)	6.56(s)	6.59 (s)
3,5 - OCH ₃	3.87 (s)	3.87 (s)	3.88 (s)
4 - OCH ₃	3.86 (s)	3.86 (s)	3.86 (s)
H-3'	7.76(dd, J=4.9, 1.1)	7.79 (brd, J=1.1)	8.28 (s)
H-4'	7.19(dd, J=4.9, 3.9)	-	7.94-7.89(m)
4'-CH ₃	-	2.31(s, -CH ₃)	-
H-5'	8.01(dd, J=3.9, 1.1)	7.23 (d, J=1.2)	7.54-7.41 (m)
H-6'	-	-	7.54-7.41 (m)
H-7'	-	-	7.94-7.89(m)
H-1''	4.13 (d, J=1.7)	4.12 (d, J=1.8)	4.19 (d, J= 1.7)
H-2''	4.03 (d, J=1.8)	4.00 (d, J=1.8)	4.15 (d, J= 1.8)

Table 16: ¹³C NMR data of epoxide derivatives **P0-epo**, **P4-epo** and **BT-epo**.

	P0-epo	P4-epo	BT-epo
C-1	130.9	131.3	130.8
C-2,-6	102.5	102.4	102.5
C-3,-5	153.7	153.7	153.7
3,5-OCH ₃	56.2	56.2	56.2
C-4	138.5	139.4	139.1
4-OCH ₃	60.9	60.9	60.9
CO	186.3	186.2	187.8
C-2'	140.9	140.6	140.7
C-3'	135.3	135.4	131.0
C-4'	128.5	139.4	125.3
4'-CH ₃	-	15.5	-
C-5'	133.7	131.0	126.4
C-6'	-	-	125.5
C-7'	-	-	123.0
C-8'	-	-	142.8
C-9'	-	-	138.6
C-1''	59.7	59.6	59.0
C-2''	62.0	61.8	60.9

Values in parts per million (δc). Measured in CDCl₃ at 75.47 MHz.

2.2.5. Pyrazole derivative **P0-pyrrz**

In the IR spectrum of chalcone derivative **P0-pyrrz** (**Table 17**) no band of stretching vibration characteristic of an α,β -unsaturated carbonyl system is observed, indicating the molecular modification of this moiety. This spectrum also revealed the presence of large bands of stretching vibration at 1634 cm⁻¹ (C-N) and 3454 cm⁻¹ (N-H), suggesting the formation of pyrazole ring. In addition, bands at 2919-2850 cm⁻¹ (aliphatic C-H), 1591-1465 cm⁻¹ (C=C) and 1239 cm⁻¹ (C-O) are observed.

Table 17: IR data of pyrazole derivative **P0-pyrrz**.

	$\nu(\text{cm}^{-1})$
Groups	P0-pyrrz
Aliphatic C-H	2919 2850
Aromatic C=C	1591 1505 1465
C-O	1239
C-N	1634
N-H	3454

The ^1H and ^{13}C NMR data of **P0-pyrz** are reported in **Table 18**. These spectra revealed the signals of A and B rings of the precursor (**Table 8** and **Table 9**). However, instead of the signals of vinylic protons, a singlet at δ_{H} 6.66 (H-2'') correlated in the HSQC spectra with a signal at δ_{C} 100.1 (C-2'') is observed, revealing the presence of pyrazole ring.

The presence of this ring was confirmed by HMBC, which also allowed the unequivocal attribution of all carbon atoms (**Figure 44**).

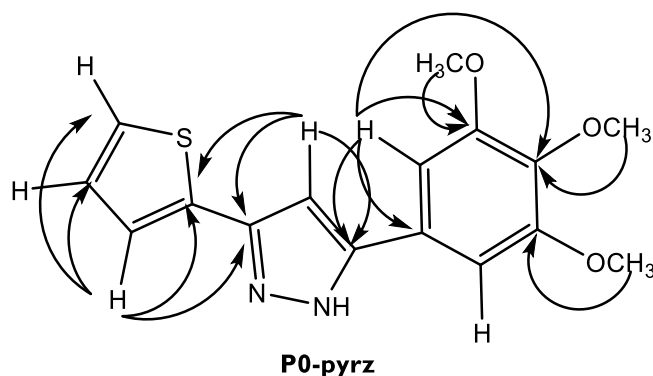


Figure 44: Main correlations found in the HMBC spectrum of **P0-pyrz**.

Table 18: ^1H NMR and ^{13}C NMR data of pyrazole derivative **P0-pyrz**.

	δ_{H}		δ_{C}
H-2,-6	6.90 (s)	C-1	126.0
3,5 - OCH ₃	3.87 (s)	C-2,-6	103.0
4 - OCH ₃	3.86 (s)	C-3,-5	153.5
H-3'	7.27 (dd, J= 5.0, 1.1)	C-4	138.4
H-4'	7.04 (dd, J= 5.0, 3.6)	3,5-OCH ₃	56.2
H-5'	7.30 (dd, J= 3.8, 1.1)	4-OCH ₃	61.0
H-2''	6.66 (s)	C-2'	144.0
5''- NH	n.o.	C-3'	125.2
-	-	C-4'	127.8
-	-	C-5'	124.3
-	-	C-1''	147.5
-	-	C-2''	100.1
-	-	C-3''	134.0

^an.o. not observed; Values in parts per million (δ_{H} and δ_{C}). Measured in CDCl₃ at 300.13 MHz and 75.45 MHz. J values (Hz) are presented in parentheses.

2.2.6. Chalcone bromine P0-br

As expected in the IR spectrum of derivative **P0-br** the band of carbonyl group appears at 1668 cm^{-1} (**Table 19**) instead of 1645 cm^{-1} observed for the building block (**Table 8** and **Table 9**), indicating that a molecular modification occurred at the α,β -unsaturated ketone system. Moreover, this spectrum revealed the presence of bands at $2918\text{-}2850\text{ cm}^{-1}$ (aliphatic C-H), $1485\text{-}1412\text{ cm}^{-1}$ (C=C), 1288 cm^{-1} (C-O) and $600\text{-}592$ (C-Br) that were in agreement with the expected structure for **P0-br**.

Table 19: IR data of chalcone derivative **P0-br**.

Groups	$\nu(\text{cm}^{-1})$	
	P0	P0-br
Aliphatic C-H	2971	2918
	2919	2850
	2832	
C=O	1645	1668
C=C	1577	
	1467	1485
	1434	1412
	1415	
C-O	1267	1288
C-Br	-	600
		562

The ^1H and ^{13}C NMR data of **P0-br** are reported in **Table 20**. As in the spectra of the precursor **P0** (**Table 8** and **Table 9**) characteristic signals of thiophene A ring are observed. On the other hand, instead of the signals of vinylic protons, two doublets at $\delta_{\text{H}} 6.29$ (H-1'') and $\delta_{\text{H}} 5.53$ (H-2'') correlated in the HSQC with the signals of carbon atoms at $\delta_{\text{C}} 48.0$ (C-1'') and $\delta_{\text{C}} 59.9$ (C-2'') can be detected, putting in evidence the bromination of C- α and C- β . In addition, regarding the signals of B ring, instead of two aromatic protons signals at $\delta_{\text{H}} 6.87$ (H-2, -6), only one aromatic proton is observed at $\delta_{\text{H}} 6.90$ (H-6) indicating the substitution of H-6 by a bromine atom.

Figure 45 shows the main correlations observed in the HMBC spectrum that confirmed the structure of **P0-br**.

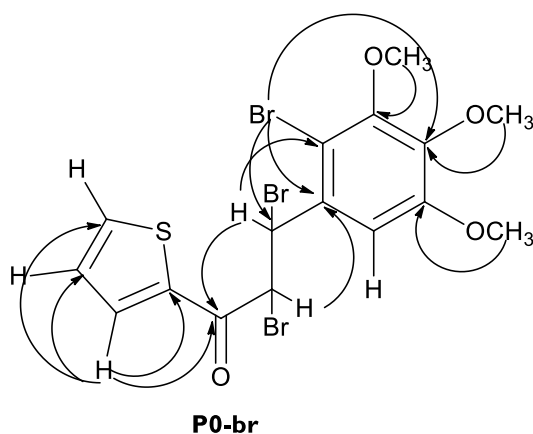


Figure 45: Main correlations found in the HMBC spectrum of **P0-br**.

Table 20: ^1H NMR and ^{13}C NMR data of chalcone derivative **P0-br**.^a

δ	P0-br		
H-6	6.93 (s)	C-1	132.6
3,5 - OCH ₃	3.93 (s)	C-6	107.8
4 - OCH ₃	3.92 (s)	C-3	150.9
H-3'	7.81 (dd, J= 5.0, 1.1)	C-4	144.0
		C-5	153.3
H-4'	7.04 (dd, J= 5.0, 3.7)	3-OCH ₃	61.1
H-5'	7.96 (dd, J= 3.8, 1.1)	4-OCH ₃	61.0
		5-OCH ₃	56.5
H-1''	6.29 (d, J= 11.0)	C-2'	140.8
H-2''	5.53 (d, J= 11.0)	C-3'	135.9
		C-4'	128.6
		C-5'	133.3
		C-2''	48.0
		C-1''	50.9
		CO	183.6

^an.o. not observed; Values in parts per million (δ_{H} and δ_{C}). Measured in CDCl₃ at 300.13 MHz. and at 75.45 MHz. J values (Hz) are presented in parentheses.

2.3. Peak Purity

For all the chalcones represented in **Table 21** prior to their biological activity evaluation, their purity was evaluated by HPLC-DAD as described in chapter 3. A percentage of purity greater than 95 % was found for all chalcones. The detector was set at a wavelength range of 220– 800 nm with a spectral resolution of 1 nm. The purity parameters included a 90% active peak region and a scan threshold of 5 mAU.

Table 21: Purity values of chalcones **P0**, **P4**, **P5**, **BT** and **BF**.

Compound	Peak purity
P0	98.6%
P4	95%
P5	95%
BT	94.5%
BF	95%

2.4. Docking studies

Molecular modeling studies were performed to predict the binding ability of chalcones **P0**, **P4**, **P5**, **BT**, **BF** and **CI**, as well as their isoxazole and pyrazole derivatives to the colchicine binding site of α,β -tubulin (PDB: 4o2b). In addition to that compounds, docking studies were performed for the chalcone **CPX (60)**, already described as having antimitotic activity. Autodock Vina was employed to investigate the docking between these compounds and 3 controls (podophylotoxin, combretastatin-A4 and colchicine) and tubulin (**Figure 46; A**).

Prior to this study, the reliability of the docking method was tested by docking colchicine to its binding site (**Figure 46; B**). Colchicine was able to bind to colchicine binding site with a similar conformation of the X-ray structure of the colchicine (RMSD of 0.86Å), indicating that the docking method is reliable and it could be employed for the docking of tested compounds. The RMSD value is $<2 \text{ \AA}$, value usually considered a good threshold value for validating a structure for use in molecular docking. This is a strong evidence that AutodockVina can predict docking poses accurately.

It is well established that the colchicine site is positioned at the interface of α and β protein heterodimers. Docking studies revealed that all tested compounds occupy the colchicine binding site of α,β -tubulin mostly buried in the β subunit (**Figure 46; A**). Colchicine interacts with tubulin with a free energy of $-10.1 \text{ kcal.mol}^{-1}$; interactions are mainly hydrophobic, and a hydrogen interaction is also established between carbonyl group of the cycloheptatrienone ring and αVal181 (**Figure 46; A and B**). Tested compounds revealed docking scores between -8.7 and $-7.3 \text{ kcal.mol}^{-1}$ (**Table 22**), all of them lower (higher affinity) than the known inhibitor podophylotoxin. Compounds **BF-iso**, **BF-pyr**, **BF**, and **BT-pyr** presented the lowest negative docking score (highest affinity to tubulin target), and therefore are predicted as having more affinity to tubulin than the known tubulin inhibitors podophylotoxin e combretastatin A4 (-7.1 and $-7.3 \text{ kcal.mol}^{-1}$, respectively). This observation supports the potent ability shown by some of these trimethoxyphenyl derivatives to disrupt the microtubule assembly by inhibiting tubulin polymerization.

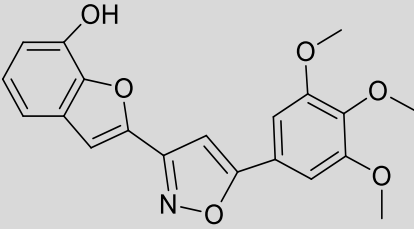
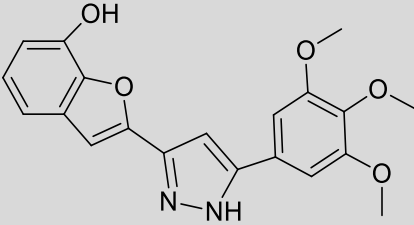
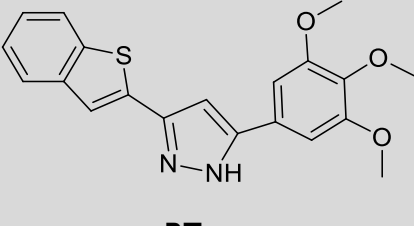
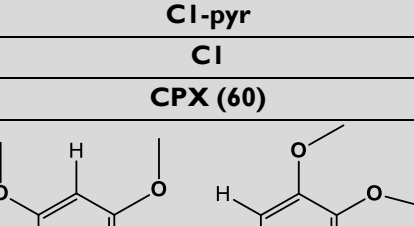
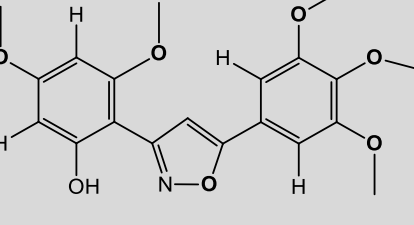
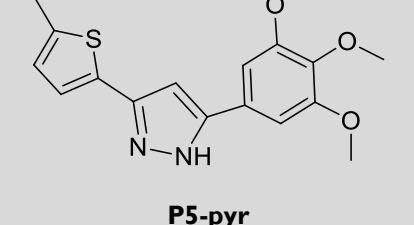
The docking pose observed for all tested compounds (**Figure 46; A**), except **CI-pyr**, showed a binding mode very similar to the one of cocrystallized colchicine. Trimethoxyphenyl groups of all tested compounds occupy a similar position to the trimethoxyphenyl ring (A-ring) of colchicine. Superimposed poses explain the importance of the basic unit, a trimethoxyphenyl ring, of both colchicine and the tested derivatives, which occupies the exact same location in

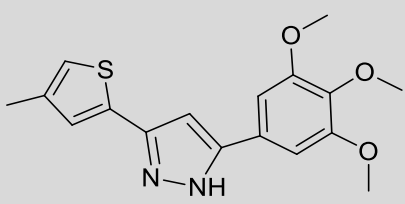
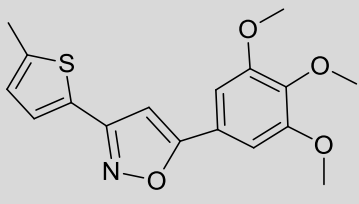
the β subunit (exemplified for **BF-iso** and **BF-pyr** on (Figure 46; C). Only **CI-pyr** is an exception, with its trimethoxyphenyl group superimposed with colchicine ring-B (not shown). The 3,4,5-trimethoxyphenyl group in **BF-iso** is predicted to form hydrophobic interactions with β Leu255, β Ala250, β Asp251, and β Leu248 (Figure 46; E). These resemble the interactions of the 3,4,5-trimethoxyphenyl group of colchicine in the hydrophobic cavity of tubulin (Figure 46; D) (167-170). The binding pose of **BF-iso** suggests that the oxazole and benzofuranol rings form hydrogen interactions with α Asn101, β Lys254, and β Asn258 (Figure 46; E). Several hydrophobic interactions are also established by **BF-pyr** 3,4,5-trimethoxyphenyl group, involving residues such as β Leu255, β Asn258, β Ala250, β Leu248, β Asp251, β Val238, β Cys241, and β Leu242 (Figure 46; E). Benzofuranol group of **BF-pyr** establishes hydrogen interactions with β Lys254 and β Asn249; pyrazole ring establishes those type of interactions with β Lys254 and β Asn258; and 4-methoxy group of trimethoxyphenyl ring establishes those type of interactions with β Val238 (Figure 46; F).

CPX (60), a compound already described by our group as a mitosis inhibitor (171), had a low docking score (high affinity), suggesting a possible mechanism of action by tubulin inhibition. Compared with **CPX (60)**, *in silico* studies suggest that molecular modifications result in improved binding interactions with colchicine binding domain in the tubulin dimer, as **BF**, **BT**, and **CI** derivatives have lower docking scores.

As already reported for the trimethoxyphenyl group in A ring, the presence of the same group on B ring is confirmed as being the key motif for binding to tubulin (172-174). *In vitro* experiments will be performed in order to confirm these *in silico* findings.

Table 22: Docking scores (Kcal.mol⁻¹) for tubulin target for the compounds **P0**, **P4**, **P5**, **BT**, **BF**, **P0-iso**, **P4-iso**, **P0-pyrz**, **P4-pyrz** and **BT-pyrz** and controls (**podophylotoxin**, **combretastatin-A4** and **colchicine**).

Docking score (kcal.mol ⁻¹)	
 <p>BF-iso</p>	-8.7
 <p>BF-pyr</p> <p>BF</p>	-8.6
 <p>BT-pyr</p> <p>BT-iso</p> <p>BT</p>	-8.2
 <p>BT-iso</p> <p>BT</p>	-8.1
<p>BT-iso</p> <p>BT</p>	-8
<p>BT</p>	-8
<p>CI-pyr</p>	-7.9
<p>CI</p>	-7.9
<p>CPX (60)</p>	-7.9
 <p>CI-iso</p>	-7.8
 <p>P5-pyr</p>	-7.7

Docking score (kcal.mol⁻¹)	
P4-iso	-7.6
 P4-pyr	-7.6
 P5-iso	-7.6
P0-pyr	-7.5
P5	-7.5
P0-iso	-7.4
P0	-7.3
P4	-7.3
Controls	
Podophylotoxin	-7.1
Combretastatin-A4	-7.3
Colchicine	-10.1

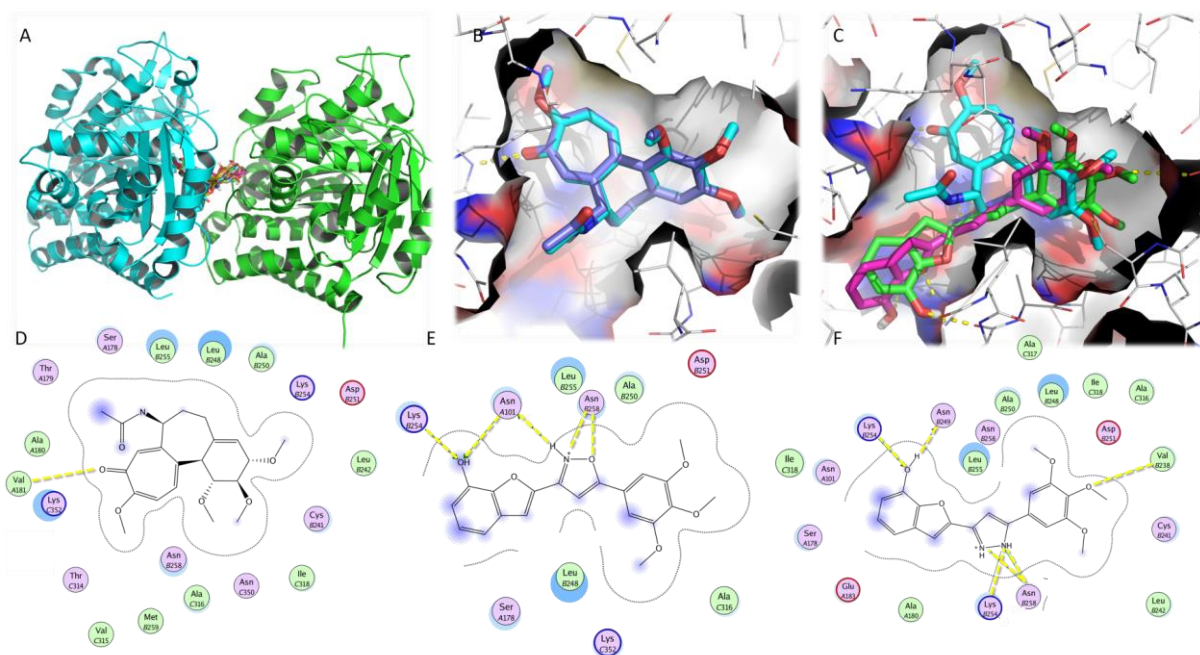


Figure 46: The molecular docking model of tested and control models with tubulin. (A) All tested molecules and controls docked in the interface between tubulin α (green) and β (blue) units. (B) A closer view of crystallographic (light blue) and docked (dark blue) colchicine. (C) A closer view of **BF-pyr** (green), **BF-iso** (magenta), and crystallographic colchicine (light blue). Hydrogen interactions are represented as yellow broken lines. 2D depiction of crystallographic colchicine (C), **BF-iso** (D), and **BF-pyr** (E) in colchicine binding site. Hydrogen interactions are represented as yellow broken lines. Receptor residues that are close to the ligand, but whose interactions with the ligand are weak or diffuse, such as collective hydrophobic or electrostatic interactions, are also represented (all the ones that have no indication for hydrogen-bonding). Solvent accessible surface area of the ligand is plotted directly onto the atoms in the form of a blue smudge. Solvent accessible surface area for the receptor residues is plotted as a blue halo.

2.5. Biological Activity

The effect of chalcones on the *in vitro* growth of three human tumor cell lines, A375-C5 (melanoma,) MCF-7 (breast adenocarcinoma) and NCI-H460 (non-small cell lung cancer) was evaluated according to the procedure adopted by the National Cancer Institute (NCI, USA) which uses the protein-binding dye sulforhodamine B (SRB) to assess cell growth (171, 175-176). By this procedure, a dose response curve was obtained for each cell line with each tested compound and the concentration that caused cell growth inhibition of 50% (GI_{50} , corresponding to the concentration of compound that inhibited 50% of net cell growth), was determined as described elsewhere (171, 175).

From **Table 23** it can be seen that, all tested chalcones revealed a potent growth inhibition of the three human tumor cell lines, exhibiting **P4** the higher potency ($3.02 < GI_{50} < 3.26 \mu\text{M}$) against the three human tumor cell lines studied.

Table 23: GI_{50} values obtained for chalcones **P0**, **P4**, **P5**, **BT** and **BF** on the growth of human tumor cell Lines^a.

Compounds	GI_{50} (μM) ^b		
	A375-C5	MCF-7	NCI-H460
P0	3,63±0,58	5,95± 0,88	5,06±0,20
P4	3,21±0,45	3,26±0,11	3,02±0,01
P5	5,70±1,45	5,56±1,51	6,28±0,31
BT	6,90±1,10	6,89±0,41	6,61±0,63
BF	8.57±1.06	9.57±1.24	8.35±0.31

^a) Data represent mean \pm SEM from at least three independent experiments performed in duplicate.

^b) Concentration that was able to cause 50% of cell growth inhibition after a continuous exposure of 48 h.

Chapter 3:

Conclusions

Natural chalcones have been intensively studied for their wide range of biological activities, namely antitumor, being this activity associated with, at least in part, to their ability to promote cell cycle arrest by interference with mitosis. Moreover, these compounds are precursors of a variety of heterocyclic compounds, such as isoxazoles and pyrazoles.

Inspired by the potential of natural chalcones as antimitotic agents, six structure related B ring analogues of chalcone **CPX (60)**, already described as antimitotic agent, were synthesized (**P0**, **P4**, **P5**, **BT**, **BF** and **CI**). Furthermore, seven chalcone derivatives have been prepared, including epoxide (**P0-epo**, **P4-epo**, **BT-epo**), tribromide (**P0-br**), isoxazole (**P0-iso**), pyrazoline (**CI-pyr**) and pyrazole (**P0-pyr**) derivatives, using classic and MAOS methodologies.

The antiproliferative effect of chalcones **P0**, **P4**, **P5**, **BT** and **BF** on three human tumor cell lines, A375-C5 (melanoma), MCF-7 (breast adenocarcinoma) and NCI-H460 (non-small cell lung cancer) was evaluated using the SRB assay. All tested chalcones revealed a potent growth inhibitory effect against the three human tumor cell lines, exhibiting **P4** the higher potency ($3.02 < GI_{50} < 3.26 \mu\text{M}$).

Molecular modeling studies were performed to predict the binding ability of chalcones **P0**, **P4**, **P5**, **BT**, **BF** and **CI**, as well as their isoxazole and pyrazole derivatives to the colchicine binding site of α,β -tubulin. In addition to that compounds, these studies were performed for **CPX (60)**, and the tubulin polymerization inhibitors podophylotoxin, combretastatin-A4 and colchicine, used as positive controls. Tested compounds revealed higher affinity than the known inhibitor podophylotoxin. Particularly, **BF**, **BF-pyr**, **BT-pyr** and **BF-iso** presented the highest affinity to tubulin target, and therefore are predicted as having more affinity to tubulin than podophylotoxin and combretastatin A4. These results support the possibility of these compounds to disrupt the microtubule assembly by inhibiting tubulin polymerization. As such, in the future pyrazole derivatives of chalcones **BF** and **BT**, as well as the isoxazole derivative of chalcone **BF**, should be synthesized in order to verify this expected effect. Additionally, the effects of chalcones on the *in vitro* growth of human tumor cell lines and as tubulin polymerization inhibitors should be investigated in the future.

Chapter 4:

Experimental Procedures

3.1. Chemistry

3.1.1. Synthesis

3.1.1.1. General Methods

MW reactions were performed using a glassware setup for atmospheric-pressure reactions and a 100 mL or 30 ml Teflon reactor (internal reaction temperature measurements with a fiber-optic probe sensor) and were carried out using an Ethos MicroSYNTH 1600 Microwave Labstation from Milestone.

All the reactions were monitored by TLC.

Purifications of compounds were carried out by flash CC using Macherey-Nagel silica gel 60 (0.04-0.063 mm), preparative TLC using Macherey-Nagel silica gel 60 (GF254) plates, and crystallization.

Melting points were obtained in a Köfler microscope and are uncorrected.

IR spectra were obtained in KBr microplate in a FTIR spectrometer Nicolet iS10 from Thermo Scientific with Smart OMNI-Transmission accessory (Software OMNIC 8.3).

^1H and ^{13}C NMR spectra were taken in CDCl_3 at r.t., on Bruker Avance 300 and 500 instruments (300.13 MHz for ^1H and 75.47 MHz for ^{13}C , 500 MHz for ^1H and 120 MHz for ^{13}C , respectively). Chemical shifts are expressed in δ (ppm) values relative to tetramethylsilane (TMS) used as an internal reference; ^{13}C NMR assignments were made by 2D (HSQC and HMBC) NMR experiments (long-range ^{13}C - ^1H coupling constants were optimized to 7 Hz).

The commercial available reagents were purchased from Sigma Aldrich Co.

All commercially available reagents were purchased from Sigma Aldrich Co. Reagents and solvents were purified and dried according to the usual procedures described elsewhere (177) (**Perrin**). The following materials were synthesized and purified by the described procedures.

3.1.2. Synthesis of Chalcone P5 by conventional heating

To a solution of 2-acetyl-5-methylthiophene (7 mmol, 1 g) in methanol (25 mL) an aqueous solution of 40 % sodium hydroxide was added until pH 13 – 14. Then a solution of 14 mmol (2.80 g) of 3,4,5-trimethoxybenzaldehyde in methanol was slowly added to the reaction mixture. The reaction was stirred during 24 h 30 min at 65 °C. The reaction was monitored by TLC (*n*-hexane: ethyl acetate, 7:3) and after completion, the reaction mixture was poured into ice and the pH was adjusted to approximately 5 with diluted HCl. The solution was then extracted with chloroform (3 x 50 mL). The organic phase was collected and further rinsed with brine and water, dried over with anhydrous sodium sulfate to remove excess water. The mixture was concentrated under reduced pressure. The obtained residue was purified by flash CC (*n*-hexane: ethyl acetate, 7:3) followed by crystallization (methanol / chloroform), being obtained pure yellow crystals. Mother liquor was then purified by flash CC (*n*-hexane: ethyl acetate, 7:3) followed by crystallization (methanol: chloroform) in order to enhance the reaction yield.

(E)-1-(5-methylthiophen-2-yl)-3-(3,4,5-trimethoxyphenyl)prop-2-en-1-one (P5):
Yield: 16 %; mp (methanol: chloroform) 126-128 °C; IR (KBr) ν_{max} : 2997-2849, 1647, 1578-1420, 1283 cm^{-1} ; ^1H NMR (CDCl_3 , 300.13 MHz) δ = 7.74 (1H, d, J = 15.4, H- β), 7.70 (1H, d, J = 3.5, H-3'), 7.26 (1H, d, J = 15.5, H- α), 6.87 (1H, d, J = 3.5, H-4'), 6.85 (2H, s, H-2,-6), 3.93 (6H, s, 3, 5-OCH₃), 3.90 (3H, s, 4-OCH₃), 2.57 (3H, s, 5'-CH₃); ^{13}C NMR (CDCl_3 , 75.47 MHz) δ = 181.5 (C=O), 153.5 (C-3, -5), 150.1 (C-5'), 143.6 (C-2'), 143.4 (C- β), 140.3 (C-4), 132.4 (C-3'), 130.4 (C-1), 126.9 (C-4'), 120.8 (C- α), 105.6 (C-2, 6), 61.0 (4-OCH₃), 56.2 (3,5-OCH₃), 16.2 (5'-CH₃).

3.1.3. Synthesis of Chalcone P0, P4, P5, BT, BF and CI by MW irradiation

To a solution of appropriately substituted ketone (2-acetylthiophene, 2-acetyl-4-methylthiophene, 2-acetyl-5-methylthiophene, 2-acetylbenzothiophene, 1-(7-hydroxybenzofuran-2-yl)ethanone or 1-(2-hydroxy-4,6-dimethoxyphenyl) ethanone) (2.83-7.93 mmol) in methanol (25mL) was added an aqueous solution of 40 % sodium hydroxide until pH 13 – 14. Then a solution of 14 mmol (2.80 g) of 3,4,5-trimethoxybenzaldehyde in

methanol was slowly added to the reaction mixture. The reaction was submitted to 30 min period of microwave irradiation at 180 W of power. Total irradiation time was 3-4 h hours and the final temperature was 75 °C. After cooling, the reaction mixture was purified as described bellow.

(E) -1-(thiophen-3-yl)-3-(3,4,5-trimethoxyphenyl)prop-2-en-1-one (P0): Purified by crystallization from chloroform and methanol. Yield: 61% as yellow crystals; mp (methanol : chloroform) 128-130°C; IR(KBr) ν_{max} : 2971-2832, 1645, 1577-1415, 1287; ¹H NMR (CDCl₃, 300.13 MHz): δ 7.89 (1H, dd, J= 3.8, 1.1, H-5'), 7.78 (1H, d, J=15.5, H- β), 7.69 (1H, dd, J=5.0, 1.1, H-3'), 7.31 (1H, d, J=15.6, H- α), 7.20 (1H, dd, J= 5.0, 3.8, H-4'), 6.87 (2H, s, H-2,-6), 3.93 (6H, s, 3,5- OCH₃), 3.90 (3H, s, 4-OCH₃); ¹³C NMR (CDCl₃, 75.47 MHz): δ 182.0 (C=O), 153.5 (C-3,-5), 145.5 (C-2'), 144.3 (C- β), 140.5 (C-4), 133.9 (C-3'), 131.8 (C-5'), 130.2 (C-1), 128.2 (C-4'), 120.9 (C- α), 105.7 (C-2,-6), 61.0 (4-OCH₃), 56.3 (3,5-OCH₃).

(E) -1-(4-methylthiophen-2-yl)-3-(3,4,5-trimethoxyphenyl)prop-2-en-1-one (P4): Purified by crystallization from chloroform and methanol. Yield: 55%, yellow crystals; mp (chloroform: methanol) 140-142°C; IR (KBr) ν_{max} : 2963- 2823, 1648, 1578-1416, 1248; ¹H NMR (CDCl₃, 300.13 MHz): δ 7.76 (1H, d, J=15.5 Hz, H- β), 7.69 (1H, brd, J=1.2, H-3'), 7.27 (1H, d, J =15.5 Hz, H- α), 7.23 (1H, dd, J=1.3, 1.1, H-5'), 6.86 (2H, s, H-2,-6), 3.93 (6H, s, 3-,5-OCH₃), 3.90 (3H, s, 4-OCH₃); ¹³C NMR (CDCl₃ 75.47 MHz): δ 181.9 (C=O), 153.5 (C- 3,-5), 145.0 (C-2'), 144.0 (C- β), 140.4 (C-4), 139.0 (C-4'), 133.7 (C-3'), 129.8 (C-5'), 130.7 (C-1), 120.9 (C- α), 105.7 (C-2,-6), 61.0 (4-OCH₃), 56.3 (3-,5-OCH₃), 15.5 (4'-CH₃).

(E) -2'-Hydroxy-3,4,4',5,6'-pentamethoxychalcone (C1): Purified by flash CC (SiO₂; n-hexane: EtOAc, 7:3) followed by crystallization from chloroform and methanol. Yield: 13 % as yellow crystals; mp (metanol: chloroform) 175- 178°C; IR (KBr) ν_{max} : 3469, 3401, 2966-2831, 1627, 1572-1403, 1268; ¹H NMR (CDCl₃, 300.13 MHz): δ 14.32 (1H, s, 2'-OH), 7.80 (1H, d, J=15.6 Hz, H- β), 7.70 (1H, d, J=15.6 Hz, H- α), 6.84 (2H, s, H-2,-6), 6.11 (1H, d, J=2.4 Hz, H-5'), 5.96 (1H, d, J=2.4 Hz, H-3'), 3.92 (6H, s, 3,5-OCH₃), 3.90 (3H, s, 4-OCH₃), 3.91 (3H, s, 4'-OCH₃), 3.84 (3H, s, 6'-OCH₃); ¹³C NMR (CDCl₃ 75.47 MHz): δ 192.3 (C=O), 168.4 (C-4'), 166.2 (C-6'), 162.4 (C-2'), 153.4 (C-3,-5), 142.4 (C- β), 140.1 (C-4), 131.1 (C-1), 126.9 (C- α), 105.6 (C-2,-6), 93.8 (C-3'), 91.3 (C-5'), 61.0 (4-OCH₃), 56.6 (3-,5-OCH₃), 55.8 (4'-OCH₃), 52.8 (6'-OCH₃).

(E)-1-(benzo[b]thiophen-2-yl)-3-(3,4,5-trimethoxyphenyl)prop-2-en-1-one (BT): Purified by flash CC (SiO₂; n-hexane: EtOAc, 7:3) followed by crystallization from chloroform

and methanol. Yield: 38 % as yellow crystals; mp (metanol: chloroform) > 350°C; IR (KBr) $\nu_{\text{máx}}$: 2961- 2849, 1641, 1583-1422, 1250; ^1H NMR (CDCl_3 , 300.13 MHz): δ 8.13 (1H, s, H-3'), 7.95-7.90 (2H, m, H-4,-7'), 7.83 (1H, d, $J=15.5$ Hz, H- β), 7.58 (1H, d, $J=15.5$ Hz, H- α), 7.52-7.41 (2H, m, H-5',-6'), 6.91 (2H, s, H-2,-6), 3.96 (6H, s, 3,5-OCH₃), 3.92 (3H, s, 4-OCH₃); ^{13}C NMR (CDCl_3 75.47 MHz): δ 171.2 (C=O), 153.5 (C-3,-5), 144.6 (C- β), 143.0 (C-2'), 145.2 (C-8'), 139.3 (C-9'), 140.7 (C-4), 130.1 (C-1), 128.8 (C-3'), 125.1 (C-6'), 127.4 (C-7'), 123.1 (C-5'), 125.9 (C-4'), 120.4 (C- α), 105.8 (C-2,-6), 61.1 (4-OCH₃), 56.3 (3,5-OCH₃).

(E)-1-(7-hydroxybenzofuran-2-yl)-3-(3,4,5-trimethoxyphenyl)prop-2-en-1-one

(BF): Purified by flash CC (SiO_2 ; n-hexane: EtOAc, 5:5) followed by flash CC (SiO_2 ; n-hexane: EtOAc, 5:5). Yield: 12 % as yellow crystals; mp (metanol: chloroform) 190-192°C; IR (KBr) $\nu_{\text{máx}}$: 3447, 2918, 2849, 1648, 1597-1484, 1287; ^1H NMR (CDCl_3 , 300.13 MHz): δ 7.89 (1H, d, $J = 15.6$ Hz, H- β), 7.68 (1H, s, H-3'), 7.43 (1H, d, $J=15.6$ Hz, H- α), 7.29 (1H, dd, $J=7.8$, 1.1 Hz, H-4'), 7.21 (3H, t, $J=7.8$ Hz, H-5'), 7.06 (1H, dd, $J=7.7$, 1.1 Hz, H-6'), 6.91 (2H, s, H-2,-6), 3.94 (6H, s, 3-,5-OCH₃), 3.92 (3H, s, 4-CH₃); ^{13}C NMR (CDCl_3 75.47 MHz): δ 179.5 (C=O), 153.6 (C-2'), 153.5 (C-3,5), 145.3 (C- β), 128.8 (C-9'), 144.6 (C-8'), 140.9 (C-4), 130.0 (C-1), 115.0 (C-4'), 125.9 (C-6'), 120.1 (C- α), 114.2 (C-3'), 114.2 (C-5'), 141.8 (C-7'), 106.1 (C-2,-6), 61.1 (4-OCH₃), 56.3 (3-,5-OCH₃).

3.1.4. Synthesis of Isoxazole derivative P0-iso

Anhydrous sodium acetate (2 mmol) dissolved in glacial acetic acid (10 ml) was added to a solution of $\text{NH}_2\text{OH}\cdot\text{HCl}$ (1mmol) dissolved in absolute ethanol (10 mL-20 mL). Subsequently, the obtained solution was added to a solution of chalcone **P0** (0.200 g, 00.628 mmol) in ethanol. The reaction mixture was submitted to successive 30 min of MW irradiation at 180 W of potency. The total irradiation time was 3h and the final temperature was 80 °C. After cooling, the solid was filtered, washed with ethanol and then purified by flash CC (SiO_2 ; n-hexane: EtOAc, 7:3) followed by preparative TLC (SiO_2 ; n-hexane: EtOAc, 7:3).

(E)3-(thiophen-2-yl)-5-(3,4,5-trimethoxyphenyl)isoxazole (P0-iso): Yield: 22%; mp 128-130°C (chloroform); IR (kBr) ν_{max} : 3444, 2963-2850, 1540-1426, 1387, 1261; ^1H NMR (CDCl_3 , 300.13 MHz): δ 7.57 (1H, dd, $J=3.8, 1.1$ Hz, H-5'), 7.48 (1H, dd, $J=5.1, 1.1$ Hz, H-3'), 7.15 (1H, dd, $J=5.5, 3.8$, H-4'), 7.07 (2H, s, H-2,-6), 6.66 (1H, s, H-2''), 3.95 (6H, s, 3-,5-OCH₃), 3.91 (3H, s, 4-OCH₃); ^{13}C NMR (CDCl_3 75.47 MHz): δ 162.8 (C-1''), 165.5 (C-3''), 153.6 (C-3,-5), 140.0 (C-4), 129.2 (C-2'), 128.2 (C-3'), 127.1 (C-4'), 128.1 (C-5'), 124.3 (C-1), 104.1 (C-2,-6),

3.1.5. Synthesis of Pyrazoline C1-pyr

To a solution of chalcone **C1** (0.140 g, 0.374 mmol) in sodium acetate (5 mL) hydrazine hydrate (3 mL) was added and then the reaction mixture was stirred at 100 °C during 4h. After, I₂ (0.37 mmol) was added and the reaction continued at 100°C during more 4 h. After the completion of the reaction, the reaction mixture was poured into crushed ice and treated with sodium hydrogen carbonate and sodium sulphite. The precipitated solid was filtered, washed with water and dried. The crude product was purified by flash CC (SiO₂; n-hexane: EtOAc, 7:3) and preparative TLC (SiO₂; n-hexane: EtOAc, 7:3).

(E)3,5-dimethoxy-2-(5-(3,4,5-trimethoxyphenyl)-1H-pyrazol-3-yl)phenol (C1-pyrz): Yield: 48.2%; mp (ethanol): 170-174°C; IR (kBr) ν_{max} : 3431, 2919, 2830, 1619, 1593-1459, , 1266; ^1H NMR (CDCl_3 , 300.13 MHz): δ = 6.18 (1H, d, $J=2.3$, H-3'), 6.11 (1H, d, $J=2.3$, H-5'), 6.68 (2H, s, H-2,-6), 3.03 (1H, dd, $J=16.5, 13.3$, H-2''a), 3.91 (3H, s, OCH₃- 4), 3.90 (1H, s, H-4'), 3.89 (6H, s, OCH₃- 3, 5), 3.83 (1H, s, 6'-OCH₃), 2.79 (1H, dd, $J=16.5, 2.9$, H-2''b), ^{13}C NMR (CDCl_3 , 75.47 MHz) δ = 164.9 (C-2'), 166.0 (C-4'), 164.9 (C-3''), 162.3 (C-6'), 153.5 (C-3,-5), 138.2 (C-4), 134.3 (C-1), 105.9 (C-1'), 103.2 (C-2,-6), 93.6 (C-3'), 93.3 (C-5'), 56.2 (3,5- OCH₃), 55.7 (4'-OCH₃), 56.2 (6'-OCH₃), 79.5 (C-1''), 60.9 (4-OCH₃), 45.8 (C-2'').

3.1.6. Epoxide derivatives P0-epo, P4-epo, P5-epo and BT-epo

The required chalcone (**P0**, **P4**, **P5** and **BT**) (0,0471-0.628 mmol) was dissolved in methanol (20 mL). To the solution was added powdered K₂CO₃ (0.194 g, 0,141 mmol) followed by the dropwise addition of an excess of H₂O₂ (160.1-213.5 mg, 4.71-6.28 mmol)

over 10 min. The mixture was stirred at room temperature for 4 h. After the completion of the reaction, MeOH was removed by Nitrogen Stream, the residue was extracted with CH₂Cl₂. After that, the CH₂Cl₂ was washed with water, dried with anhydrous sodium sulfate and evaporated by Nitrogen Stream. The solid obtained was purified by crystallization (dichloromethane: methanol).

(E)Thiophen-2-yl-(3-(3,4,5-trimethoxyphenyl)oxiran-2-yl)methanone

(P0-epo): Yield: 46% ; mp (dichloromethane: methanol): 111-113 °C; IR (kBr) ν_{max} : 2920-2848, 1659, 1590-1417, 1239; ¹H NMR (CDCl₃, 300.13 MHz) δ = 8.01 (1H, dd, J=3.9, 1.1, H-5'), 7.76 (1H, dd, J=4.9, 1.1, H-3'), 7.19 (1H, dd, J= 4.9, 3.9, H-4'), 6.57 (2H, s, H-2,-6), 4.13 (1H, d, J= 1.7, H-1''), 4.03 (1H, d, J= 1.8, H-2''), 3.87 (6H, s, 3, 5- OCH₃), 3.86 (3H, s, 4- OCH₃); ¹³C NMR (CDCl₃, 75.47 MHz) δ = 186.3 (C=O), 153.7 (C-3, -5), 140.9 (C-2'), 138.5 (C-4), 135.3 (C-3'), 133.7 (C-5'), 130.9 (C-1), 128.5 (C-4'), 102.5 (C-2, -6), 62.0 (C-2''), 60.9 (4-OCH₃), 59.7 (C-1''), 56.2 (3,5- OCH₃).

(E)I-(4'-methylthiophen-2'-yl)-(3-(3,4,5-trimethoxyphenyl)oxiran-2-

yl)methanone (P4-epo): Yield: 41%; mp (dichloromethane: methanol): 104-108 °C; IR (kBr) ν_{max} : 2996-2939, 1654, 1594-1424, 1245; ¹H NMR (CDCl₃, 300.13 MHz) δ = 7.79 (1H, d, J=1.1, H-3'), 7.23 (1H, d, J= 1.2, H-5'), 6.56 (2H, s, H-2,-6), 4.12 (1H, d, J= 1.8, H-1''), 4.00 (1H, d, J= 1.8, H-2''), 3.87 (6H, s, 3, -5- OCH₃), 3.86 (3H, s, 4- OCH₃), 2.31 (1H,s, 4' -CH₃); ¹³C NMR (CDCl₃, 75.47 MHz) δ = 186.2 (C=O), 153.7 (C-3,-5), 140.6 (C-2'), 139.4 (C-4), 135.4 (C-3'), 131.3 (C-1), 131.0 (C-5'), 139.4 (C-4'), 102.4 (C-2,-6), 61.8 (C-2''), 60.9 (4-OCH₃), 59.6 (C-1''), 56.2 (3,5-OCH₃).

(E)I-(benzo(b)thiophen-2-yl)-(3-(3,4,5-trimethoxyphenyl)oxiran-2-yl)methanone

(BT-epo): Yield: 23%; mp (dichloromethane: methanol) 155-157 °C; IR (kBr) ν_{max} : 2961-2850, 1679, 1593-1429, 1246; ¹H NMR (CDCl₃, 300.13 MHz) δ = 8.28 (1H, s, H-3'), 7.94-7.89 (2H, m, H- 4',-7'), 7.54-7.41 (2H, m, H- 5',-6'), 6.59 (2H, s, H-2,-6), 4.19 (1H, d, J= 1.7, H-1''), 4.15 (1H, d, J= 1.8, H2''), 3.88 (6H, s, OCH₃- 3,5), 3.86 (3H, s, 4- OCH₃); ¹³C NMR (CDCl₃, 75.47 MHz) δ = 187.8 (C=O), 153.7 (C-3,-5), 140.7 (C-2'), 139.1 (C-4), 131.0 (C-3'), 130.8 (C-1), 126.4 (C-5'), 125.5 (C-6'), 125.3 (C-4'), 138.6 (C-9'), 123.0 (C-7'), 102.5 (C-2, -6), 60.9 (C-2''), 60.9 (4- OCH₃-), 59.0 (C-1''), 56.2 (3,-5 OCH₃).

3.1.7. Synthesis of Pyrazole derivative P0-pyr

To a solution of chalcone epoxide **P0-epo** (0.170 g, 0.47mmol) in xylenes (4 mL) and dichloromethane (2 mL) was added *p*-toluenesulfonic acid monohydrate (0.23 mmol, 11.25 mg) and hydrazine hydrate (0.23 mL). The reaction mixture was stirred during 3 h at 100 °C and controlled by TLC (SiO₂: n-Hexane: EtOAc, 5:5). The xylenes were removed under reduced pressure and the obtained solid was washed with *n*-hexane. The solid obtained after evaporation with reduce pressure was purified by flash CC (SiO₂: n-hexane: EtOAc, 5:5) followed by preparative TLC (SiO₂: n-hexane: EtOAc, 5:5).

(E)3-(thiophen-2-yl)-5-(3,4,5-trimethoxyphenyl)-1H-pyrazole (P0-pyr): Yield: 4%; mp 70-72°C ; IR (kBr) ν_{max} : 3454, 2919, 2850, 1636, 1591-1465, 1249; ¹H NMR (CDCl₃, 300.13 MHz): δ 7.30 (1H, dd, J= 3.8, 1.1, H-5'), 7.27 (1H, dd, J=5.0, 1.1, H-3'), 7.04 (1H, dd, J= 5.0, 3.6, H-4'), 6.90 (2H, s, H-2,-6), 6.66 (1H, s, H-2''), 3.87 (6H, s, 3,5-OCH₃), 3.86 (3H, s, 4-OCH₃); ¹³C NMR (CDCl₃, 75.47 MHz) δ = 153.5 (C-3,-5), 147.5 (C-1''), 139.0 (C-3''), 138.4 (C-4), 144.0 (C-2'), 127.8 (C-4'), 126.0 (C-1), 125.2 (C-3'), 124.3(C-5'), 103.0 (C-2, -6), 100.1 (C-2''), 61.0 (4- OCH₃), 56.2 (3,5- OCH₃).

3.1.8. Synthesis of Chalcone bromine P0-br

To a solution of chalcone **P0** (0.250 g, 1.9 mmol) in carbon tetrachloride (40 mL) bromine was slowly added until the reaction mixture became red. The reaction mixture was stirred at room temperature during 3 h until the consumption of the starting material was complete. The resulting brown solid was filtrated, washed with carbon tetrachloride (2 x 10 mL), and then purified by crystallization from methanol and chloroform.

(E)2,3-dibromo-1-(thiophen-2-yl)-3-(3,4,5-trimethoxyphenyl)propan-1-one (P0-br): Yield: 78%; mp (methanol: chloroform) 120-122 °C; IR (kBr) ν_{max} : 2918, 2850, 1668,1485, 1412, 1288, 600, 562; ¹H NMR (CDCl₃, 300.13 MHz) δ = 7.96 (1H, dd, J= 3.8, 1.1 H-5'), 7.81 (1H, dd, J=5.0, 1.1, H-3'), 7.04 (1H, dd, J= 5.0, 3.7, H-4'), 6.93 (1H, s, H-6), 6.29 (1H, d, J= 11.0, H-1''), 5.53 (1H, d, J=11.0, H-2''), 3.93 (6H, s, 3-,5-OCH₃), 3.92 (3H, s, 4-

OCH₃); ¹³C NMR (CDCl₃, 75.47 MHz) δ= 183.6 (C=O), 153.3 (C-5), 150.9 (C-3), 144.0 (C-4), 144.0 (C-4), 140.8 (C-2'), , 135.9 (C-3'), 133.3 (C-5'), 132.6 (C-1), 128.6 (C-4'), 107.8 (C-6), 61.1 (3- OCH₃), 61.0 (4- OCH₃), 56.5 (5- OCH₃), 50.9 (C-1''), 48.0 (C-2'').

3.2. Peak Purity

Analytical HPLC-DAD analyses were performed on a SpectraSYSTEM (Thermo Fisher Scientific, Inc, USA) equipped with a P4000 pump, a AS3000 autosampler and a diode array detector UV8000. The separation was carried out on a 250 x 4.6 mm i.d. FortisBIO C18 (5 µm) (Fortis™ Technologies Ltd, Cheshire, UK). LC analysis was performed by isocratic elution using a mixture of MeOH: H₂O (80:20 v/v) as mobile phase and the flow rate was set at 1 mL/ min. The injected volume was 20 µL and the eluent was monitored at 254 nm. The detector was set at a wavelength range of 190–800 nm with a spectral resolution of 1 nm. The purity parameters included a 95% active peak region and a scan threshold of 5 mAU. ChromQuest 5.0 (version 3.2.1) software (Thermo Fisher Scientific Inc.) managed chromatographic data. Methanol (HPLC grade) was obtained from Carlo Erba Reagents (Val de Reuil, Italy) and HPLC grade water obtained from a Simplicity® UV Ultrapure Water System, Millipore Corporation, USA. Prior to use, mobile phase solvents were degassed in an ultrasonic bath for 15 min. All the analyses were performed in triplicate.

3.3. Docking Studies

Crystal structure of tubulin (PDB code: 4o2b) (178), downloaded from the protein databank (PDB) (179), was used for the study. Structure files of 3 known tubulin inhibitors - colchicines, podophylotoxin, and combretastatin A4 - and 19 tested molecules were created and minimized using the chemical structure drawing tool Hyperchem 7.5 (Hypercube, FL, USA) (180). Structure-based docking was carried out using AutoDock Vina (Molecular Graphics Lab, CA, USA) (181). The active site was defined as the region of tubulin engulfing crystallographic ligand colchicine. Default settings for small molecule-protein docking were used throughout the simulations. Top 9 poses were collected for each molecule and the lowest docking score value was associated with the more favorable binding conformation. PyMol 1.3 (Schrödinger, NY, USA) (182) and MOE v2008 (Chemical Computing Groups, Montreal, Canada) (183) were used for visual inspection of results and graphical representations.

3.4. Biological Activity

3.4.1. Cell Culture

The following three human tumor cell lines were used: MCF-7 (breast adenocarcinoma, ECACC, UK), NCI-H460 (non-small cell lung cancer, a kind gift from NCI, Bethesda, USA) and A375-C5 (melanoma, ECACC, UK). All cell lines were grown as monolayer and routinely maintained in RPMI-1640 medium with ultraglutamine supplemented with 5% heat-inactivated fetal bovine serum (FBS) at 37°C in a humidified atmosphere containing 5% CO₂.

3.4.2. Growth Inhibition Assay

Cells were plated in 96-well plates at appropriate densities in order to ensure exponential growth throughout the experimental period (5.0×10^3 cells/well for MCF-7 and NCI-H460 and 7.5×10^3 cells/well for A375-C5) and then allowed to adhere overnight. Cells were then treated for 48 h with five serial dilutions of each compound (1:2 or 1:3). Following this incubation period, cells were fixed *in situ* with trichloroacetic acid, washed and stained with SRB (175). The bound stain was then solubilized with Tris and the absorbance was measured at 492 nm in a plate reader (Biotek Instruments Inc. PowerWave XS, Winooski, USA). The effect of the vehicle solvent (DMSO) on the growth of these cell lines was evaluated by exposing untreated control cells to the maximum concentration of DMSO used in each assay (0.25%).

Chapter 5:

References

The search for the references used in the present dissertation was made using the following browsers (last access in August of 2016).

<http://apps.isiknowledge.com/>
<http://www.scopus.com/scopus/home.url>
<http://onlinelibrary.wiley.com/advanced/search>
<https://scholar.google.com/>
<http://sciencedirect.com/>

References

1. RAVISHANKAR, D. [et.al.] - Flavonoids as prospective compounds for anti-cancer therapy. *Int J Biochem Cell Biol.* 45 (2013) 2821-2831.
2. FERLAY, J. [et.al.] - Cancer incidence and mortality worldwide: sources, methods and major patterns in GLOBOCAN 2012. *International journal of cancer.* 136 (2015) 359-86.
3. FERLAY, J- Preventing cancer - The European code against cancer, 2016 [accessed 04-02-2016]. Available on the Internet: <http://www.euro.who.int/en/health-topics/noncommunicable-diseases/cancer/news/news/2016/02/preventing-cancer-the-european-code-against-cancer>
4. JEMAL, A. [et.al.] - Global cancer statistics. *CA. A cancer journal for clinicians.* 61 (2011) 69-90.
5. MASAWANG, K. [et.al.] - Evaluation of 2', 4'-dihydroxy-3, 4, 5-trimethoxychalcone as antimitotic agent that induces mitotic catastrophe in MCF-7 breast cancer cells. *Toxicology letters.* 229 (2014) 393-401.
6. NAGLE, A. [et.al.] - Antimitotic agents of natural origin. *Current drug targets.* 7 (2006) 305-326.
7. MEDARDE, M. [et.al.] - Naphthalene combretastatin analogues: synthesis, cytotoxicity and antitubulin activity. *Journal of enzyme inhibition and medicinal chemistry.* 19 (2004) 521-40.
8. JORDAN, A. [et.al.] - Tubulin as a target for anticancer drugs: agents which interact with the mitotic spindle. *Medicinal research reviews.* 18 (1998) 259-96.
9. DOMINGUEZ-BRAUER, C. [et.al.] - Targeting Mitosis in Cancer: Emerging Strategies. *Molecular cell.* 60 (2015) 524-36.
10. B. ALBERTS- **Molecular Biology of the Cell.** 5^a Ed. New york: Taylor & Francis Group, 2008. ISBN 13 978-081534105-5
11. MOLLINEDO, F. [et.al.] - Microtubules, microtubule-interfering agents and apoptosis. *Apoptosis. An international journal on programmed cell death.* 8 (2003) 413-50.
12. DEBONO, A. [et.al.] - Progress Toward the Development of Noscapine and Derivatives as Anticancer Agents. *Journal of medicinal chemistry.* 58 (2015) 5699-5727
13. JORDAN, M. A. - Mechanism of action of antitumor drugs that interact with microtubules and tubulin. *Current medicinal chemistry. Anti-cancer agents.* 2 (2002) 1-17.
14. LI, Q. [et.al.] - Discovery and development of antimitotic agents that inhibit tubulin polymerisation for the treatment of cancer. *Expert Opinion on Therapeutic Patents.* 12 (2002) 1663-1702.
15. NEGI, A. S. [et.al.] - Natural antitubulin agents: importance of 3,4,5-trimethoxyphenyl fragment. *Bioorg Med Chem.* 23 (2015) 373-389.

16. GUPTA, S. - Delineation of Current Development of Antimitotic Compounds Targeting Cytoskeletal Protein Tubulin and Microtubule in the Cancer Therapy. *Current Chemical Biology*. 8 (2014) 165-183.
17. JORDAN, M. A. [et.al.]- Microtubules as a target for anticancer drugs. *Nature reviews. Cancer*. 4 (2004) 253-65.
18. STANTON, R. A. [et.al.] - Drugs that target dynamic microtubules: a new molecular perspective. *Medicinal research reviews*. 31 (2011) 443-481.
19. ZHOU, B. [et.al.] - Diverse Molecular Targets for Chalcones with Varied Bioactivities. *Medicinal Chemistry*. 5 (2015) 388-404
20. DALL'ACQUA, S. - Natural products as antimitotic agents. *Current topics in medicinal chemistry*. 14 (2014) 2272-2285.
21. KAUR, R. [et.al.] - Recent developments in tubulin polymerization inhibitors: An overview. *European Journal of Medicinal Chemistry*. 87 (2014) 89-124.
22. MUKHTAR, E. [et.al.] - Targeting microtubules by natural agents for cancer therapy. *Molecular cancer therapeutics*. 13 (2014) 275-284.
23. NOBLE, R. [et.al.]- Role of chance observations in chemotherapy: Vinca Rosea. *Annals of the New York Academy of Sciences*. 76 (1958) 882-894.
24. LU, Y. [et.al.] - An overview of tubulin inhibitors that interact with the colchicine binding site. *Pharmaceutical research*. 29 (2012) 2943-2971.
25. SONIA ARORA, A. F. G., Khushbu Solanki - Combretastatin A-4 and its Analogs in Cancer Therapy. *Int. J. Pharm. Sci. Rev. Res*. 22 (2013) 168-174.
26. CRAGG M.G. [et.al.]- **Anticancer Agents from Natural Products**. 2^a Ed. U.S.A: Taylor & Francis Group, (2011). ISBN 9781439813829
27. KERR, D. J. [et.al.] - The concise synthesis of chalcone, indanone and indenone analogues of combretastatin A4. *Bioorganic & medicinal chemistry*. 15 (2007) 3290-3298.
28. TRON, G. C. [et.al.] - Medicinal chemistry of combretastatin A4: present and future directions. *J Med Chem*. 49 (2006) 3033-44.
29. LUDUENA, R. F. [et.al.] - Tubulin sulfhydryl groups as probes and targets for antimitotic and antimicrotubule agents. *Pharmacology & therapeutics*. 49 (1991) 133-152.
30. VAN VUUREN, R. J. [et.al.] - Antimitotic drugs in the treatment of cancer. *Cancer chemotherapy and pharmacology*. 76 (2015) 1101-12.
31. LIU, Y.T. [et.al.] - Synthesis and biological activity of chalcones-imidazole derivatives. *Research on Chemical Intermediates*. 39 (2013) 1037-1048.
32. KONG, Y. [et.al.] - A boronic acid chalcone analog of combretastatin A-4 as a potent anti-proliferation agent. *Bioorganic & Medicinal Chemistry*. 18 (2010) 971-977.
33. HAMEL, E. [et.al.] - Synergistic effects of peloruside A and laulimalide with taxoid site drugs, but not with each other, on tubulin assembly. *Mol Pharmacol*. 70 (2006) 1555-1564.
34. GNANAMBAL. K, M. E. [et.al.] - Dictyoceratidan poisons: Defined mark on microtubule-tubulin dynamics. *Life sciences*. 148 (2016) 229-240.
35. TER HAAR, E. [et.al.] - Discodermolide, a cytotoxic marine agent that stabilizes microtubules more potently than taxol. *Biochemistry*. 35 (1996) 243-250.
36. NEWMAN, D. J. [et.al.] - Advanced preclinical and clinical trials of natural products and related compounds from marine sources. *Current medicinal chemistry*. 11 (2004) 1693-1713.
37. EDLER, M. C. [et.al.] - Demonstration of microtubule-like structures formed with (-)-rhazinilam from purified tubulin outside of cells and a simple tubulin-based assay for evaluation of analog activity. *Archives of biochemistry and biophysics*. 487 (2009) 98-104.
38. CHENG, A.-X. [et.al.] - The function and catalysis of 2-oxoglutarate-dependent oxygenases involved in plant flavonoid biosynthesis. *International journal of molecular sciences*. 15 (2014) 1080-1095.
39. WINKEL-SHIRLEY, B. [et.al.] - Flavonoid Biosynthesis. A Colorful Model for Genetics, Biochemistry, Cell Biology, and Biotechnology. *Plant Physiology*. 126 (2001) 485-493.

40. CABRERA, M. [et.al.] - Synthetic chalcones, flavanones, and flavones as antitumoral agents: Biological evaluation and structure–activity relationships. *Bioorganic & Medicinal Chemistry*. 15 (2007) 3356-3367.
41. SAHU, N. K. [et.al.] - Exploring pharmacological significance of chalcone scaffold: a review. *Current medicinal chemistry*. 19 (2012) 209-25.
42. MT ALBUQUERQUE, H. [et.al.] - Chalcones as Versatile Synthons for the Synthesis of 5-and 6-membered Nitrogen Heterocycles. *Current Organic Chemistry*. 18 (2014) 2750-2775.
43. ORLIKOVA, B. [et.al.] - Dietary chalcones with chemopreventive and chemotherapeutic potential. *Genes & Nutrition*. 6 (2011) 125-147.
44. BATOVSKA, D. I. [et.al.] - Trends in utilization of the pharmacological potential of chalcones. *Current Clinical Pharmacology*. 5 (2010) 1-29.
45. NASIR ABBAS BUKHARI, S. [et al.] - Synthesis and biological evaluation of chalcone derivatives (mini review). *Mini reviews in medicinal chemistry*. 12 (2012) 1394-1403.
46. MATOS, M. J. [et.al.] - Potential pharmacological uses of chalcones: a patent review (from June 2011-2014). *Expert opinion on therapeutic patents*. 25 (2015) 351-366.
47. SHEN, J. [et. al.] - Brønsted acidic ionic liquids as dual catalyst and solvent for environmentally friendly synthesis of chalcone. *Journal of Molecular Catalysis A: Chemical*. 280 (2008) 24-28.
48. MERRIFIELD, R. B. [et.al.] - Solid phase peptide synthesis. I. The synthesis of a tetrapeptide. *Journal of the American Chemical Society*. 85 (1963) 2149-2154.
49. MERRIFIELD, R. B. - Solid phase synthesis. *Angewandte Chemie International Edition in English*. 24 (1985) 799-810.
50. NEVES, M. P. [et.al.] - Solid-phase synthesis of 2'-hydroxychalcones. Effects on cell growth inhibition, cell cycle and apoptosis of human tumor cell lines. *Bioorg Med Chem*. 20 (2012) 25-33.
51. YIN B.T. [et.al.] - Synthesis and biological evaluation of α -triazolyl chalcones as a new type of potential antimicrobial agents and their interaction with calf thymus DNA and human serum albumin. 71 (2014) 148-159.
52. CLIMENT, M. [et.al.] - Zeolites as catalysts in organic reactions. Claisen-Schmidt condensation of acetophenone with benzaldehyde. *Catalysis letters*. 4 (1990) 85-91.
53. VARMA, R. S. [et.al.] - Microwave-assisted deacetylation on alumina: a simple deprotection method. *Journal of the Chemical Society, Perkin Transactions I*. (1993) 999-1000.
54. AGUILERA, A. [et.al.] - Ba (OH)₂ as the catalyst in organic reactions. Part XIV. Mechanism of Claisen-Schmidt condensation in solid-liquid conditions. *Canadian journal of chemistry*. 65 (1987) 1165-1171.
55. DREXLER, M. T. [et.al.] - The effect of solvents on the heterogeneous synthesis of flavanone over MgO. *Journal of Catalysis*. 214 (2003) 136-145.
56. SOLHY, A. [et.al.] - Efficient synthesis of chalcone derivatives catalyzed by re-usable hydroxyapatite. *Applied Catalysis A: General*. 374 (2010) 189-193.
57. FUENTES, A. [et.al.] - Catalyzed synthesis of chalcones under interfacial solid-liquid conditions with ultrasound. *Tetrahedron letters*. 28 (1987) 4541-4544.
58. WANG, X. [et.al.] - Direct synthesis and catalytic applications of ordered large pore aminopropyl-functionalized SBA-15 mesoporous materials. *The Journal of Physical Chemistry B*. 109 (2005) 1763-1769.
59. WELTON, T. - Room-temperature ionic liquids. Solvents for synthesis and catalysis. *Chemical reviews*. 99 (1999) 2071-2084.
60. WASSERSCHIED, P. [et.al.] - Ionic liquids—New “solutions” for transition metal catalysis. *Angewandte Chemie International Edition*. 39 (2000) 3772-3789.
61. ZHAO, D. [et.al.] - Ionic liquids: applications in catalysis. *Catalysis today*. 74 (2002) 157-189.

62. WILKES, J. S. - Properties of ionic liquid solvents for catalysis. *Journal of Molecular Catalysis A: Chemical*. 214 (2004) 11-17.
63. COLE, A. C. [et.al.] - Novel Brønsted acidic ionic liquids and their use as dual solvent-catalysts. *Journal of the American Chemical Society*. 124 (2002) 5962-5963.
64. C. OLIVER, K. A. [et.al.] - *Microwaves in Organic and Medicinal Chemistry*. 2^o Ed. Germany: Wiley-VCH Verlag GmbH & Co. KGaA, 2012. ISBN 978-3-527-32094-4
65. SRIVASTAVA, Y. [et.al.] - Ecofriendly microwave assisted synthesis of some chalcones. *Rasayan J. Chem.* 1 (2008) 884-886.
66. KRISHNAKUMAR, B. [et.al.] - $\text{TiO}_2\text{-SO}_4^{2-}$ as a novel solid acid catalyst for highly efficient, solvent free and easy synthesis of chalcones under microwave irradiation. *Catalysis Communications*. 12 (2011) 375-379.
67. RATEB, N. M. [et.al.] - Atom-efficient, solvent-free, green synthesis of chalcones by grinding. *Synthetic Communications*. 39 (2009) 2789-2794.
68. KUMAR, S. [et.al.] - An efficient green procedure for the synthesis of chalcones using C-200 as solid support under grinding conditions. *Green Chemistry Letters and Reviews*. 1 (2008) 123-125.
69. ZANGADE, S. [et. al.] - An efficient and operationally simple synthesis of some new chalcones by using grinding technique. *Chemical Sciences Journal*. 13 (2011) 110-115
70. LEANNE, C. D. [et.al.] - New method for producing alpha,beta-unsaturated carbonyl compounds by using one-pot condensation reaction. *CN103254053B*. 2012.
71. XU. [et al.] - Process for preparation of chalcone compounds. 2012.
72. AL-MASUM, M. [et.al.] - Palladium-catalyzed direct cross-coupling of potassium styryltrifluoroborates and benzoyl chlorides—A one step method for chalcone synthesis. *Tetrahedron Letters*. 52 (2011) 1008-1010.
73. EDDARIR, S. [et.al.] - An efficient synthesis of chalcones based on the Suzuki reaction. *Tetrahedron letters*. 44 (2003) 5359-5363.
74. SELEPE, M. A. [et al.] - Application of the Suzuki-Miyaura reaction in the synthesis of flavonoids. *Molecules*. 18 (2013) 4739-4765.
75. BOHM, B. A.- **Introduction to Flavonoids**. 1^a Ed. Canada: Harwood Academic Pub, 2 (1998). 90-5702-353-9
76. KUMAR, A. [et.al.] - Synthesis of chalcones and flavanones using Julia–Kocienski olefination. *Tetrahedron*. 66 (2010) 9445-9449.
77. BIANCO, A. [et. al.] - A new synthesis of flavonoids via Heck reaction. *Tetrahedron letters*. 44 (2003) 9107-9109.
78. BHAT, B. [et.al.] - Synthesis of 3, 5-Diphenyl-1 H-Pyrazoles. *Synthetic communications*. 35 (2005) 1135-1142.
79. PONNALA, S. [et.al.] - Iodine-Mediated Synthesis of 2-Arylbenzoxazoles, 2-Arylbenzimidazoles, and 1, 3, 5-Trisubstituted Pyrazoles. *Synthetic communications*. 36 (2006) 2189-2194.
80. LOKHANDE, P. [et.al.] - Regioselective one-pot synthesis of 3, 5-diaryl-pyrazoles. *Indian journal of chemistry section b*. 44 (2005) 2338.
81. WANG, B. [et al.] - A novel method for the synthesis of 1, 3, 5-triarylpyrazoles. *Chemical Journal of Chinese Universities*. 24 (2002) 648-650.
82. ZHANG, Z.[et.al.] - One-pot synthesis of 3, 5-diphenyl-1H-pyrazoles from chalcones and hydrazine under mechanochemical ball milling. *Heterocycles. An international journal for reviews and communications in heterocyclic chemistry*. 89 (2014) 103-112.
83. OUTIRITE, M. [et. al.] - New one step synthesis of 3,5-disubstituted pyrazoles under microwave irradiation and classical heating. *Journal of Heterocyclic Chemistry*. 45 (2008) 503-505.
84. LANDGE, S. M. [et.al.] - Synthesis of pyrazoles by a one-pot tandem cyclization-dehydrogenation approach on Pd/C/K-10 catalyst. *Synlett*. 2007 (2007) 1600-1604.

85. VYAS, R. [et. al.] - Heterocyclization of some chalcones to isoxazoles, pyrazoles and pyrimidine nuclei under microwave irradiation and their biological profile. *Journal of the Indian Chemical Society.* 85 (2008) 1217-1226.
86. HAMADA, N. [et.al.] - Synthesis And Spectral Studies Of Some Novel Pyrazole Derivatives From Chalcones Precursors. *Heterocyclic Communications.* 15 (2009) 327-334.
87. AGRAWAL, N. N.[et al.] - Synthesis of pyrazole and isoxazole in triethanolamine medium. *Indian journal of chemistry section b.* 46 (2007) 532.
88. PINTO, D. C. [et. al.] - New bis (chalcones) and their transformation into bis (pyrazoline) and bis (pyrazole) derivatives. *European Journal of Organic Chemistry.* 2003 (2003) 747-755.
89. KALIRAJAN, R. [et.al.] - Microwave Irradated Synthesis, Characterization and Evaluation for their Antibacterial and Larvicidal Activities of some Novel Chalcone and Isoxazole Substituted 9-Anilino Acridines. *Peertechz J Med Chem Res.* 1 (2015) 001-007
90. MOUSTAFA, O. S. [et.al.] - Synthesis and Antimicrobial Activity of Some New Cyanopyridines, Isoxazoles, Pyrazoles, and Pyrimidines Bearing Sulfonamide Moiety. Phosphorus, Sulfur, and Silicon and the Related Elements. 178 (2003) 475-484.
91. PATIL, S. [et.al.] - Novel pyrimidines, isoxazols and pyrazoles—their synthesis, characterization and microbial evaluation. *An International Quarterly Journal of Heterocycles.* 1 (2014) 35-39
92. PRAKASH, O. [et.al.] - The chemistry of α , β -ditosyloxyketones: new and convenient route for the synthesis of 1, 4, 5-trisubstituted pyrazoles from α , β -chalcone ditosylates. *Tetrahedron.* 65 (2009) 10175-10181.
93. LEBLANC, R. [et. al.] - Synthesis and cytotoxicity of epoxide and pyrazole analogs of the combretastatins. *Bioorg Med Chem.* 13 (2005) 6025-34.
94. TERESA, M. V. D. P. e. M. - Recent Advances on the Synthesis and Reactivity of Isoxazoles. *Current Organic Chemistry.* 9 (2005) 925-958.
95. ARCHANA, A. [et. al.] - Synthesis of Potential Quinazolinonyl Pyrazolines and Quinazolinyl Isoxazolines as Anticonvulsant Agents. *ChemInform.* 34 (2003)
96. GAUTAM, N. [et.al.] - Synthesis, characterization, antimicrobial, insecticidal and anthelmintic screening of some new s-triazine derivatives of pyrazoline, pyrimidine, isoxazoline and isothiazoline moiety. *Indian J. Chem. B.* 51 (2012) 1400-1410.
97. KUMBHARE, R. M. [et.al.] - Synthesis and biological evaluation of novel triazoles and isoxazoles linked 2-phenyl benzothiazole as potential anticancer agents. *Bioorganic & medicinal chemistry letters.* 22 (2012) 5424-7.
98. ANTO, R. J. [et.al.] - Anticancer and antioxidant activity of synthetic chalcones and related compounds. *Cancer Letters.* 97 (1995) 33-37.
99. WON, S. J. [et.al.] - Synthetic chalcones as potential anti-inflammatory and cancer chemopreventive agents. *Eur J Med Chem.* 40 (2005) 103-12.
100. NOWAKOWSKA, Z. - A review of anti-infective and anti-inflammatory chalcones. *Eur J Med Chem.* 42 (2007) 125-37.
101. LAHTCHEV, K. L. [et.al.] - Antifungal activity of chalcones: A mechanistic study using various yeast strains. *European Journal of Medicinal Chemistry.* 43 (2008) 2220-2228.
102. GUTTERIDGE, C. E. [et.al.] - Antileishmanial and Antimalarial Chalcones: Synthesis, Efficacy and Cytotoxicity of Pyridinyl and Naphthalenyl Analogs. *Medicinal Chemistry.* 3 (2007) 115-119.
103. SALEM, M. M.; WERBOVETZ, K. A. - Antiprotozoal compounds from *Psorothamnus polydenius*. *Journal of natural products.* 68 (2005) 108-11.
104. SASHIDHARA, K. V. [et.al.] - Identification of quinoline-chalcone hybrids as potential antiulcer agents. *European Journal of Medicinal Chemistry.* 89 (2015) 638-653.
105. ROSSI, G. V. [et.al.] - An evaluation of the antihistaminic activity of a new series of chalcone derivatives. *American journal of pharmacy and the sciences supporting public health.* 129 (1957) 324-31.

106. SIVAKUMAR, P. M. [et.al.] - Antibacterial activity and QSAR of chalcones against biofilm-producing bacteria isolated from marine waters. SAR and QSAR in environmental research. 21 (2010) 247-63.
107. MAHAPATRA, D. K. [et.al.] - Anti-cancer chalcones: Structural and molecular target perspectives. Eur J Med Chem. 98 (2015) 69-114.
108. KARTHIKEYAN, C. [et.al.] - Advances in Chalcones with Anticancer Activities. Recent patents on anti-cancer drug discovery. 10 (2015) 97-115.
109. SYAM, S. [et.al.] - Synthesis of Chalcones with Anticancer Activities. Molecules. 17 (2012) 6179.
110. DUCKI, S. [et.al.] - Antimitotic chalcones and related compounds as inhibitors of tubulin assembly. Anti-cancer agents in medicinal chemistry. 9 (2009) 336-347.
111. DUCKI, S. [et.al.] - Potent antimitotic and cell growth inhibitory properties of substituted chalcones. Bioorganic & medicinal chemistry letters. 8 (1998) 1051-1056.
112. LAWRENCE, N. J. [et.al.] - Linked parallel synthesis and MTT bioassay screening of substituted chalcones. Journal of combinatorial chemistry. 3 (2001) 421-426.
113. LAWRENCE, N. J. [et.al.] - The chemistry and biology of antimitotic chalcones and related enone systems. Curr Pharm Des. 11 (2005) 1679-1693.
114. LAWRENCE, N. J. [et.al.] - Effects of α -substitutions on structure and biological activity of anticancer chalcones. Bioorganic & medicinal chemistry letters. 16 (2006) 5844-5848.
115. KAMAL, A. [et.al.] - Synthesis of chalcone-amidobenzothiazole conjugates as antimitotic and apoptotic inducing agents. Bioorganic & medicinal chemistry. 20 (2012) 3480-3492.
116. ALIAS, Y. [et.al.] - An antimitotic and cytotoxic chalcone from *Fissistigma lanuginosum*. Journal of natural products. 58 (1995) 1160-1166.
117. BEUTLER, J. A. [et.al.] - Two new cytotoxic chalcones from *Calythropsis aurea*. Journal of natural products. 56 (1993) 1718-1722.
118. BOUMENDJEL, A. [et.al.] - Antimitotic and antiproliferative activities of chalcones: forward structure-activity relationship. J Med Chem. 51 (2008) 2307-2310.
119. ROBINSON, M. W. [et.al.] - Synthesis and evaluation of indole-based chalcones as inducers of methuosis, a novel type of nonapoptotic cell death. J Med Chem. 55 (2012) 1940-1956.
120. RAO, Y. K. - Differential effects of synthesized 2'-oxygenated chalcone derivatives: modulation of human cell cycle phase distribution. Bioorg Med Chem. 12 (2004) 2679-86.
121. HSU, Y. L. [et.al.] - Isoliquiritigenin induces apoptosis and cell cycle arrest through p53-dependent pathway in Hep G2 cells. Life sciences. 77 (2005) 279-92.
122. EDWARDS, M. L. [et.al.] - Chalcones: a new class of antimitotic agents. J Med Chem. 33 (1990) 1948-54.
123. PEYROT, V. [et.al.] - Mechanism of binding of the new antimitotic drug MDL 27048 to the colchicine site of tubulin: equilibrium studies. Biochemistry. 31 (1992) 1125-1132
124. PEYROT, V. [et.al.] - Interaction of tubulin and cellular microtubules with the new antitumor drug MDL 27048. A powerful and reversible microtubule inhibitor. J Biol Chem. 264 (1989) 21296-301.
125. CHIRON, M. [et.al.] - Novel use of chalcone class compounds for inhibiting tumoral mass vascularization. WO2002047604 A3. 2002.
126. DUCKI, S. [et.al.] - The development of chalcones as promising anticancer agents. IDrugs. 10 (2007) 42-46.
127. DUCKI, S. [et.al.] - Potent antimitotic and cell growth inhibitory properties of substituted chalcones. Bioorganic & medicinal chemistry letters. 8 (1998) 1051-1056.
128. FONSECA, J. [et.al.] - Prenylated Chalcone 2 Acts as an Antimitotic Agent and Enhances the Chemosensitivity of Tumor Cells to Paclitaxel. Molecules. 21 (2016) 982.

129. LEE, J. M. [et al.] - A new synthetic 2'-hydroxy-2,4,6-trimethoxy-5',6'-naphthochalcone induces G2/M cell cycle arrest and apoptosis by disrupting the microtubular network of human colon cancer cells. *Cancer Lett.* 354 (2014) 348-354.
130. SALUM, L. B. [et.al.] - Cytotoxic 3,4,5-trimethoxychalcones as mitotic arresters and cell migration inhibitors. *Eur J Med Chem.* 63 (2013) 501-510.
131. SHIN, S. Y. [et.al.] - Novel antimetabolic activity of 2-hydroxy-4-methoxy-2',3'-benzochalcone (HymnPro) through the inhibition of tubulin polymerization. *Journal of agricultural and food chemistry.* 61 (2013) 12588-12597.
132. TATSUMI, Y. [et.al.] - Enhancement of in vivo Antitumor Activity of a Novel Antimetabolic 1-Phenylpropenone Derivative, AM-132, by Tumor Necrosis Factor- α or Interleukin-6. *Japanese journal of cancer research.* 92 (2001) 768-777.
133. IKEDA, S. [et.al.] - Preparation of chalcone derivatives as antitumor agents. *Jpn Kai Tokkyo Koho.* 8 (1999) 188,546.
134. ZHANG, H. [et.al.] - Design, synthesis and biological evaluation of novel chalcone derivatives as antitubulin agents. *Bioorganic & medicinal chemistry.* 20 (2012) 3212-3218.
135. BOUMENDJEL, A. [et.al.] - A novel chalcone derivative which acts as a microtubule depolymerising agent and an inhibitor of P-gp and BCRP in in-vitro and in-vivo glioblastoma models. *BMC cancer.* 9 (2009) 242.
136. WANG, G. [et.al.] - Design, synthesis, and structure-activity relationship studies of novel millepachine derivatives as potent antiproliferative agents. *Eur J Med Chem.* 54 (2012) 793-803.
137. WANG, G. [et.al.] - Design, synthesis and biological evaluation of a series of pyrano chalcone derivatives containing indole moiety as novel anti-tubulin agents. *Bioorg Med Chem.* 22 (2014) 2060-2079.
138. KAMAL, A. [et.al.] - Synthesis and anti-cancer activity of chalcone linked imidazolones. *Bioorganic & medicinal chemistry letters.* 20 (2010) 4865-4869.
139. RAMAIAH, M. J. [et.al.] - Chalcone-imidazolone conjugates induce apoptosis through DNA damage pathway by affecting telomeres. *Cancer cell international.* 11 (2011) 1-11.
140. RUAN, B.-F. [et.al.] - Synthesis, biological evaluation, and molecular docking studies of resveratrol derivatives possessing chalcone moiety as potential antitubulin agents. *Bioorganic & Medicinal Chemistry.* 19 (2011) 2688-2695.
141. TU, H.Y. [et.al.] - Synthesis and biological evaluation of 2', 5'-dimethoxychalcone derivatives as microtubule-targeted anticancer agents. *Bioorganic & medicinal chemistry.* 18 (2010) 2089-2098.
142. LIN, C.N. [et.al.] Synthesis and biological evaluation of 2', 5'-dimethoxychalcone derivatives as microtubule-targeted anticancer agents. *US20110306775 A1.* 2011.
143. KIM DO, Y. [et.al.] - Design and biological evaluation of novel tubulin inhibitors as antimetabolic agents using a pharmacophore binding model with tubulin. *J Med Chem.* 49 (2006) 5664-5670
144. CAO, D. [et.al.] - Synthesis and biological evaluation of novel pyranochalcone derivatives as a new class of microtubule stabilizing agents. *Eur J Med Chem.* 62 (2013) 579-89.
145. DYRAGER, C. [et.al.] - Inhibitors and promoters of tubulin polymerization: synthesis and biological evaluation of chalcones and related dienones as potential anticancer agents. *Bioorganic & medicinal chemistry.* 19 (2011) 2659-2665.
146. MARTEL-FRACHET, V. [et.al.] - Investigation of a new 1, 3-diarylpropenone as a potential antimetabolic agent targeting bladder carcinoma. *Anti-cancer drugs.* 20 (2009) 469-476.
147. MARTEL-FRACHET, V. [et.al.] - IPP51, a chalcone acting as a microtubule inhibitor with in vivo antitumor activity against bladder carcinoma. *Oncotarget.* 6 (2015) 14669.
148. ROMAGNOLI, R. [et.al.] - Hybrid alpha-bromoacryloylamido chalcones. Design, synthesis and biological evaluation. *Bioorganic & medicinal chemistry letters.* 19 (2009) 2022-8.

149. ZHU, C. [et.al.] - Discovery of potent cytotoxic ortho-aryl chalcones as new scaffold targeting tubulin and mitosis with affinity-based fluorescence. *J Med Chem.* 57 (2014) 6364-6382.
150. KAMAL, A. [et.al.] - Synthesis of phenstatin/isocombretastatin-chalcone conjugates as potent tubulin polymerization inhibitors and mitochondrial apoptotic inducers. *Organic & biomolecular chemistry.* 13 (2015) 3963-3981.
151. KONIECZNY, M. T. [et.al.] - Structural factors affecting affinity of cytotoxic oxathiole-fused chalcones toward tubulin. *European journal of medicinal chemistry.* 89 (2015) 733-742.
152. KONIECZNY, M. T. [et.al.] - Structural factors affecting cytotoxic activity of (E)-1-(Benzo[d][1,3]oxathiol-6-yl)-3-phenylprop-2-en-1-one derivatives. *Chemical biology & drug design.* 84 (2014) 86-91.
153. FOROUMADI, A. [et.al.] - Chromene-Based Synthetic Chalcones as Potent Antileishmanial Agents: Synthesis and Biological Activity. *Chemical biology & drug design.* 75 (2010) 590-596.
154. NAZARIAN, Z. [et.al.] - Novel antileishmanial chalconoids: synthesis and biological activity of 1- or 3-(6-chloro-2H-chromen-3-yl)propen-1-ones. *Eur J Med Chem.* 45 (2010) 1424-1429.
155. TSENG, C. H. [et.al.] - Discovery of 3-phenylquinolinylchalcone derivatives as potent and selective anticancer agents against breast cancers. *Eur J Med Chem.* 97 (2015) 306-19.
156. LESLIE, B. J. [et.al.] - Phenylcinnamides as novel antimitotic agents. *Journal of medicinal chemistry.* 53 (2010) 3964-3972.
157. YIN, Y. [et.al.] - Design, synthesis and biological evaluation of (E)-3-(3, 4-dihydroxyphenyl) acrylylpiperazine derivatives as a new class of tubulin polymerization inhibitors. *Bioorganic & medicinal chemistry.* 22 (2014) 4285-4292.
158. LUO, Y. [et.al.] - Synthesis, biological evaluation, and molecular modeling of cinnamic acyl sulfonamide derivatives as novel antitubulin agents. *Bioorganic & medicinal chemistry.* 19 (2011) 4730-4738.
159. FATHALLA, O. A. [et.al.] - Synthesis of new 2-thiouracil-5-sulphonamide derivatives with antibacterial and antifungal activity. *Archives of pharmacal research.* 28 (2005) 1205-1212.
160. MURTHY, Y. [et.al.] - Synthesis and characterization of a new chromanoisoxazole. *Indian Journal of Chemistry Section B.* 45 (2006) 532.
161. MURTHY, Y. [et.al.] - Synthesis, characterisation of new chromanoisoxazoles and investigation of optical power limiting properties. *Indian journal of chemistry. Sect. B: Organic chemistry, including medical chemistry.* 43 (2004) 361-366.
162. SOLANKEE, A. [et.al.] - Antimicrobial evaluation of some novel isoxazoles, cyanopyridines and pyrimidinthiones. *Indian J. Chem., Sect B.* 52 (2013) 671-676.
163. SUWUNWONG, T. [et.al.] - Influence of trimethoxy-substituted positions on fluorescence of heteroaryl chalcone derivatives. *Chemical Papers.* 65 (2011) 890-897.
164. RAMESH, B. [et.al.] - Synthesis, spectral studies and anti-inflammatory activity of 2-acetyl thiophene. *Journal of Chemistry.* 7 (2010) 433-436.
165. LAWRENCE, N. J. [et.al.] - The interaction of chalcones with tubulin. *Anti-cancer drug design.* 15 (2000) 135-141.
166. PASSADOR, E. A. P. [et.al.] - The International Journal of Plant Biochemistry and Molecular Biology A pyrano chalcone and a flavanone from *Neoraputia magnifica*. *Phytochemistry.* 45 (1997) 1533-1537.
167. BOMBUWALA, K. [et.al.] - Colchitaxel, a coupled compound made from microtubule inhibitors colchicine and paclitaxel. *Beilstein journal of organic chemistry.* 2 (2006) 13.
168. PEREZ-RAMIREZ, B. [et.al.] - Linkages in tubulin-colchicine functions: the role of the ring C (C') oxygens and ring B in the controls. *Biochemistry.* 37 (1998) 1646-1661.
169. FOURNIER-DIT-CHABERT, J. [et.al.] - Synthesis and biological evaluation of colchicine C-ring analogues tethered with aliphatic linkers suitable for prodrug derivatisation. *Bioorganic & medicinal chemistry letters.* 22 (2012) 7693-7696.

170. YANG, B. [et.al.] - Syntheses and biological evaluation of ring-C modified colchicine analogs. *Bioorganic & medicinal chemistry letters*. 20 (2010) 3831-3833.
171. NEVES, M. P. [et.al.] - Synthesis of a natural chalcone and its prenyl analogs--evaluation of tumor cell growth-inhibitory activities, and effects on cell cycle and apoptosis. *Chem Biodivers*. 9 (2012) 1133-1134.
172. ANDREU, J. M. [et.al.] - Role of the colchicine ring A and its methoxy groups in the binding to tubulin and microtubule inhibition. *Biochemistry*. 37 (1998) 8356-8368.
173. GUPTA, S. [et.al.] - Biphasic kinetics of the colchicine-tubulin interaction: role of amino acids surrounding the A ring of bound colchicine molecule. *Biochemistry*. 44 (2005) 10181-1018.
174. TORIN HUZIL, J. [et.al.] - Computational design and biological testing of highly cytotoxic colchicine ring A modifications. *Chemical biology & drug design*. 75 (2010) 541-550.
175. MONKS, A. [et.al.] - Feasibility of a high-flux anticancer drug screen using a diverse panel of cultured human tumor cell lines. *Journal of the National Cancer Institute*. 83 (1991) 757-766.
176. SKEHAN, P. [et.al.] - New colorimetric cytotoxicity assay for anticancer-drug screening. *Journal of the National Cancer Institute*. 82 (1990) 1107-1112.
177. Wilfred, L.F. [et.al.] - **Purification of Laboratory Chemicals**. 3^o Ed. Oxford: 1988. ISBN 9780080515465
178. PROTA, A. E. [et.al.] - The Novel Microtubule-Destabilizing Drug BAL27862 Binds to the Colchicine Site of Tubulin with Distinct Effects on Microtubule Organization. *Journal of Molecular Biology*. 426 (2014) 1848-1860.
179. BERMAN, H. [et.al.] - The worldwide Protein Data Bank (wwPDB): ensuring a single, uniform archive of PDB data. *Nucleic Acids Res*. 35 (2007) 301-303.
180. FROIMOWITZ, M. [et.al.] - HyperChem: a software package for computational chemistry and molecular modeling. *Biotechniques*. 14 (1993) 1010-1013.
181. JAGHOORI, M. M. [et.al.] - 1001 Ways to run AutoDock Vina for virtual screening. *J Comput Aided Mol Des*. 30 (2016) 237-249.
182. SEELIGER, D. [et.al.] - Ligand docking and binding site analysis with PyMOL and Autodock/Vina. *J Comput Aided Mol Des*. 24 (2010) 417-422.
183. VILAR, S. [et.al.] - Medicinal chemistry and the molecular operating environment (MOE): application of QSAR and molecular docking to drug discovery. *Curr Top Med Chem*. 8 (2008) 1555-1572.